Functional Morphology and Development of Veliger Larvae of the European Oyster, *Ostrea edulis* Linné

THOMAS R. WALLER

SMITHSONIAN CONTRIBUTIONS TO ZOOLOGY • NUMBER 328

SERIES PUBLICATIONS OF THE SMITHSONIAN INSTITUTION

Emphasis upon publication as a means of "diffusing knowledge" was expressed by the first Secretary of the Smithsonian. In his formal plan for the Institution, Joseph Henry outlined a program that included the following statement: "It is proposed to publish a series of reports, giving an account of the new discoveries in science, and of the changes made from year to year in all branches of knowledge." This theme of basic research has been adhered to through the years by thousands of titles issued in series publications under the Smithsonian imprint, commencing with *Smithsonian Contributions to Knowledge* in 1848 and continuing with the following active series:

Smithsonian Contributions to Anthropology
Smithsonian Contributions to Astrophysics
Smithsonian Contributions to Botany
Smithsonian Contributions to the Earth Sciences
Smithsonian Contributions to Paleobiology
Smithsonian Contributions to Zoology
Smithsonian Studies in Air and Space
Smithsonian Studies in History and Technology

In these series, the Institution publishes small papers and full-scale monographs that report the research and collections of its various museums and bureaux or of professional colleagues in the world of science and scholarship. The publications are distributed by mailing lists to libraries, universities, and similar institutions throughout the world.

Papers or monographs submitted for series publication are received by the Smithsonian Institution Press, subject to its own review for format and style, only through departments of the various Smithsonian museums or bureaux, where the manuscripts are given substantive review. Press requirements for manuscript and art preparation are outlined on the inside back cover.

S. Dillon Ripley
Secretary
Smithsonian Institution

SMITHSONIAN CONTRIBUTIONS TO ZOOLOGY • NUMBER 328

Functional Morphology and Development of Veliger Larvae of the European Oyster, *Ostrea edulis* Linné

Thomas R. Waller

SMITHSONIAN INSTITUTION PRESS
City of Washington
1981

ABSTRACT

Waller, Thomas R. Functional Morphology and Development of Veliger Larvae of the European Oyster, *Ostrea edulis* Linné. *Smithsonian Contributions to Zoology*, number 328, 70 pages, 152 figures, 1 table, 1981.—Veliger larvae of the European oyster taken seven days and 15 days after release from parent were anesthetized, fixed, critical-point dried, and examined with scanning electron microscopes. Study of body and shell in a growth series revealed many structures and patterns of development previously poorly known or unknown: (1) the presence of four ciliary bands on the velum, not three; (2) the heel-first development of the foot, with medial ciliation of the toe preceding complete ciliation; (3) the order of appearance and structure of major duct openings on the foot and body wall; (4) the beginning of larval eyes as hemispherical tufts of elongate microvilli; (5) the early development of gill primordia; and (6) the early appearance of a prominent gill bridge, which originates by cross-contact of cilia on the mantle margins followed by migration of epithelial cells and tissue fusion.

A striking posterodorsal notch and growth track on the left valve of prodissoconch II of many Ostreidae and Gryphaeidae is formed by postanal cilia, which deform the fragile calcifying edge of the left valve but are unable to deform the more massive margin of the right valve.

The transition from shell gland to mantle occurs very early in the prodissoconch-I stage, and increasing specialization of the mantle edge produces a three-layered shell well before the prodissoconch-I/II boundary, which merely marks the moment when the valves first completely enclose the body and close against one another. Shell microstructure does not change until metamorphosis, at which time the aragonitic microstructures disappear and are succeeded by far coarser calcitic structures. The postmetamorphic myostracum is an exception. It remains aragonitic and is possibly a continuation of the inner layer of the larval shell. The prodissoconch ligament is formed by periostracum, the fibrous resilium appearing later near the time of metamorphosis. The larval shells of oviparous and larviparous oysters differ, those of the former having a prodissoconch I that is smaller compared to prodissoconch II.

OFFICIAL PUBLICATION DATE is handstamped in a limited number of initial copies and is recorded in the Institution's annual report, *Smithsonian Year*. SERIES COVER DESIGN: The coral *Montastrea cavernosa* (Linnaeus).

Library of Congress Cataloging in Publication Data
Waller, Thomas R.
Functional morphology and development of veliger larvae of the European oyster, Ostrea edulis Linné
(Smithsonian contributions to zoology ; no. 328)
Bibliography: p.
1. European oyster—Development. 2. Mollusks—Larvae. 3. Mollusks—Development. I. Title. II. Title: Veliger larvae of the European oyster, Ostrea edulis Linné. III. Series: Smithsonian Institution. Smithsonian contributions to zoology ; no. 328.
QL1.S54 no. 328 [QL430.7.09] 591s [594'.11] 80-23129

Contents

Functional Morphology and Development of Veliger Larvae of the European Oyster, *Ostrea edulis* Linné

Thomas R. Waller

Introduction

Two groups of oysters may be distinguished on the basis of their breeding habits (Morton, 1958; Galtsoff, 1964; Stenzel, 1971). An "oviparous" or nonincubatory group, which includes the American oyster, *Crassostrea virginica* (Gmelin), the Japanese oyster, *C. gigas* (Thunberg), and other species, discharges eggs and sperm directly into the surrounding seawater. Fertilization is thus external, and the developing planktonic larvae are afforded no parental protection. In contrast, "larviparous" or incubatory oysters, such as the European oyster, *Ostrea edulis* Linné, and the Pacific oyster, *O. lurida* Carpenter, cast only sperm into the surrounding water. Eggs are retained within the shell of the female and are fertilized internally by sperm drawn into the mantle cavity with the incurrent stream. Early development occurs within the shell of the parent, and when the larvae are finally released (some 6 to 18 days after fertilization depending on temperature) they pursue a short planktonic life (generally 0 to 17 days, also depending on temperature) before permanently settling on a suitable substrate (Erdman, 1935; Korringa, 1941; Chanley, pers. comm., 1979).

The present study is concerned primarily with larval development in the larviparous group, specifically in the European oyster, *Ostrea edulis*. Descriptions deal with larval morphology from time of release from parent to just before eyespots become pigmented and the foot becomes fully functional. Emphasis is on structure of the velum, development of organs in the mantle cavity, ultrastructure and development of shell and mantle, and relationship between features of shell and body. For comparison, larval shells of some oviparous species, particularly of *Crassostrea gigas* and *C. virginica*, are discussed briefly.

ACKNOWLEDGMENTS.—I thank Paul Chanley, Fundacion Chile, Coquimbo, whose shipment of living larvae from the Shelter Island Oyster Company launched this project. Warren Blow, Walter R. Brown, Mary-Jaque Mann, Duane Hope, John Harshbarger, and Kenneth M. Towe of the Smithsonian Institution, Ruth D. Turner of Harvard University, and Melbourne R. Carriker of the University of Delaware provided technical assistance. Critical reviews were provided by Chanley, Turner, and Carriker, as well as Frank R. Bernard and Daniel B. Quayle, Nanaimo Biological Station, British Columbia, Dale Bonar

Thomas R. Waller, Department of Paleobiology, National Museum of Natural History, Smithsonian Institution, Washington, D.C. 20560.

and Robert D. Burke, University of Maryland, Richard A. Lutz, Yale University, and P. Dinamani, Fisheries Research Division, Wellington, New Zealand. The artwork is by Lawrence B. Isham, Department of Paleobiology, Smithsonian Institution.

Background

In the vast literature on the biology of oyster larvae that has accumulated since Brach (1690) and Leeuwenhoeck (1695) first trained their early compound microscopes on these tiny organisms, there are still relatively few detailed studies of bivalve larval development and morphology (see reviews by Horst, 1883–1884, Korringa, 1941, and Galtsoff, 1964). The most complete description of cell lineage and early development of the preveliger stages of oyster larvae remains that of Horst (1883–1884), which describes the development of larvae of *Ostrea edulis* from fertilization up to the moment of release from parent. Other studies of these early stages are more limited in scope or lack detail, e.g., Davaine (1853) and Fernando (1931) on *O. edulis*, Hori (1933) on *O. lurida*, Brooks (1880) and Galtsoff (1964) on *Crassostrea virginica*,, and Fujita (1929, 1934) on *C. gigas*. More detailed information on early development can be obtained from studies of unrelated bivalves, particularly the work of Meissenheimer (1900) on *Dreissena*, Hatschek (1880) on *Teredo*, and Allen (1961) on *Pandora*.

The gross anatomy of more advanced oyster larvae is known primarily through the exhaustive study of Erdmann (1935), which is again concerned with the European oyster. Erdmann began his study with a brief description of the oldest growth stage considered by Horst (1883–1884), the newly released larva, and finished with an extensive description of the oldest free-swimming stage, the 'ansatzreife' (attachment-ready) larva, now generally referred to as the pediveliger (Carriker, 1961). Millar (1955) studied the mechanism of food movement in the gut of larval *Ostrea edulis* of unspecified growth stage, but presumably the pediveliger stage, and updated information previously furnished by Yonge (1926) and Erdmann (1935). Cole (1938) and Hickman and Gruffydd (1971) concentrated on growth stages beyond those studied by Erdmann and dealt with the fate of larval organs of *O. edulis* through metamorphosis. Cranfield (1973a, b, c, 1974) described the ultrastructure and histochemistry of the foot and mantle edge of the pediveliger of *Ostrea edulis* and the function of these organs during settlement and cementation.

Until recently investigation of the larval shell of the oyster has lagged far behind the study of soft tissue. Most papers dealing with larval shells of oysters have been concerned primarily with identification and hence have concentrated on shell outline and the configuration of hinge teeth, both of which are within the range of light microscopy. Most of these studies deal only with late larval stages and present the hinge in a highly diagrammatic fashion (e.g., Rees, 1950; Ranson, 1960; Stenzel, 1971). Pascual (1971, 1972), however, published exceptionally high-quality light micrographs showing the development of the hinge of both oviparous and larviparous species, including *Ostrea edulis*, and Dinamani (1973) used light microscopy to show hinge development in the oviparous species, *Saccostrea glomerata*. Dinamani (1976) also used scanning electron microscopy to demonstrate differences in the development of the provinculum (larval hinge) of oysters in the genera *Crassostrea*, *Saccostrea*, and *Ostrea*. Carriker and Palmer (1979a) used scanning electron microscopy to study the shell of *Crassostrea virginica*, including microsculpture, microstructure, and a peculiar posterodorsal notch. The notch was discussed from a functional point of view by Waller (1979) in abstract and will be examined in detail in the present study.

In 1975 Turner and Boyle published the first scanning electron micrographs of whole, anesthetized bivalve larvae prepared by critical-point drying, a technique first developed by Anderson (1951, 1956) and now widely applied in biology and medicine (see Becker and Johari, 1978, for extent of application). Boyle and Turner (1976) later used this technique to illustrate the velar

and pedal ciliation of a pholad, *Martesia striata*, and Waller (1980) demonstrated the extent to which critical-point drying could be used in studies of cell surfaces, micro-anatomy, and mantle-shell relationships in mature bivalves in the Order Arcoida.

Review of Larval Development

The diameter of the spherical egg of *Ostrea edulis* is about 150 μm when it is released from the gonad (Orton, 1937; Korringa, 1941; Yonge, 1960). This size is at least two or three times that of the eggs of oviparous species (Amemiya, 1926; Hori, 1933).

Differing accounts of cell lineage and gastrulation were given by Horst (1883-1884) and Fernando (1931). Basically, cleavage follows the typical molluscan spiral pattern. Micromeres spread from the animal pole over the surface of the macromeres toward the vegetal pole, and gastrulation is intermediate between epiboly and emboly. It is unclear whether the blastopore remains open to become the mouth at a later stage (Horst's view and also Fujita's, 1934) or closes and subsequently becomes the site of a stomodaeum and later the mouth (Fernando's view). The morphological outcome in either case is an embryo that is spheroidal, with the animal pole domed and the vegetal pole concave and bearing the presumptive mouth opening (Figure 1*a*). No cilia have been reported on the surface of the embryo at this point in the development of *Ostrea edulis*, although the embryo of *Crassostrea virginica* at a comparable stage has been shown with a covering of fine cilia (Galtsoff, 1964). Amemiya (1926) mentioned that the blastula of *C. virginica* rotates, and Senô (1929) described the gastrula of *Ostrea denselamellosa* as being ciliated and motile.

Two important structures, a crown of motile cilia (prototroch) and an ectodermal invagination (shell gland), disrupt the outline of the embryo as it enters the trochophore stage. The prototroch is centered on the animal pole; the shell gland appears on one side, nearer to the animal pole than to the vegetal pole (Figure 1*b*,*c*). Authors do not agree, however, on the order of appearance of these structures. In *Ostrea edulis*, Davaine (1853) observed that the shell gland appears at the same time as the earliest prototroch. Horst (1883–1884) showed the shell gland appearing even before gastrulation is completed and well before the earliest appearance of the prototroch (Figure 1*b*), implying that the first appearance of the shell gland in *Ostrea edulis* is earlier than in other bivalve larvae. Finally, Fernando (1931) showed the prototroch appearing shortly after gastrulation and the shell gland definitely following the earliest appearance of the prototroch. In *Crass-*

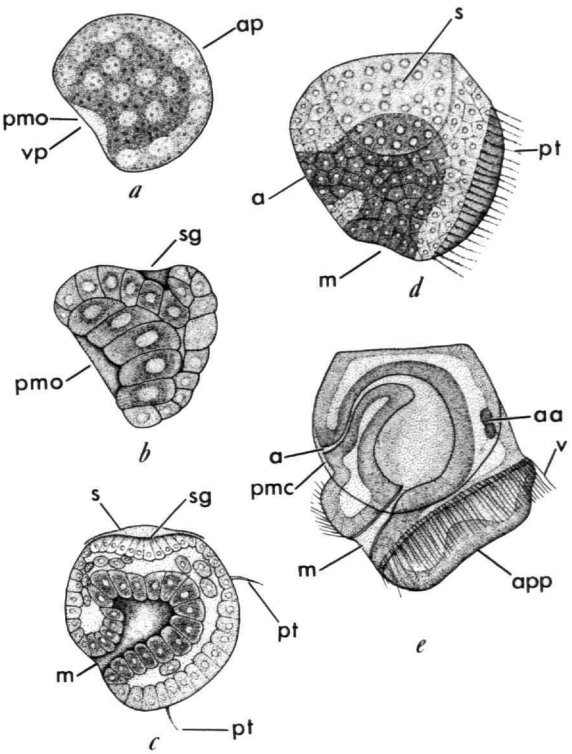

FIGURE 1.—Early development of *Ostrea edulis*, redrawn from Horst (1883–1884) with presumptive dorsal region (shell gland and later the hinge) at top and anterior to right: *a*, gastrula; *b*, early trochophore; *c*, middle trochophore; *d*, late trochophore; *e*, early veliger. (a = anus, aa = anterior adductor, ap = animal pole, app = apical pit, m = mouth, pmc = presumptive mantle cavity, pmo = presumptive mouth opening, pt = prototroch, s = shell, sg = shell gland, v = velum, vp = vegetal pole.)

ostrea gigas, Fujita (1934) found that the shell-gland invaginates about the same time the blastopore begins to close and before development of the prototroch.

Descriptions of the early prototroch also differ. Horst (1883–1884) showed that in *Ostrea edulis* the prototrochal cilia stem from a single ring of cells (trochoblasts), the center of the ring being a simple dome (Figure 1*c*). Neither Davaine (1853) nor Horst observed any cilia on the dome, whereas Fernando (1931) illustrated an apical tuft of cilia from the earliest appearance of the prototroch onward. In *Crassostrea gigas*, Fujita (1934) described an apical "flagellum" six or seven times as long as the surrounding velar cilia in veliger larvae that were in the early D-shaped phase of shell development (probably earliest prodissoconch II). This "flagellum" gradually became shorter relative to surrounding cilia as development proceeded, but Fujita did not specify whether or not it eventually disappeared during the veliger stage. It is not yet known whether these developmental patterns represent real variation due to environmental or genetic differences or whether they are artifacts of techniques.

Subsequent changes in the external morphology of the trochophore and veliger involve evagination of the shell gland, secretion and enlargement of a shell, formation of the anal tuft and anus, gradual elaboration of the prototroch into the velum, and formation of the mantle cavity in which the foot and other structures develop (Figures 1*d*,*e*, 2, 3).

The structure of the shell gland and the earliest formed shell are among the most poorly known aspects of larval morphology. Early authors debated whether the initial shell of a bivalve is a single structure or a paired structure. These differences are readily resolved, however, when it is noted that authors referring to a single structure, such as Horst (1883–1884), were referring to the first-formed uncalcified cuticle, whereas those referring to a paired structure, such as Lacaze-Duthiers (1854) and Brooks (1880), were describing the first calcified structures; which are indeed paired (Raven, 1958). Obviously the organic structure must precede calcification, for, as discussed below and as noted by Carriker and Palmer (1979a) and Kniprath (1979), it is the periostracum that separates the microenvironment for initial calcification from the surrounding seawater.

Secretion of the initial organic periostracum is by cells that border the nearly closed opening of the shell-gland invagination (Kniprath, 1979), and it seems that some trace of this earliest portion of the shell should be detectable on the surface of prodissoconch I. Unfortunately, descriptions of the form of the invagination and its opening are incomplete. Horst (1883–1884) showed the invagination as a transverse groove in *Ostrea edulis*, attenuating at its ends, with the plane of the groove inclined to the surface of the embryo and passing inward toward the posterior (Figure 1*b*). Lacaze-Duthiers (1854) referred to the calcified valves as being formed from two thickenings of the epiblast on each side of a dorsal depression, and Brooks (1880) observed a similar origin in the American oyster. The first-formed shell, including the initial organic cuticle (or periostracum) and the paired calcified valves, must therefore be a transversely elongate structure, which indeed it is as revealed by scanning electron microscope.

When the shell gland, which is the rudiment of the mantle, actually becomes the mantle is a matter of definition made difficult by the fact that the change is gradual. It is implicit in the terms "gland" and "mantle" that the former is specialized epithelium and the latter is a sheet-like fold of epithelium enclosing a mantle cavity. It is also generally understood that a "mantle" has a specialized edge having either a periostracal groove or a commarginal band of specialized cells capable of secreting a periostracum. Unfortunately, however, there are no detailed studies of the histology of the transition between shell gland and mantle in the Bivalvia, and it is necessary to look to studies of gastropod larvae for a clearer understanding of the changes that take place.

Cather (1967), who extended the previous work of Raven (1958), found that in the gastropod

Ilyanassa, secretion of a thin membrane (initial periostracum) by the shell gland begins in the invaginated stage (see also Demian and Yousif, 1973a, b). The membrane is at first attached by microvilli to the apical ends of all of the cells in the invagination but subsequently lifts from the central cells and closes the opening of the invagination. From this point on, the periostracum is attached only to the leading edge of the shell gland. Calcification begins after the shell gland evaginates. The calcium carbonate is aragonite, which, as noted by Cather, is formed in a viscous matrix that underlies the periostracum. After secretion of the first calcified shell, the central cells of the shell gland change from columnar to squamous and no longer show evidence of secretory activity. The marginal cells, however, remain in their original columnar, active state. It is at this point that Cather prefers to use the term "mantle" rather than "shell gland," because an initial phase of calcification has been completed and there is a clear differentiation in the cells which comprise the structure. Subsequent growth of the mantle edge in the larva is by incorporation of surrounding ectodermal cells as well as by proliferation of the cells in the mantle.

Kniprath (1977) found a different ontogeny of shell gland and mantle in the gastropod *Lymnaea stagnalis*. The initial periostracum is not secreted by the invaginated cells of the shell gland, but only by the rosette of cells surrounding the invagination. Functional activation of other cells proceeds from the peripheral rosette inward. The initial periostracum is therefore a ring consisting of the same type of material that in subsequent stages will form the outermost layer of the periostracum. More centrally located cells secrete inner layers and close the central hole in the initial periostracal ring. After evagination of the shell gland, the free mantle edge forms when the peripheral cells of the gland arch upward and a second arched ring of cells differentiates on the outside of the first arched ring. These two ridges become opposed to one another, forming the periostracal groove between them.

Both of these patterns of development in gastropods demonstrate that commarginal differentiation of secretory cells occurs very early in the development of the shell gland and that the change from shell gland to mantle is gradual and transitional. In contrast, students of bivalve larvae have long considered the shell-gland phase to extend through the prodissoconch-I stage of shell development and have assumed that the prodissoconch-I/II boundary represents an abrupt change from calcification by the shell gland to calcification by the mantle (e.g., Bernard, 1896; Ansell, 1962; Ockelmann, 1965; Kumé and Dan, 1968; Calloway and Turner, 1979). This assumption, however, has been based on a change in external sculpture rather than on actual observation of histological or shell ultrastructural changes. It will be argued in the present study that the prodissoconch-I/II boundary represents nothing more than the onset of valve closure.

In oyster larvae, the calcified shell valves extend laterally as the shell gland or mantle increases in area, and at the stage represented by Figure 1*d* the valves cover nearly half the dorsoventral dimension of the trochophore. The cilia of the prototroch increase in size, but the pretrochal region remains dome-shaped. According to Horst (1883–1884), it is at about this stage that the intestine first communicates with the exterior by way of the anus.

At the point where the anus forms, a tuft of cilia also appears on the epiderm. In fact, ciliation probably precedes formation of the anus, as shown by Hatschek (1880) in *Teredo*, Meisenheimer (1900) in *Dreissena*, and Allen (1961) in *Pandora*. This ciliary tuft was unknown to Horst (1883–1884) and therefore is absent from Figures 1*d* and 1*e*. Dantan (1916) first noted its presence in the larva of the European oyster and described it in detail, noting that short cilia surround the anus and that longer cilia occur just dorsal to the anus. He considered this "postanal ciliary crown" to be homologous with the telotroch generally present in trochophores of the mollusk-annelid line, and Fernando (1931) actually called the tuft the "telotroch."

Elaboration of the prototroch to a velum in-

volves five main events: (1) doubling of the ring of trochoblasts to produce a double row of cilia, (2) elongation and clustering ("compounding") of the cilia, (3) subsidence in the center of the apical dome to form an apical pit, (4) enlargement of the tissue in the apical pit to produce an apical organ and eventually a cerebral ganglion, and (5) the formation of velar retractor muscles inserted into the shell and complexly ramified in the velum. Aside from the apical cilia, authors differ on whether or not cilia are present on the epiderm central to the preoral ring of locomotory cilia in the developing prototroch. Horst (1883–1884) and Fernando (1931) found none, but Dantan (1916) showed fine cilia present over the entire apical dome except at the center, where he maintained that cilia are absent.

Authors have also differed in their ideas on how the mantle cavity develops. Meisenheimer (1900) thought that it formed by an actual infolding of the body wall. However, Erdmann (1935) maintained, probably correctly, that the precursor of the mantle cavity is the flattened posteroventral region of the trochophore lying between mouth and anus. This area becomes the mantle cavity not through any infolding but simply because it is overgrown by advancing edges of the mantle and shell that are curved rather than flattened.

With the ontogenetic developments described above, the trochophore of the European oyster becomes a veliger and is ready for release from its parent. From this stage up to the end of larval development, Erdmann's (1935) reconstructions, reproduced in Figures 2 and 3, are the most informative. External features of interest in the present study are the velum, mouth region, structures in the mantle cavity, and the anal region.

In the newly released larva (Figure 2), Erdmann distinguished only one clearly delimited ciliary band, preoral in position and containing long, locomotory cilia stemming from a double row of large cells. The entire subvelar area was said to be covered with fine cilia that move particles indiscriminately toward the mouth. In the pediveliger stage (Figure 3), however, he was able to distinguish three ciliary bands separated from one another by narrow non-ciliated spaces: a preoral locomotory band, a subvelar adoral band of short cilia, and a second subvelar band bearing longer cilia and said to be postoral in position. Erdmann did not specifically refer to the long cilia in the preoral band as being compound but clearly stated that they occur in tufts lying parallel to one another.

Erdmann also found that in both early and late veligers a conical apical pit occurs slightly posterior to the center of the velum. The posterior slope of the pit is steep and without cilia, whereas the anterior slope is shallow and bears short cilia. During development the epithelium underlying the anterior slope of the pit thickens and projects further into the lumen of the velum, where it is underlain by the cerebral (cephalic) ganglion. According to Erdmann, throughout the veliger stage the mouth is actually a part of the velar mass, occurring on a lobe on the posterior subvelar region (Figures 2, 3). Some investigators (Horst, 1883–1884; Yonge, 1926, 1960) have confused this mouth lobe with the rudiment of the foot.

There has been no general agreement on the nature of ciliation about the mouth. Dantan (1916) described only a postoral ciliary tuft, which he considered to be a remnant of the postoral band found in some other bivalves. Erdmann (1935), on the other hand, found no tuft but considered the mouth to be surrounded by cilia of the adoral and postoral velar bands. Dantan (1916) also observed invaginations on the borders of the mouth which he interpreted to be buccal glands.

Erdmann (1935) showed that the foot develops medially from an outgrowth of the ectoderm of the body wall. In the newly released larva (Figure 2), there is little external expression of the foot primordium other than an invagination marking the site of the byssal gland. An elevated, ciliated papilla, the heel or metapodium, then appears dorsal to the byssal-gland invagination. Later, the epithelium ventral to the byssal gland proliferates and grows outward to produce the toe or

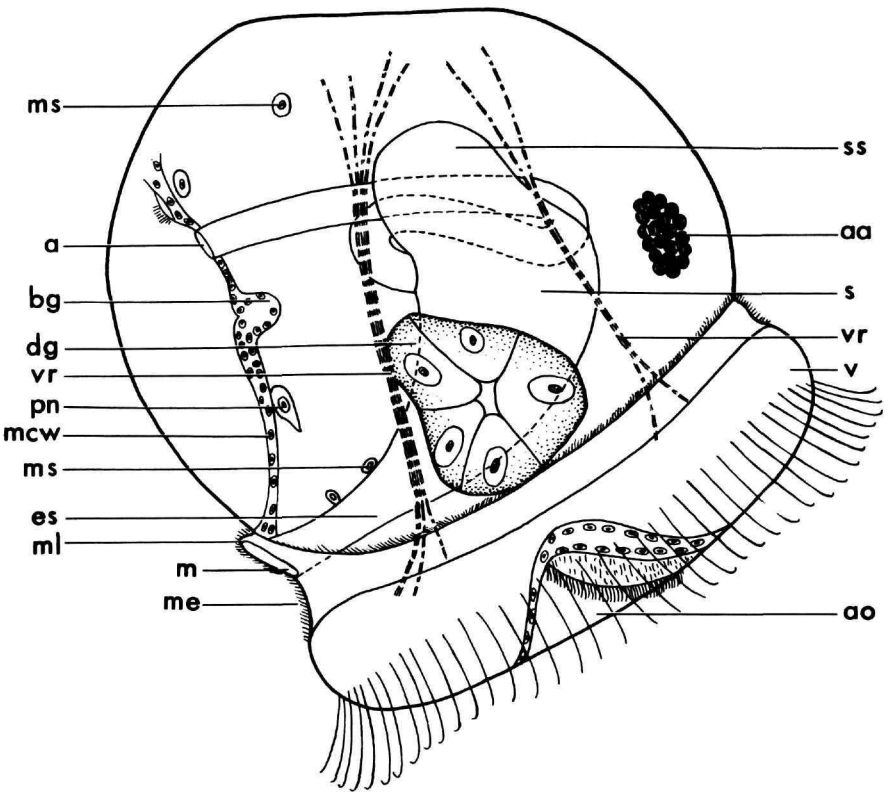

FIGURE 2.—Anatomy of a young, newly released, six-day-old veliger larva of *Ostrea edulis*, redrawn from Erdmann (1935) (a = anus, aa = anterior adductor, ao = apical organ, bg = primordial byssal gland, dg = digestive gland, es = esophagus, m = mouth, mcw = mantle-cavity wall, me = mouth embayment, ml = mouth lobe, ms = free mesenchymal cell, pn = protonephridium, s = stomach, ss = style sac, v = velum, vr = velar retractor).

propodium, which becomes a prominent structure by the end of the veliger stage.

Soon after release from parent, deep gill cavities or "kiemenhohlen" (Hatschek, 1880) form on each side of the foot by infolding of the body wall. A single gill primordium also forms on each side as an ectodermal ridge of the mantle. As in all bivalve larvae thus far studied, this is the primordium of the inner demibranch (e.g., Lacaze-Duthiers, 1854; Rice, 1908; Raven, 1958; Knight-Jones, 1954b). Later, papillae which are the primordia of the gill filaments form on the ridges, and the ridges themselves elongate posteriorly, nearly to the edge of the mantle. At this point in *Ostrea edulis*, the ridges on each side join to one another by a bridge of epithelium (Erdmann, 1935, and Figure 3). The outer demibranchs do not develop until after metamorphosis (Yonge, 1926).

Medially, on each side of the base of the primordial foot, tiny invaginations form the paired statocysts, which, according to Erdmann (1935), maintain openings into the mantle cavity only for a brief time before being closed off. The primordia of the eyes also appear early as outgrowths from the body wall in the gill cavities lateral and slightly anterior to the base of the foot. Lastly, paired protonephridia also appear very early, but Erdmann could detect openings to the exterior only late in the veliger stage and

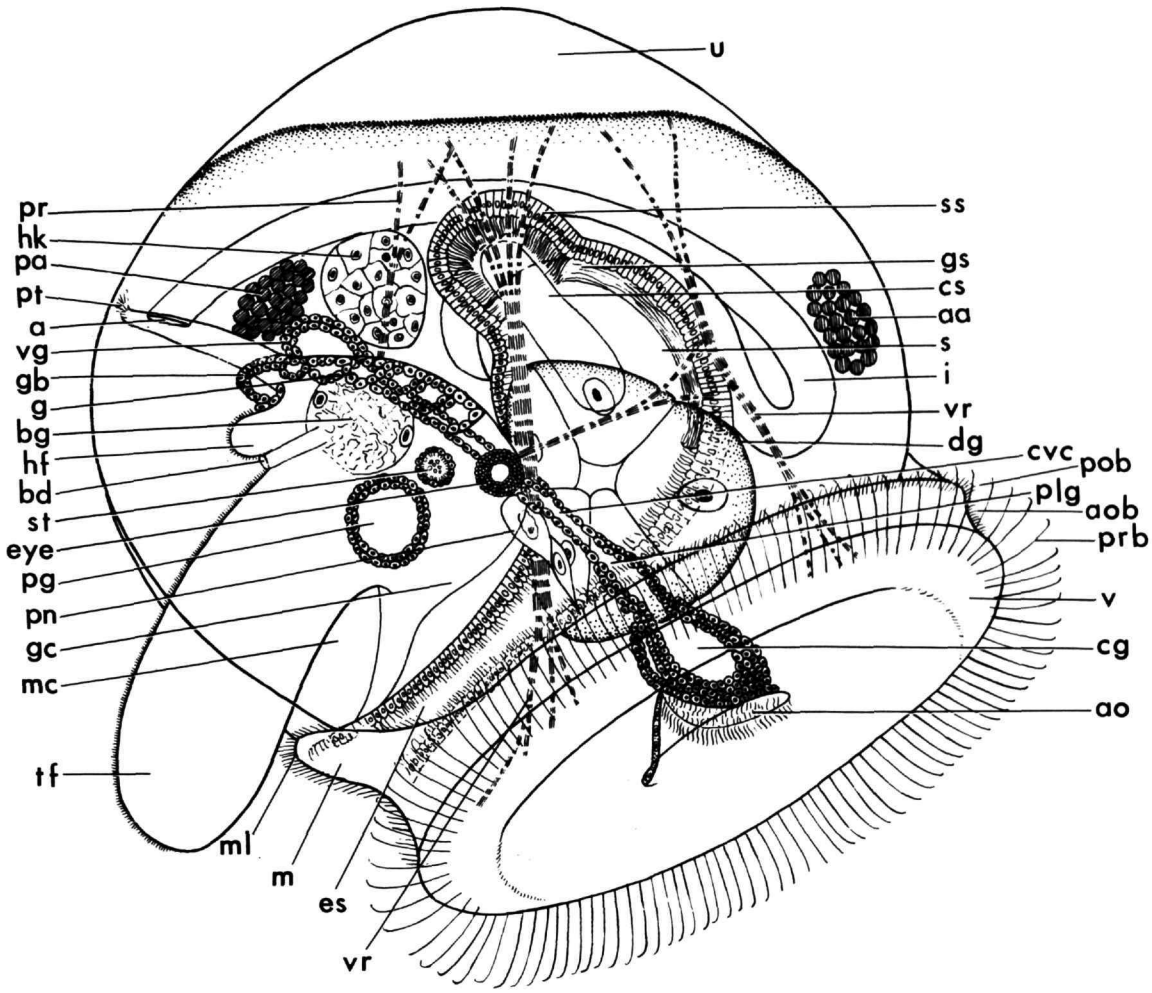

FIGURE 3.—Anatomy of a pediveliger larva of *Ostrea edulis*, redrawn from Erdmann (1935) (a = anus, aa = anterior adductor, ao = apical organ, aob = adoral ciliary band, bd = byssal gland duct, bg = byssal gland, cg = cerebral ganglion, cs = crystalline style, cvc = cerebro-pleural-visceral connective, dg = digestive gland, es = esophagus, eye = eye, g = gill primordium, gb = gill bridge, gc = gill cavity, gs = gastric shield, hf = heel of foot, hk = primordium of heart and kidney, i = intestine, m = mouth, mc = mantle cavity, ml = mouth lobe, pa = posterior adductor, pg = pedal ganglion, plg = pleural ganglion, pn = protonephridium, pob = postoral ciliary band, pr = pedal retractor, prb = preoral ciliary band, pt = postanal ciliary tuft, s = stomach, ss = style sac, st = statocyst, tf = toe of foot, u = umbo, v = velum, vg = visceral ganglion, vr = velar retractor).

then only with difficulty by repeated sectioning. These three pairs of structures—the static ducts, eye primordia, and protonephridial ducts—all occur close to one another. The only other structures present in the mantle cavity of the veliger are the anus and the postanal tuft (Figures 2 and 3), developed at the dorsal extremity of the mantle cavity.

The structure of the shell of the veliger stage is somewhat better known than that of the preveliger shell. As is generally the case with bivalve larvae having planktonic planktotrophic stages, a boundary line separates a pitted and radially striate prodissoconch I from a commarginally striate prodissoconch II (Werner, 1939; Ockelmann, 1965). As previously mentioned another prominent sculptural feature of the prodissoconch II of oysters is a posterodorsal notch and resultant spiral growth track (Tanaka, 1960; Waller, 1979; Carriker and Palmer, 1979a). The shell is oval in lateral view, with a shape somewhat like that of a small Nuculacean clam. The hinge line is short but with strong interlocking hinge teeth in the prodissoconch-II stage. Some authors (e.g., Ranson, 1960; Stenzel, 1971) have described a central resilium (or internal fibrous ligament) as being present between the teeth, but this is now known to be incorrect (Pascual, 1971, 1972; Carriker and Palmer, 1979a). The resilium does not appear until at or near metamorphosis, and it is then at the anterior edge of the anterior hinge teeth, not in the center.

The ultrastructure of the larval shell of *Ostrea edulis* has not been described, although Carriker and Palmer (1979a) have dealt with the ultrastructure of the prodissoconch II of another species, *Crassostrea virginica.*

In *Ostrea edulis*, metamorphosis involves permanent cementation of shell to substrate, disappearance of the velum, foot, anterior adductor muscle, and eyespots, appearance of labial palps, and elaboration of gills and mantle edges. These events and changes have been thoroughly described by Cole (1938), Hickman and Gruffydd (1971), and Cranfield (1973a, b, c, 1974) and need not be reviewed here. Relatively little attention has been given to the abrupt changes in shell fabric and mineralogy that occur at metamorphosis. Carriker and Palmer (1979a) showed that in *Crassostrea virginica* the finely textured aragonite of the prodissoconch changes abruptly to coarsely prismatic and foliated calcite at metamorphosis. Descriptions of dissoconch shell mineralogy and fabric can be found in Galtsoff (1964), Taylor, Kennedy, and Hall (1969), and Stenzel (1971).

Materials and Methods

Two samples of living veliger larvae of *Ostrea edulis* were received from the Shelter Island Oyster Company, Greenport, Long Island, New York. The specimens of one sample were anesthetized and fixed when they were still in an early prodissoconch-II stage, seven days from time of release from parent. The specimens of the second sample were anesthetized and fixed when they had reached an advanced prodissoconch-II stage, 15 days after release.

Specimens were anesthetized by transferring them to a 50-ml culture dish half filled with seawater and adding one or two drops of 2-phenoxyethanol (Eastman Kodak Co.) to the seawater in the dish. These specimens, which were still capable of swimming but incapable of retracting their velum, were then transferred to a 2-ml dish and were killed by adding a drop of fixative consisting of 2% glutaraldehyde buffered with sodium cacodylate (0.025 M in seawater) prepared according to the method of Turner and Boyle (1975). When the beating of velar cilia ceased, the seawater was drawn off and replaced by the fixative. Specimens were dehydrated with a graded series of ethanols and amyl acetate and critical-point dried in a Denton DCP-1 unit.

Short pieces of No. 39 coated copper wire were shaped so that each piece would stand on its coiled base with an upright stalk. The critical-point dried specimens were placed on a clean glass surface; the tip of the wire stalk was dipped in glue (polyvinyl acetate), which was allowed to dry to a "tacky" consistency; and this glued tip was then touched to a larva at a point which would allow the velum and gaping mantle cavity to be viewed with the scanning electron microscope. The wires bearing the larvae were then set on their bases on a glass coverslip and fastened to the coverslip with a dilute water-soluble glue (trade name, "Elmer's Glue-all," Borden, Inc.). The cover-slip was then fastened to a standard

aluminum stub by means of a carbon suspension. Mounting the specimens on wires permitted subsequent reorientation on the stub simply by bending the wire. The specimens were sputter-coated under vacuum first with a thin layer of carbon and then with gold-palladium and were studied with Coates and Welter 106B and Cambridge Mark-IIA scanning electron microscopes.

Some of the fresh larval shells of *Ostrea edulis*, ethanol-preserved shells of *Crassostrea gigas* (Thunberg, 1793), and dried postlarval museum specimens of *Neopycnodonte cochlear* (Poli, 1795) were mechanically fractured, cleaned ultrasonically in neutral distilled water, and mounted directly on glass coverslips. Other shells were etched in an oxygen plasma in a Tegal "Plasmod" low-temperature asher or were treated with commercial grade laundry bleach (5% NaOCl) to remove the periostracum. During the period of nearly two years during which this study was in progress, critical-point dried specimens were stored in a glass silica-gel dessicator and showed no evidence of deterioration or change in appearance at the levels of magnification of the scanning electron microscopes.

The illustrated specimens of larval shells of *Ostrea edulis* and *Crassostrea gigas* were numbered to permit the reader to determine whether or not the micrographs are of the same or different individuals. Each microscope stub was given a separate number, and if the stub contained more than one specimen, each specimen was lettered. These specimens will not become part of the permanent collection of the Museum because of their small size, fragile mounts, and likelihood that the dried tissues will deteriorate. Specimens of *Neopyonodonte cochlear* from the museum collections bear USNM (National Museum of Natural History, formerly United States National Museum) catalog numbers.

Terms, Measurements, and Limitations

The terms "prodissoconch I" and "prodissoconch II," first used by Werner (1939), refer to successive stages of development of the larval shell as well as to the shell itself. The prodissoconch-I stage extends in time from the beginning of calcification to the end of development of prodissoconch I. The end of this stage on the shell exterior is indicated by a more or less abrupt change in sculpture from faintly radially striate without prominent commarginal growth ridges to commarginally ridged without significant radial striae. In oyster larvae, this boundary also coincides with the origin of the posterodorsal notch and its growth track. The prodissoconch-II stage extends in time from the end of the prodissoconch-I stage to metamorphosis and the beginning of the postmetamorphic shell, the "dissoconch." The prodissoconch-II shell includes the entire prodissoconch-I shell plus whatever new growth has been added, both to the periphery and to the interior surfaces. The dissoconch stage spans the entire time from metamorphosis to death. The relationships of these terms to others currently in use are shown in Figure 4.

Directional terms are with respect to the larval shell. "Dorsal" is toward the larval hinge, "ventral" away from the hinge; "anterior" and "posterior" refer to directions parallel to the hinge and toward the sites of the anterior and posterior larval adductors. "Proximal" and "distal" have been used in the customary anatomical sense, meaning toward earlier formed parts and toward later formed parts, respectively. "Apical" and "basal" are used as in histology, meaning away from or toward the basal lamina of an epithelial cell. "Commarginal" refers to sculptural or structural features of the shell that are parallel to the shell margins or to previous traces of the shell margin; the term is being increasingly used in molluscan morphology in place of the geometrically inaccurate term "concentric." "Radial" refers to elements of the shell that radiate from the umbo and are approximately perpendicular to the shell margin. "Length" is the anterior-posterior dimension of the shell parallel to the hinge line; "height" is the dorsal-ventral dimension perpendicular to the hinge. "Convexity" (= depth) is the maximum transverse width perpendicular to the plane of commissure.

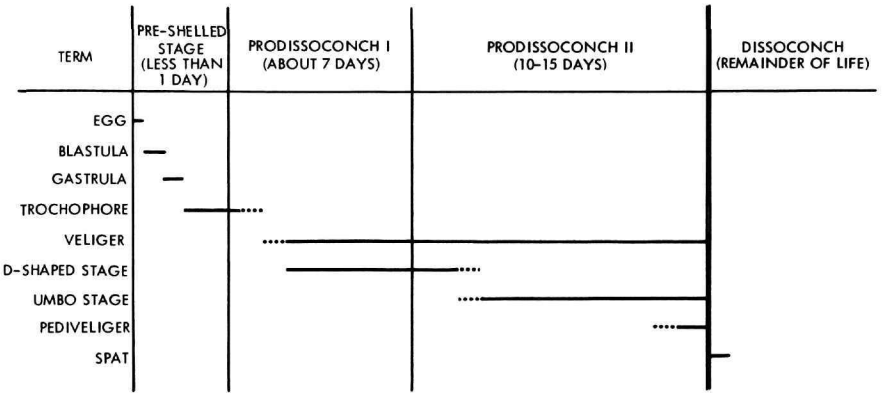

FIGURE 4.—Relationship of stages of development of the prodissoconch to other common terms used to describe the larval shell and body of *Ostrea edulis* (dashed lines indicate uncertainty or transition; durations of stages may be highly variable).

Measurements based on scanning electron micrographs are subject to inaccuracies due to the tremendous foreshortening of depth of field and the difficulty of knowing whether the end-points of a measurement are in the plane of focus. The accuracy of observation may also be affected by the state of preservation of the specimen. Chemicals used in preservation and preparation may cause slight etching or rearrangement of shell microstructural components. In general, however, calcified surfaces described herein have similar appearances regardless of mode of preparation (e.g., air-dried without preservation in alcohol, air-dried from alcohol, critical-point dried, plasma etched). An additional inaccuracy may be introduced by the shrinkage of soft tissues during dehydration and critical-point drying (estimated by Boyde, 1978, to be up to 25% linear). As noted in a previous study (Waller, 1980), this problem is not serious at the levels of interpretation involved, and shrinkage-induced fracturing along cell boundaries may be useful in that it reveals the outlines of cells and the relationship between cell surfaces and adjacent structures.

Finally, cultured specimens may differ from individuals living under natural conditions, and both genetic and environmental factors may affect larval morphology (Culliney, Boyle, and Turner, 1972). In the present study, the larvae of *Ostrea edulis* are from the same parents, and the degree to which morphological features and developmental patterns in different breeding stocks vary has not been investigated.

Observations and Functional Interpretations

BEHAVIOR

Erdmann (1935) described the behavior of veliger larvae of *Ostrea edulis*, but certain observations relevant to functional morphology and the relationship of body and shell are repeated here. Swimming larvae seven days after release from parent were in an early prodissoconch-II stage, with straight dorsal margin unobscured by umbones, valves of about equal convexity and 200 to 210 μm in length, no apparent foot, and no eyespots (Figure 5).

When the valves were closed, the larvae were distinctly negatively buoyant and lay on the bottom of the container with their infolded velar cilia quiescent. Because valves were transparent at this stage, the velum, velar retractors, and rotating stomach contents were visible. Rotation of stomach contents in all specimens observed was clockwise when viewed from the anterior. As pointed out by Millar (1955), anti-clockwise movement is inhibited by the internal profile of the stomach floor.

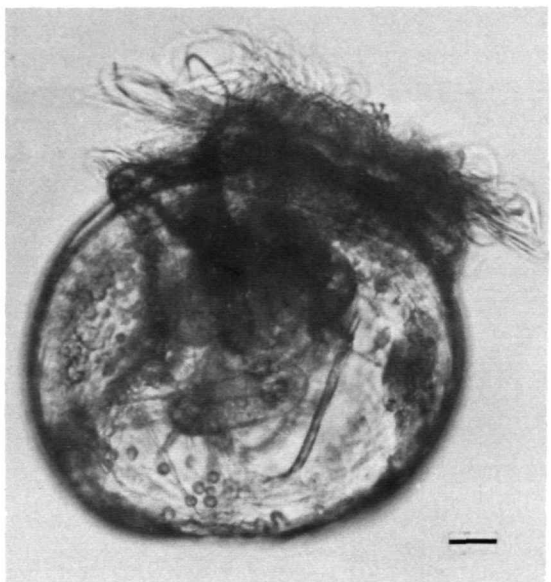

FIGURE 5.—Transmitted-light micrograph of living *Ostrea edulis* in early predissoconch-II stage (about × 350, bar = 20 μm).

When swimming was about to begin, the valves gaped slightly, and velar cilia began to vibrate and protrude from between the valves. Most specimens extruded and unfolded their velum very rapidly. Other specimens, possibly sick or injured, extruded their velum but did not unfold it, which caused them to spiral on the bottom of the container. When the velum unfolded completely and became an oval disk, the velar (anteroventral) side of the larva rotated upward and the larva swam upward from the bottom. The direction of movement was with the anterior end first, with the plane of the velar crown slightly declined toward the anterior. An apt analogy is the flight of a helicopter, which is pulled upward and forward by its rotor. As noted by Knight-Jones (1954a), larvae of *Ostrea edulis* viewed from above spiral in a clockwise direction as they move forward.

When the velum was extended but still folded, so that the shell was still on its side, it could be seen that the gut and stomach were pushed anteroventrally with the velum to a position in the ventral half of the shell. The dorsal half was then a void except for the posterior portion of the gut, which remained relatively fixed in position. In fact the anus showed no movement at all relative to the shell margin during extrusion of the velum. Velar retractors crossing the void converged to their insertions in the velar mass and branched to their insertions near the dorsal margins of the valves.

On the posterior side of the velar crown, the lobe containing the mouth was visible in some living specimens. The ventral side of the mouth was bordered by a tuft of relatively inactive and stiff cilia, and a fine stream of fluid interpreted as mucus could be seen exiting posteriorly from this tuft. Yonge (1926) noted that surplus food which is not ingested leaves by the same route as this stream, "so that a larva swimming through a thick suspension of food leaves behind it a trail of particles embedded in a long string of mucus."

All views of swimming larvae were necessarily ventral because of their consistent orientation with the velar crown upward. By focusing below the velum on a point along the posterodorsal shell margin, however, it was possible to observe defecation by active specimens. Feces were in the form of tiny rods or strings, and their forceful expulsion appeared to be directly from the anus. No rolling of fecal material in the mantle cavity by cilia, which was suggested by Yonge (1926), was observed. The trajectory of expelled feces did not lie in the plane of commissure but rather was in a posterior direction slanting from the left side of the veliger toward the right side.

Larvae 15 days beyond release from parent reached 280 μm in shell length and had valves that were coiled sufficiently so that umbones were beginning to obscure the hinge. The left valve had also surpassed the right in convexity. No significant behavioral modifications were observed, except that when the velum was withdrawn and the valves were shut, the larva was more likely to land on its larger, left valve. These specimens were not yet in the pediveliger stage. Although the foot was present in most specimens, it was not yet sufficiently developed for crawling.

TABLE 1.—Transitional stages in development of observed specimens of *Ostrea edulis* from near time of release from parent (early prodissoconch II) to near time of appearance of pigmented eyespots (late prodissoconch II)

Growth stage	*Approximate shell length (in microns)*	*Foot*	*Gill bridge*
1	190	heel only, no toe	absent
2	200	heel only, no toe	absent
3	250	faint toe primordium	ciliary tufts on posterior mantle edge, unfused
4	250	toe primordium is a prominent bulge	ciliary tufts, unfused
5	265	toe beginning to project from mantle	ciliary tufts, unfused
6	280	toe of moderate length, unciliated and without cement-gland opening	ciliary tufts, unfused
7	290	toe of moderate length, ciliated along midline, with cement-gland duct opening	weak ciliary fusion
8	300	elongate toe, medially ciliated	weak tissue fusion in addition to ciliary fusion
9	310	toe further elongated, ciliated on all surfaces and capable of lateral movement	epithelial bridge

Few of the specimens had pigmented eyespots, but black pigment was present around the base of the velum and on the ventral mantle edges.

MORPHOLOGY

Length of time from spawning is not an accurate predictor of developmental stage. Erdmann (1935) found that rate of development is strongly influenced by temperature, and Culliney, Boyle, and Turner (1972) stressed the variability of cultured populations. It is not surprising, therefore, that the two samples of larvae seven and fifteen days from release contained a variety of growth stages and that these stages actually overlapped between the samples. Because there is little variation in relative rates of development of one organ with respect to another, these stages represented a continuum of development. To facilitate description in the present study, however, this continuum was divided arbitrarily into nine stages, which are outlined in Table 1. Figures 9 through 84 are arranged in sequence according to these stages.

The following observations are presented in the form of a travel with the scanning electron microscope, starting with the velum, plunging dorsally into the mantle cavity, then emerging on the posterior side of the hinge and passing across the exterior of the shell. Next, the microstructure of the shell is viewed by means of fractures, and

then the relationship between mantle and shell and the inner shell surface, particularly the hinge apparatus, are examined after the removal of soft tissues. The final section deals with changes observable in the early dissoconch following metamorphosis.

Velum

During growth of the veliger, the velar crown retains its oval shape but increases in size, ranging (in micrographs of fixed specimens) from a length of about 150 μm and width of 110 μm in Stage 1 (Figure 19) to about 200 by 140 μm by Stage 3 (Figures 33, 34). (Fully extended vela were not observed in later stages of fixed specimens.)

The central region of the velar disk bears a deep apical pit, which in surface view is nearly circular with a diameter of 10 to 15 μm (Figures 21, 30, 37). In all cases the pit slopes toward the posterior so that its anterior slope is shallow and posterior slope steep, as shown in Figure 30 and also by Erdmann (1935, Figures 2 and 3 herein) in longitudinal section. A tuft of from 20 to 100 fine cilia 6 to 8 μm in length stems from the anterior floor of the pit. These cilia barely project above the sides of the pit, which is itself in the center of the broadly concave central region of the velar disk. No ontogenetic trends in the size, depth, or degree of ciliation of the pit could be detected from the surface views, nor was it possible to observe the floor of the pit. According to Hickman and Gruffydd (1971), the very center of the floor of the pit is occupied by the apical organ, which differs in cellular arrangement from the surrounding velar tissue.

In some bivalve groups, particularly the Veneridae, a long apical flagellum or tuft of very long cilia is present throughout larval life and is said to be sensory (Ansell, 1962; see also Boyle and Turner, 1976). It is tempting to postulate a similar function for the short apical cilia of *Ostrea edulis*, because they are unsuited for locomotion and food-gathering and are underlain by the cerebral ganglion (Hickman and Gruffydd, 1971).

The epithelium surrounding the apical pit is devoid of cilia and bears microvilli, some 5 or 6 per micron, over its entire surface (Figures 19, 21, 30, 31, 34, 37). In general, the apical surfaces of the cells comprising the epithelium of the disk are flat, except immediately surrounding the apical pit, where they are commonly strongly tumescent. A mucus-like substance coats the tips of the microvilli, and where microvillous surfaces of adjacent cells come into contact the microvilli appear to adhere to one another (Figure 21).

The periphery of the velar crown is girdled by four bands of cilia (Figures 6, 31, 33), not three as described by Erdmann (1935). Two of the bands are preoral in position, one is adoral, and the fourth is postoral.

The inner preoral band (Figure 31), described here for the first time, is about 8 to 10 μm in width and forms a complete oval separated from the outer preoral band by a nonciliated space

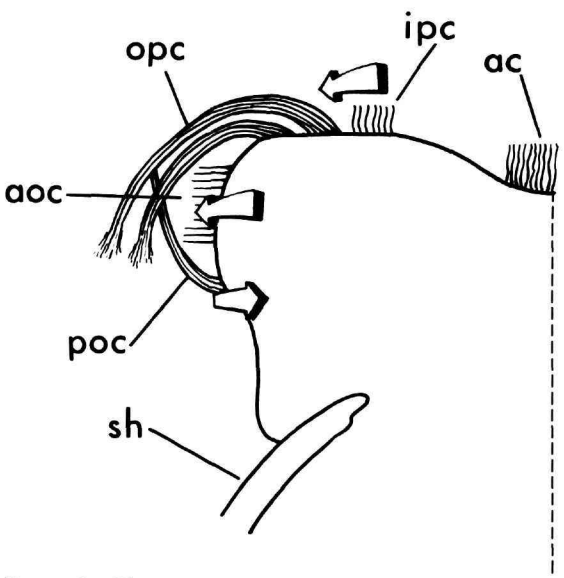

FIGURE 6.—Diagrammatic cross section of right half of velum of *Ostrea edulis* viewed from anterior (outer preoral cilia and postoral cilia are at bottom of effective beat; arrows show directions of metachronal waves; ac = apical cilia, aoc = adoral cilia, ipc = inner preoral cilia, opc = outer preoral (locomotory) cilia, poc = postoral cilia, sh = shell).

that varies in width depending on the degree of extension of the velum. The dense cilia of the band are no longer than about 20 μm and randomly arranged, showing no clumping or fusion nor any indication of coordinated metachronal movement. The band is indistinct and possibly incompletely developed in Stage 1, fairly distinct by Stage 2, and apparently fully developed by Stage 3.

The function of the inner preoral band is unknown. Both the size and arrangement of its cilia resemble those of the adoral band, which receives food particles from the compound cilia of the outer preoral band and transports them to the mouth (Yonge, 1926). Although the inner preoral band is in a position to receive food particles directly from the water that impinges on the surface of the velum during swimming, there is no connection with the mouth because the outer preoral band intervenes. If the inner preoral band is involved in food-gathering, it would have to pass the food particles to the compound cilia of the outer preoral band, which would then transfer the particles to the adoral band, whence they would pass to the mouth. A more likely functional interpretation is that the band is an upcurrent tactile receptor.

The outer preoral ciliary band, which is concerned with locomotion and feeding, dominates the velum because of its width and the size and complexity of its cilia (Figures 9, 19, 28, 31–34). The cilia are clustered in a manner that has led some investigators to refer to them as "compound cilia", consisting of numerous single cilia which arise from a limited area of the same cell, contact one another a short distance above their bases, and remain in contact for nearly their entire length before splaying apart at their tips. Total length of a cluster is in the neighborhood of 50 to 70 μm, and the number of individual cilia in one cluster can only be guessed from the scanning electron micrographs—perhaps 20 to 80. Erdmann (1935) determined from sections that in fact the outer preoral band is a double row of ciliary clusters stemming from a double row of large cells.

Knight-Jones (1954a, b) found a common plan in the locomotory bands of many molluscan veligers, including both bivalves and gastropods. In swimming position the effective beat of the locomotory cilia is downward over the edge of the velum. The beats are coordinated so that metachronal waves are generated along the band approximately at a right angle to the plane of beat of each cilium. These "diaplectic" waves are termed "dexioplectic" if the effective beat of the cilia is to the right of the direction of propagation of the metachronal wave and "laeoplectic" if the beat of the cilia is to the left. Knight-Jones applied the same terms to the orientation of the rows of cilia in each compound cilium, which he found were always aligned parallel ("orthoplectic" rows) or perpendicular ("diaplectic" rows) to the plane of beat. The functional outcome of this arrangement is that diaplectic metachronism permits elongation of cilia which, because of close contact or fusion, can flex more strongly. The spacing pattern of the cilia relative to the direction of propagation of metachronal waves minimizes interference between cilia, and the effective beat of the ciliary clusters generates a thrust which propels the veliger upward with the velar crown leading.

Metachronal waves, which pass continuously around the oval locomotory band, cause the veliger to rotate in a direction opposite to the direction of travel of the waves (Knight-Jones, 1954b). As noted by Knight-Jones, this rotation is countered in two ways. First, the shape of the veliger itself may produce a drag that results in a speed of rotation which is slower than the speed of the metachronal waves. Secondly, the beat of the locomotory cilia may not be perpendicular to the velar margin and to the direction of movement of the metachronal waves, but rather the cilia may beat in a plane oblique to the margin such that rotation is slowed or even completely countered (Figure 7).

Scanning electron microscopy revealed that in *Ostrea edulis* the pattern of compound cilia in the outer preoral band is as predicted by Knight-Jones (1954b). In each compound cilium the

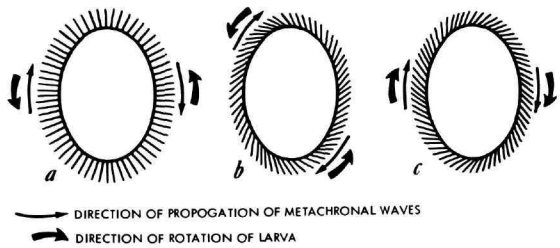

FIGURE 7.—Theoretical relationships of laeoplectic metachronal waves, obliquity of locomotory cilia, and rotation of larva during swimming: *a*, cilia strictly diaplectic, rotation of larva produced by metachronal waves; *b*, obliquity of cilia reinforcing rotation produced by metachronal waves; *c*, obliquity of cilia countering rotation produced by metachronal waves.

constituent cilia are arranged in long orthoplectic and short diaplectic rows (Figure 32). The numbers of cilia involved cannot be determined without sectioning, but it appears that 10 to 15 are aligned in the orthoplectic rows. The numbers of cilia in the diaplectic rows appear to increase from the inner edge of the band toward the outer edge, suggesting that the orthoplectic rows diverge in that direction. Contact between cilia appears to be closest within the diaplectic rows.

Knight-Jones (1954a, b) observed that in *Ostrea edulis* the metachronal waves are laeoplectic. When the velum of swimming larvae is viewed from above, metachronal waves move in a clockwise direction, but the entire specimen rotates in the *same* direction. It can therefore be predicted that the effective stroke of the cilia lies in a plane oblique to the velar margin as shown in Figure 7*c*. This is exactly the pattern shown by the locomotory cilia of each of 12 specimens fixed with velum extended (Figure 19). It appears that the obliquity and intensity of the beat of the locomotory cilia thus more than counter the rotational force imparted by metachronal waves.

The outer preoral band is separated by a narrow nonciliated space, 4 or 5 μm wide, from the adoral band, which leads to and surrounds the mouth (Figures 11, 31, 33, 39). Like the inner preoral band, the adoral band in fixed specimens consists of randomly arranged short cilia approximately 8 μm in length that show no evidence of coordinated movement. Even though the adoral band approaches 20 μm in width, it is completely overlapped by the compound cilia of the outer preoral band when they are at the bottom of their effective beat. Yonge (1926) found that food particles are thrown by the large cilia of the inner preoral band onto the adoral band where they are embedded in mucus and carried back to the mouth. Thus, the direction of the currents generated by adoral cilia would run from anterior to posterior on each side of the velum.

The postoral band of cilia, first described by Erdmann (1935), is actually a single row of compound cilia along the dorsal edge of the adoral band (Figures 6, 28). Each compound cilium is 15 to 20 μm long and consists of a single orthoplectic row of four or five cilia. Some of the scanning electron micrographs (e.g., Figure 28) suggest that the effective beat of these cilia is toward the adoral band and counter to the beat of the outer preoral, locomotory cilia (Figure 6). Strathmann, Jahn, and Fonseca (1972) found that such "opposed band" systems are common ciliary feeding mechanisms in molluscan veligers. By means of high-speed cinefilms, they determined that both the preoral and postoral bands are essential for feeding. The postoral cilia permit increased movement of the preoral cilia relative to the water in the latter half of their effective stroke, and it is at this point that most of the clearance of particles from the water occurs. They also found that some veligers could continue swimming without feeding, presumably by stopping the beat of the postoral cilia.

If the idea of Knight-Jones (1954b) that the direction of diaplectic metachronal waves is constant in an individual regardless of function is correct, then other functions for the postoral band are suggested. Metachronal waves passing along this band would be laeoplectic and would run in a direction opposite to that of the metachronal waves of the outer preoral band because the directions of effective beat are opposite. This opposition of wave patterns may facilitate cleaning of the preoral cilia by the postoral cilia. It is

also possible that cilia of the postoral band may serve to counter and adjust the rate of rotation imparted by the outer preoral band.

At the posterior end of the velar disk, the postoral band passes posterior to the mouth and appears to merge with the postoral tuft. The cilia comprising this tuft (Figures 11, 20, 25, 33, 39) tend to be more densely clustered and appear to be more rigid than those of the postoral band. Also, a portion of the tuft is out of line with the postoral band, being distinctly more posterior in position. These observations suggest that the postoral tuft is a distinct structure, a view also held by Meisenheimer (1900) and Dantan (1916). It does not appear to be merely the posterior edge of the postoral band as described by Erdmann (1935). The relative rigidity of the cilia in the postoral tuft suggest that it may serve a sensory function. It may also facilitate the posteriorward streaming of excess mucus and food, because it is at the point of egress of this stream as observed by Yonge (1926) and in the preceding section on behavior.

The cells that comprise the epithelium of the entire subvelar region are large and devoid of cilia. Like the epithelium of the apical disk, however, the surface is microvillous, the tips of the microvilli appear mucus-covered, and the microvilli of adjacent cell surfaces adhere to one another where these surfaces are brought into contact in folds or between tumescent cells (Figure 27). No sensory structures nor any glandular ducts were detected. The anterior (Figures 18, 26, 29) and lateral (Figures 43, 44, 47, 48) subvelar surfaces merge with the mantle, and the posterior surface of the stalk (Figures 11, 33, 39) passes dorsally into the mantle cavity.

Foot

The first structure to be encountered in following the body wall dorsally from the mouth is the primordium of the foot. Basically, the mode of development, with the heel first and then the toe, is as described by Erdmann (1935), but scanning electron microscopy allows the pattern of development of pedal cilia and some of the secretory ducts to be seen. (See Table 1 for the nine stages of development.)

In Stage 1, the heel of the foot is already present as a small protuberance from the body wall midway along a medial line passing from the mouth to the hinge (Figures 11, 14). It is transversely elongated and dorsoventrally compressed, about 26 by 9 μm, and is densely ciliated on its medial, ventral surface. The nonciliated dorsal surface of the heel rises sharply from the body wall. The ciliated ventral surface is more gently sloping and at its base bears a pair of large ciliated duct openings (Figure 15). The total transverse diameter of this double opening is 13 μm, each duct opening being about 7 μm. These are the openings of the byssal gland complex, which Erdmann (1935) showed to be the first of many organs to form on the ventral side of the larva. Although Erdmann referred only to a single gland, Cranfield (1973a) demonstrated that by the pediveliger stage several types of glands that share a common ciliated duct in this location are present. The double opening may represent an early stage in the development of the complex before a common duct is formed.

By Stage 3 the primordium of the toe has appeared on the ventral side of the heel, and both structures push out together from the body wall. The process is due to proliferation of epithelial cells as shown by Erdmann (1935), not to infolding of the body wall on each side as supposed by Meisenheimer (1900). Like the heel, the toe is a transversely elongated ridge, but it is larger (50 by 25 μm), has more gently sloping dorsal and ventral surfaces, and lacks cilia (Figures 40, 42).

In Stage 4, the heel and toe are more strongly elevated from the body wall, and the byssal-duct opening is clearly single, measuring 7 μm in transverse diameter. There are still no cilia on the toe primordium. In Stages 5 and 6, the ventral slope of the toe steepens as it begins to bulge ventrally, but there are as yet no cilia (Figure 52). By Stage 7, the toe of the foot has become a ventrally projecting, somewhat flattened cylindrical structure bearing cilia along its midline (Figure 58).

This band of cilia is narrow adjacent to the heel, broadens toward the tip of the toe, and remains broad as it rounds the tip onto the newly formed anterior surface that faces the inner wall of the mantle cavity. By this stage a second duct opening, about 1 μm in diameter, has appeared somewhat to the left of the midline of the foot (Figure 58). This is the opening for gland types C1 and C2 of Cranfield (1973a), which will be involved in secretion of cement after the larva settles (Cranfield, 1975).

By Stage 8 the toe has lengthened into a strongly ventrally projecting tapered cylinder with a bluntly rounded tip (Figure 68). The entire foot measures about 75 μm in length and about 53 μm in width near the heel. Cilia are still restricted to a medial band on the heel and proximal portion of the toe, but the band has become wider near the tip of the toe, covering nearly the entire width. The opening of gland-types C1 and C2, which has widened to a diameter of about 4 μm, is located at about one fourth the distance from the byssal-duct opening to the tip of the toe. The axis of the toe is still in the median plane, and there is no evidence of complex foot torsion or extension in the micrographs.

By Stage 9, the foot has about the same diameter as in Stage 8 but has lengthened to about 90 μm[1] and shows evidence in the micrographs of being able to pivot on its base (Figure 78). Dense cilia now cover nearly the entire sole. Although the size of the foot suggests that it can now probably be extended outward between the valves, observations of living specimens from the same sample, 15 days from release, revealed none which had entered the pediveliger stage with a fully functional foot. All of the cell surfaces of the foot bear microvilli like those of the velum.

Structures in Gill Cavities

Lateral to the foot, the inner wall of the mantle cavity is deeply recessed to produce a pair of ectodermal pockets. These pockets were called "kiemenhohlen" (gill cavities) by Erdmann (1935), because they contain the anterior ends of the primordial gills. In addition to the gill primordia, which are described below, three paired structures develop in each gill cavity: (1) the openings of static ducts, (2) photoreceptors (called eyespots after they become pigmented in more advanced larvae), and (3) structures which are possibly the openings of protonephridial ducts (Figures 8, 43–50). The relative positions of these structures are shown diagramatically in Figure 8, which is drawn from a specimen in developmental Stage 3, where the structures are best exposed. (See Table 1 for an outline of developmental stages.) The structures as they appear in this specimen will be described first, followed by descriptions of other stages of development.

Static-Duct Openings.—The interpretation of the first pair of structures as openings of static

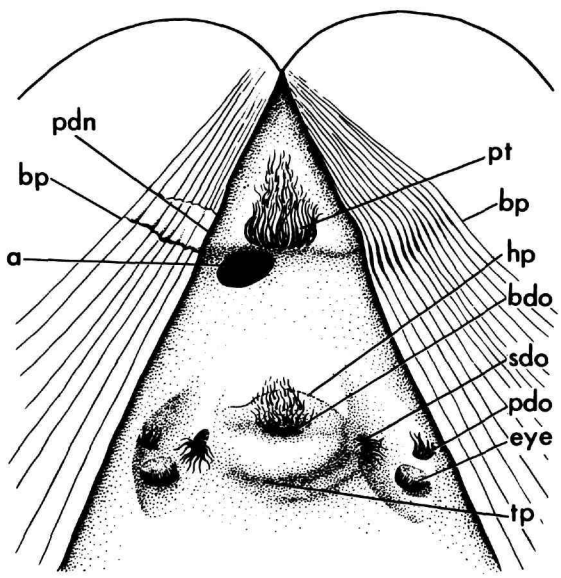

Figure 8.—Diagrammatic posterior view of body wall in mantle cavity of *Ostrea edulis* veliger, Stage 3 (a = anus, bp = boundary between prodissoconch I and II, bdo = byssal-gland duct opening, eye = microvillous eye primordium, hp = heel primordium, pdn = posterodorsal notch, pdo = protonephridial duct opening, pt = postanal tuft, sdo = static duct opening, tp = toe primordium).

[1] Because the velum of the specimen shown in Figure 78 is partially retracted, it is likely that the foot is also.

ducts, which connect statocysts to the exterior, is based on correspondence in size and position to structures so described by Erdmann (1935) in sectional views. These openings are the closest of the three structures to the midline, each opening being a circle 7 to 9 μm in diameter lying on the medial side of the gill cavity at the lateral edge of the toe primordium. Short cilia 2 to 4 μm in length originating in the walls of the duct occupy its lumen and extend across its opening, meeting at the center. The cilia must transport fluid along the axis of the duct. The majority of micrographs show that the concave side of curved cilia is toward the interior of the duct; straight cilia that are probably fixed in their effective-beat position also show slight flexure at their base toward the interior of the duct (Figures 16, 45, 46, 49, 50, 54, 57). In view of the different forms of cilia in effective and recovery beats outlined by Gray (1928, 1930; see also the reviews by Sleigh, 1962, 1974), these observations suggest that fluid is transported through the duct from the outside inward toward the statocysts.

In the Stage-3 specimen, a second incomplete ring of long vibratile organelles, interpreted as cilia rather than flagella (see following interpretation), borders the ventral edge of the duct opening. These cilia extend about 100° of arc around the periphery of the left duct and only about 45° around the periphery of the right. They reach about 14 μm in length and are therefore much longer than the cilia in the duct opening. Rather than extending over the duct opening, the long cilia extend ventrally along the epithelium of the mantle-cavity wall.

The question arises whether these long vibratile organelles are cilia or flagella. Although the internal 9 + 2 structure is known to be the same in both types of organelles, the direction of movement of a cilium is perpendicular to its long axis and parallel to the surface of the cell that bears it, whereas a flagellum generally moves in a series of waves that pass from its base upward along its long axis, thus moving fluids parallel to its length (Sleigh, 1962). In the Stage-3 specimen, the position of the long organelles is not diagnostic but suggests flagellate movement parallel to the cell surface, thereby pulling water from over the duct opening and transporting it ventrally toward the posterior edge of the mouth lobe. Specimens in developmental Stage 8, however, show these organelles in a flexed position, bent over the static-duct opening (Figure 74). Assuming that this position is not an artifact of preparation, then it appears that the long organelles are cilia. Rather than pulling water over the duct openings, they would then push water over and possibly into the openings.

Ontogenetic variation in the static-duct openings entails an apparent increase in diameter, ranging from less than 6 μm in Stage 1 (Figure 16) to about 11 μm in Stage 7 (Figures 56, 57). The presence and absence of the long marginal cilia suggest individual variation or possibly loss of cilia during fixation. In Stage 3 described above, long cilia are present on both duct openings (Figures 45, 46, 49, 50); in Stages 1 (Figure 16) and 7 (Figures 56, 57) they are lacking on both openings; in Stage 5 (Figures 53, 54) they are present on the left opening but not on the right; and in Stage 8 (Figures 73, 74) they are present on the right opening but not on the left. In Stages 4 and 9 long cilia are present on the right side, but the left side was not observable.

In the present study, static-duct openings can be demonstrated to be present from the time of release from parent to a stage just before the pediveliger in which there is still no evidence of closing. The openings thus appear to persist longer than observed by Erdmann (1935), who thought that they constrict early in the veliger stage and finally close as the statocysts migrate inward from the epithelium. Only closed statocysts are present in mature oysters (Carazzi, 1902).

A common assumption is that the static ducts of invertebrates are excretory (e.g., Barber, 1968). However, the configuration of the cilia bordering the openings and lining the walls of the static ducts of *Ostrea edulis* suggest that particles may pass inward from the exterior toward the statocysts. This may also be the case in some other

species. Cragg and Nott (1977) found inwardly pointing cilia in the static ducts of pediveliger larvae of *Pecten maximus* and suggested that statoconia of variable appearance may be introduced into the statocyst from the exterior *via* the static duct (see also Buddenbrock, 1915, and Plate, 1924).

PHOTORECEPTORS.—The second structure in the gill cavity is interpreted as an early developmental stage of the larval eye, because its position (on the medial wall of the gill cavity anterior to the static-duct opening and ventral and medial to the anterior extremity of the primordial gill axis) exactly corresponds to the position of the pigmented eyespot in the later pediveliger stage illustrated by Erdmann (1935). The flower-like structure is raised, hemispherical, approximately 6 μm in diameter, and is covered with hundreds of hair-like organelles. These organelles are interpeted as microvilli rather than cilia because they are only about 0.1 μm in diameter and no more than 1 μm long. The stem of the structure is obscured but is clearly narrower than the hemispherical head.

The primordial eye seems to show a slight ontogenetic increase in size, ranging from less than 6 μm in diameter in Stage 1 (Figure 16) to nearly 9 μm in Stage 7 (Figure 59), and also becomes more widely separated from the static-duct opening. By Stage 8, however, the structure appears submerged in the epithelium so that its apparent diameter at the epithelial surface is smaller (about 4 μm), and its microvilli are no longer as strongly projecting.

These changes are in accord with Erdmann's (1935) finding that the eye primordium in a seven-day old veliger consists of a thickening of the epithelium of the gill-cavity wall which produces a bulge on the epithelial surface. The submergence noted herein in Stage 8 seems to signify a trend toward the conditions found by Cole (1938) in the later, pediveliger stage. By that time the eye becomes an almost spherical cup of pigmented epithelium filled with a gelatinous matrix and having its aperture closed by a lens-like body. The early microvillous nature of the eye primordium suggests that the larval eyes are of rhabdomeric rather than ciliary origin (Eakin, 1965). The rhabdomeric type is prevalent in the Mollusca.

PROTONEPHRIDIAL-DUCT OPENINGS.—The third structure, which is possibly the opening of a protonephridial duct, is exceedingly difficult to resolve in the specimens observed, because it lies deep within the gill cavity and is always partially obscured by the primordial eye. Basically, the structure appears to be a small tuft of eight to ten cilia, which are 3 to 4 μm in length, lying on the dorsolateral side of and nearly in contact with the eye (Stage 3, Figures 45, 49). The cilia arise from a small depression about 2 μm in diameter, but it is not possible to determine whether it is the opening to a pit or duct. The bases of the cilia are perpendicular to the subjacent epithelial surface, and it appears that their effective beat is dorsally directed. These structures could only be detected in Stages 1 and 3. They are probably absent in Stage 5, definitely absent in Stage 7, and probably absent in Stage 8, suggesting that their duration may be variable or that they may disappear during fixation.

The interpretation of these paired structures as the openings of protonephridial ducts is speculative not only because of the obscure morphology of the structures themselves, but also because Erdmann (1935) was unable to find the precise position of these ducts even after repeated sectioning. Examination of Erdmann's figured sections reveals that the protonephridia develop early in the veliger stage and by the pediveliger stage open to the exterior through a tiny pore in the vicinity of the eye.

Gills

By means of scanning electron microscopy, the three-dimensional form of the developing gill primordia of the oyster can be described in detail. The most remarkable aspect of this development is the early formation of the bridge of tissue that in mature oysters connects the posterior ends of the left and right gills. This bridge arises by cross-contact and possibly cross-fusion of cilia in Stage

7 followed by cross-fusion of epithelium in Stage 8.

In Stage 1, the only element of the gill primordia which can be observed is a cluster of cilia at the mid-posterior edge of each mantle lobe (Figures 9, 10). It will be seen later that these cilia are the precursors of the gill bridge. They stem from the first three rows of cells along the mantle edge, whereas other marginal cilia are generally restricted to the first row. Prepared specimens in this stage and also in Stage 2 do not permit observation of gill primordia on the epithelium deeper in the mantle cavity.

In Stage 3 the right gill primordium is a low, broad epithelial ridge about 20 μm wide tending directly anteriorly along the dorsal side of the gill cavity from the mid-posterior edge of the mantle (Figures 47, 48). The ridge is low and barely discernible at the mantle edge but increases in height, possibly to about 7 μm, as it approaches the body wall. Cell boundaries are clearly discernible. The cells are variable in size, the largest approximately 3 μm in diameter; all have curved, microvillous apical surfaces. Crossing the anterior third of the ridge at a right angle are two minute transverse ridges, the primordia of the gill filaments. Each of these ridges is only one cell wide and is bordered anteriorly and posteriorly by a depression of about the same width as the ridge. The primordium of the left gill in Stage 3 presents basically the same form (Figures 43, 44), but it is not possible to determine whether it has the same number of transverse ridges. A few widely scattered cilia, no more than 3 μm in length, are present on each primordium. As in Stage 1, a cluster of cilia is present on the mid-posterior margin of each mantle lobe.

Little change occurs in the basic arrangement of the gill primordia until Stage 7. In specimens at this stage of development, only the posterior extremities of the gill ridges could be observed, but these are instructive. A few cilia stemming from the posterior extremity of each gill ridge contact one another across the midline to produce an exceedingly fine ciliary bridge (Figures 63–65). So tenuous is this connection that the electron beam of the scanning electron microscope caused some of the ciliary connections to break, a process that could be observed on the cathode-ray viewing screen. On each side the cilia arise from a mound of epithelium at the end of the gill ridge (Figure 65). The mantle edge itself has by this time extended distally from the posterior extremity of the gill ridge and still bears a cluster of long cilia on its mid-posterior margin (see Figure 71, Stage 8). Apparently the clusters of cilia described as occurring on the mantle margin in Stages 1 through 3 have lost their marginal position as new cells are added along the mantle edge. New cilia continue to form at the same location on the margin, but the original cilia have now cross-fused, and cells proliferating around the base of the ciliary bridge are beginning to push upward along the bridge.

By Stage 8, elongate epithelial cells are present across the entire bridge on its anterior side, but the bridge remains largely ciliary on its posterior side (Figures 69, 70). The diameter of the bridge at its narrowest point on the midline is scarcely more than 2 μm, but it is surely stretched and attenuated when the valves are gaping. Cells present on the bridge are elongated along the bridge axis and appear to be growing over the fused cilia while new cilia form from the new cells. The bridge widens gradually toward each side into the expanded posterior extremities of the gill ridges (Figures 71, 72).

Also by Stage 8, the gill ridges have undergone considerable change and are beginning to show unequal development, the right ridge being retarded with respect to the left. Height of the ridge has increased to about 20 μm, and in a section transverse to the ridge axis, height now exceeds width. The right primordial gill still has two transverse ridges on its anterior half. Each transverse ridge is a cluster of apically convex cells of various sizes. The anterior end of the main gill ridge has become separated from the mantle epithelium and is now the anterior end of the gill axis (Figures 71, 72). The anterior insertion point of this axis is slightly dorsal and lateral to the static-duct opening and slightly posterior and

dorsal to the primordial eye. Scattered cilia are present along the crest of the gill. The left gill ridge at this stage is about the same size as the right, but possesses an additional transverse ridge and depression.

In Stage 9, the gill bridge has increased its minimum diameter on the midline to nearly 4 μm, and the epithelial portion of the bridge looks stronger relative to the fused ciliary portion, which is still present (Figures 81, 82). The gill primordia have basically the same configuration as in Stage 8, but the transverse ridges that comprise the primordial filaments are even more prominent, and the anterior gill axis has increased in length. The number of primordial filaments is the same as in Stage 8, two on the right gill ridge and three on the left. Close examination of the depression between the two primordial filaments on the right gill ridge (Figures 83, 84) reveals that it contains a mucus-gland opening (identified by a comparison with such structures in critical-point dried gill filaments of mature pectinids shown by Owen and McCrae, 1976). It is likely that these gland openings are already present in the interfilamental depressions in Stage 8.

It is doubtful that the gills are functional in any of these early stages, except as the increased surface area which they contribute aids in respiration. The basic incurrent-excurrent pattern of the adult, however, is probably already present. As suggested by the direction of beat inferred from micrographs of the marginal cilia of the static-duct opening and the cilia adjacent to the presumed protonephridial duct openings, water flows dorsally past the primordial gills into the presumptive suprabranchial region.

Anal Region

Dorsal to the foot and gills, the mantle cavity becomes shallower and its walls converge on the shell margin at the posterior end of the hinge. In this anal region, three structures are present throughout the veliger stage: the anus, a postanal ciliary tuft, and a distinct concavity, referred to here as the posterodorsal notch, in the margin of the left valve.

The anus lies to the left of the midline. In specimens in Stages 1 and 3, where it is in a constricted stage, it is a tiny oval structure approximately 3.5 by 6 μm with the short axis transverse (Figures 17, 33, 41) and with short cilia projecting from its lumen. In Stage 8, one specimen shows the anus in a dilated condition (Figures 67, 69). In this state the anus is nearly circular (26 by 29 μm) and is filled with fecal material that obscures the cilia of the lumen. Specimens fixed in the act of defecating (Figure 75) show that waste material is compacted into feces within the rectum and is not rolled into feces in the mantle cavity as suggested by Yonge (1926). Compaction is probably by way of ciliary action wihin the rectum at times when abundant food is passing through. Peristalsis, said to be present by Yonge (1926), is unlikely, because no muscles are known to occur in the walls of the larval intestine or rectum (Erdmann, 1935).

The postanal tuft is raised and separated from the anus by a low step in the body wall (Figures 12, 33, 40, 41, 43, 47, 69). Cilia in the tuft approach 15 μm in length and are densely clustered ventrally, just dorsal to the anus; dorsally, the cilia are confined to a narrow medial band. The dense clustering of the cilia prevents determining their direction of beat from an analysis of their curvature, except for a few cilia at the ventral edge of the tuft. These appear to have a dorsally directed effective beat. As mentioned in the earlier description of behavior, living larvae propel fecal material outward from the region of the postanal tuft along a trajectory which is to the left of the plane of commissure of the valves. Presumably, some of the postanal cilia beat in that direction.

The margin of the left valve is strongly deflected adjacent to the dense postanal tuft and forms a distinct notch in the lip of the shell margin and a slight outward deflection of the outer surface of the valve. In contrast, the margin of the right valve is deflected only very slightly or not at all at this location (Figures 89–92, 94, 95,

137). In specimens that are fixed with the valves nearly or completely closed (Figures 22, 51, 76), it can be seen that the cilia of the postanal tuft project between the valves adjacent to the notch. The short cilia that lie in a medial band dorsal to the tuft align with the plane of commissure of the valves and barely project. When the valves are completely closed, an opening at the site of the shell notch may or may not be present. In all cases where an opening is present, it is a thin slit not exceeding 7 μm in maximum dimension. Removal of the periostracum by bleaching or plasma etching enlarges the opening (Figures 88, 89), indicating that the periostracum of the opposing valves at the site of the notch contributes to its closing.

Growth and extension of the shell margins preserve the locus of positions of the notch to produce a sharply delimited raised growth track on the exterior of the left valve and in some cases a very low, barely discernible ridge on the right valve (Figures 88, 90, 91). The beginning of the growth track indicates that the notch first forms at the prodissoconch-I/II boundary; the end of the track demonstrates that the notch disappears at metamorphosis, at the prodissoconch-dissoconch boundary (Figure 120). At its earliest point on the left-valve surface, the growth track is commonly narrower or unevenly constricted compared to its appearance slightly later (Figures 22, 91, 95). The width of the growth track increases very gradually from about 10 μm to about 16 μm, suggesting that the size of the postanal ciliary tuft also increases during development. This gradual increase in width of the track, however, is not completely uniform. At each growth line the growth track constricts, and between each growth line it widens.

Although waste material is ejected from the mantle cavity by the postanal cilia adjacent to the notch, the notch itself provides too small an opening for this ejection to occur when the valves are closed. Many specimens fixed with the valves closed have trapped waste material between the valves in the notch, and feces are far too large to pass by the notch even when the valves are agape (Figure 75). Furthermore, the notch is a far more common site for injury to the margin of the shell than elsewhere (Figures 12, 51, 76), suggesting that foreign particles lodged between closed valves at the notch produce the injury.

An explanation of the function of the notch, how it forms, why it is restricted largely to the left valve, and why it is present only during the prodissoconch-II stage requires an examination of the nature of the mantle edge, the configuration of the shell margin, and the mode of formation of the prodissoconch-I/II boundary. This explanation will therefore be deferred until the final discussion.

Mantle Edge

The epithelium forming the stalk of the velum and the body wall merges without change in its surface appearance into the mantle epithelium lining the inner surfaces of the valves. Microvilli are present everywhere on the surface; cilia are absent except on the mantle margin or on structures, such as the gill primordia, which form from the mantle.

The configuration of the mantle edge of veliger Stages 1 through 9 is similar to that examined in detail by Cranfield (1974) in the pediveliger stage. Two marginal folds are present, separated by the periostracal groove (Figures 36, 61, 71, 72). Widely scattered cilia on the mantle margin stem from what appears to be the first row of cells of the inner fold proximal to the periostracal groove (Figures 10, 35, 36, 38). These cells also bear elongate microvilli which appear to be swollen by and covered with secretion. The width of the microvillous band is about 3 μm. At the distal edge of this band, which forms the sharp leading edge of the inner mantle fold, microvilli as long as 1.5 μm lie against the surface of the periostracum and appear to be partially embedded in it (Figure 36). On the basis of Cranfield's (1974) description, the marginal cilia appear to represent the cilia that he shows as occurring at the apex of the inner fold. A prominent band of cilia that he described as running along the margin of the

inner fold and stemming from the third row of cells inward from the margin does not appear to be present in the stages examined in the present study. A third row of cilia, which Cranfield showed stemming from the outer surface of the inner fold and extending toward the newly generated periostracum, also could not be detected or perhaps was not distinguished from the distal band.

Radial muscles inserted in the shell and extending into the inner mantle fold were also shown to be present in the veliger by Cranfield (1974). I infer that they are already present at least by Stage 5, because at this stage the mantle edge behaved differently than in earlier stages during preparation of the specimens. In Stages 1 through 4, the mantle margin remained attached to the periostracum (Figures 10, 35). Where fracturing of tissue due to dessication occurred, it was proximal to the periostracal groove and followed no particular pattern. In Stages 5 through 9, however, the entire mantle margin pulled away from the periostracum, severing the periostracum near where it emerged from the periostracal groove so that a narrow band of periostracum remained in the groove (Figures 60, 61, 72, 79). The mantle edge then lifted up from the inner surface of the shell along a line of separation that is probably the line of attachment of the radial muscles (the pallial line). In Figures 72 and 79, radially aligned stringers of tissue that are probably muscles can be seen meeting the shell along this line.

This separation of the mantle edge from the periostracum and the inner shell surface permitted inspection of parts of the outer fold of the mantle which otherwise would have been shielded from view by the periostracum and shell. It can be seen in Figures 60–62 that the distal edge of the outer fold attenuates to a thin edge and consists of what appear to be long, densely matted microvilli or cell processes. The edge is consistently scalloped around the entire periphery of the shell, the width of the projections being 12 to 15 μm (Figures 60, 61). It is likely that the reentrants in this scalloped margin are adjacent to cell boundaries, which are not visible in the micrographs. The salients would then represent maximal growth of microvilli from centers of cells. The outer surface of the outer fold, from its distal edge to the inferred pallial line, is entirely covered by very long microvilli, many of which remain embedded in the shell and appear to be intimately connected with its secretion (Figures 72, 79, 83). The outer surface of the mantle proximal to the pallial line was not examined.

Shell

SHAPE AND SCULPTURE.—The few fully formed larval shells (prodissoconch II) of *Ostrea edulis* (Figure 118–120) observed in the present study are variable in size, ranging from 265 to 360 μm in length and 250 to 300 μm in height (measurements from the prodissoconchs of three specimens that had cemented to the bottom of a laboratory beaker). The valves are unequal in convexity, the left being more convex than the right and the convexity of closed valves being on the order of 250 μm. In contrast, prodissoconch I is less variable in size, typically measuring 170 μm long and 160 μm high with the valves equal in convexity (measurements from 17 veligers). Although none of the specimens examined permit accurate measurement of convexity, it appears that this dimension of prodissoconch I is on the order of 90 to 100 μm.

The two prodissoconch stages can generally be distinguished on the basis of three features: (1) prodissoconch I is separated from prodissoconch II by the first prominent commarginal growth line; (2) the surface of prodissoconch I is nearly smooth or very faintly radially and commarginally striate, whereas that of prodissoconch II is distinctly commarginally striate but lacks radial striae; and (3) the posterodorsal notch and its growth track begin at the prodissoconch-I/II boundary. A fourth, less consistent criterion is a change in the angle of spiral coiling at the boundary between the two stages, generally from a higher angle to a lower angle. In lateral view, prodissoconch I is D-shaped, but so also are the

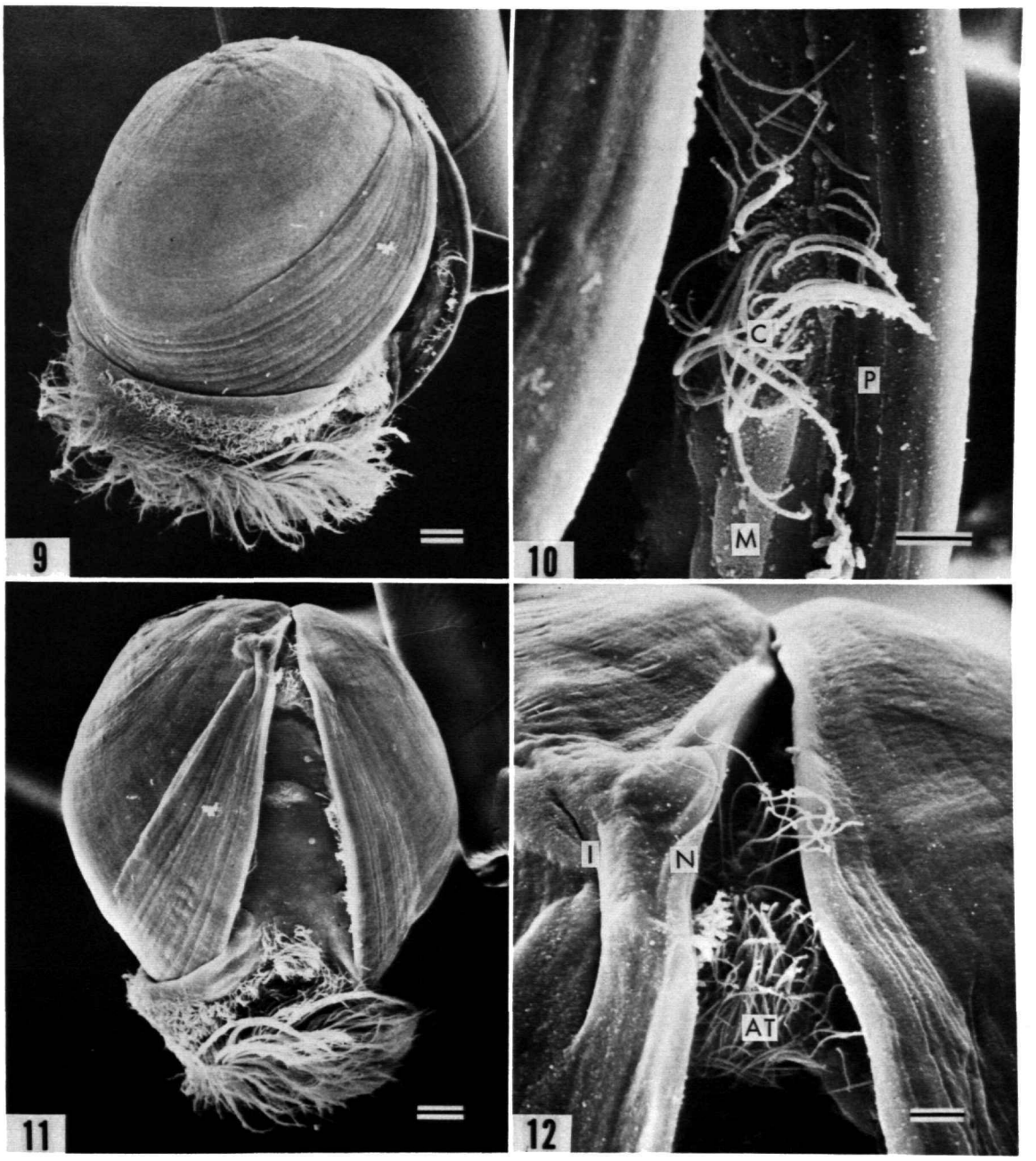

FIGURES 9–12.—*Ostrea edulis*, specimen 372A, early prodissoconch II, stage 1: 9, left posterior side (× 350, bar = 20 μm); 10, detail of Figure 9, mantle edge (M), ciliary tuft on mantle (C), and periostracum (P) (× 2500, bar = 5 μm); 11, posterior view (× 370, bar = 20 μm); 12, detail of Figure 11, posterodorsal shell notch (N) with injury (I) and postanal ciliary tuft (AT) (× 1750, bar = 5 μm).

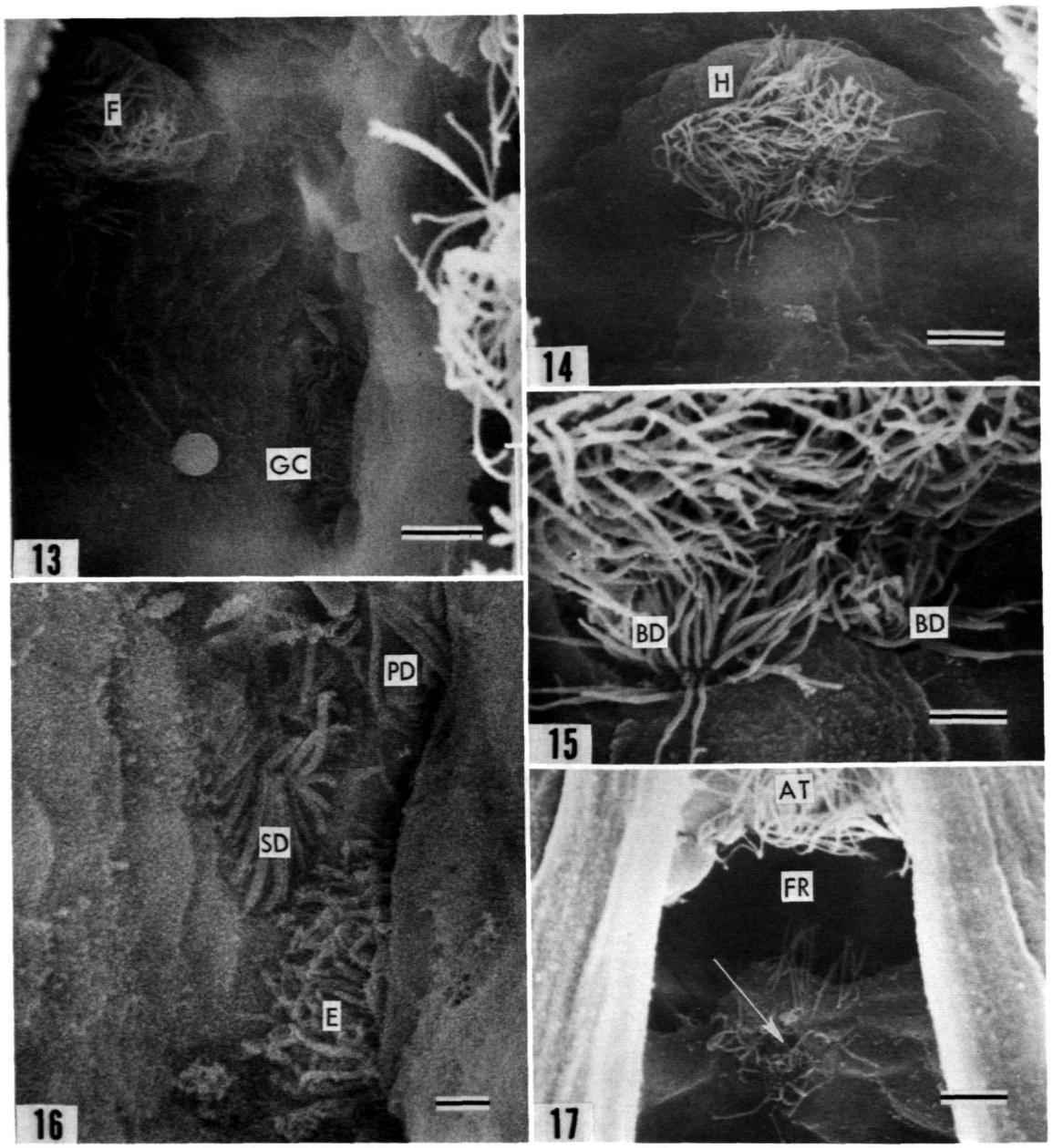

FIGURES 13–17.—*Ostrea edulis*, specimen 372A, early prodissoconch II, stage 1: 13, gill cavity (GC) on right side of foot primordium (F) (× 2500, bar = 5 μm); 14, heel primordium (H) (× 2400, bar = 5 μm); 15, detail of Figure 14, double byssus-duct opening (BD) (× 5800, bar = 2 μm); 16, gill cavity on left side of foot primordium with oblique view of static-duct opening (SD), side views of cilia of possible prontonephridial-duct opening (PD), and eye primordium (E) (× 8200, bar = 1 μm); 17, anus (arrow) and postanal ciliary tuft (AT) separated by fracture (FR) in the body wall (× 2000, bar = 5 μm).

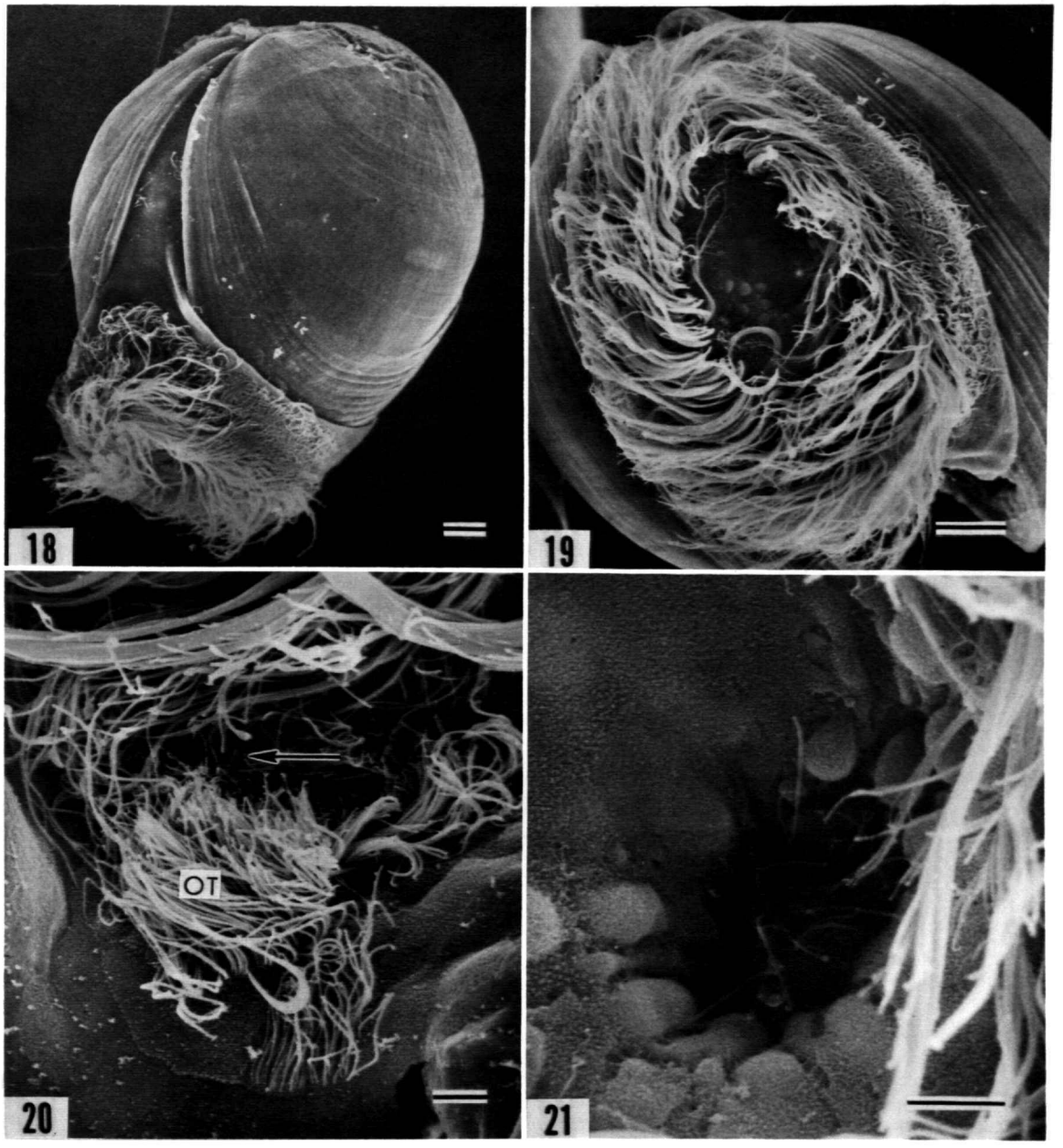

FIGURES 18–21.—*Ostrea edulis*, specimen 372A, early prodissoconch II, stage 1: 18, left anterior side (× 340, bar = 20 μm); 19, apical view of slightly retracted velum (× 520, bar = 20 μm); 20, detail of Figure 11, mouth (arrow) and postoral ciliary tuft (OT) (× 1600, bar = 5 μm); 21, detail of Figure 19, apical pit and surrounding tumescent epithelial cells (× 3000, bar = 5 μm).

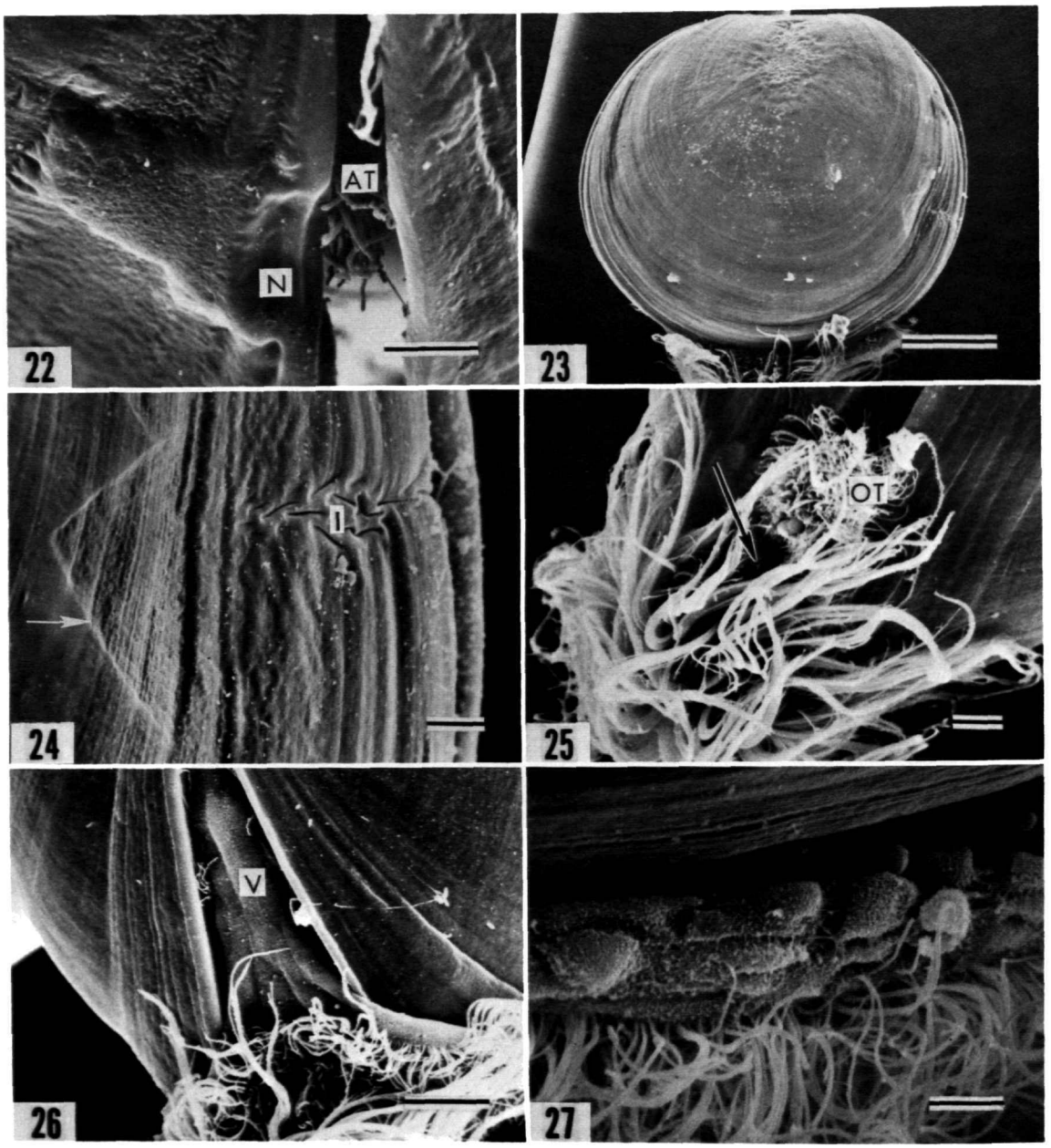

FIGURES 22–27.—*Ostrea edulis*, early prodissoconch II, between stages 1 and 2: 22, specimen 369B, posterodorsal notch (N) and postanal ciliary tuft (AT) (× 3000, bar = 5 μm); 23, specimen 369C, left side (× 300, bar = 50 μm); 24, detail of Figure 23, disturbed periostracum on prodissoconch I (arrow) and repaired injury (I) on prodissoconch II (× 1800, bar = 5 μm); 25, specimen 369C, folded velum, mouth (arrow), and postoral ciliary tuft (OT), viewed from posterior side (× 800, bar = 10 μm); 26, specimen 373D, anterior side of velar stalk (V) (× 670, bar = 20 μm); 27, specimen 372B, tumescent cells on side of folded velum (× 2300, bar = 5 μm).

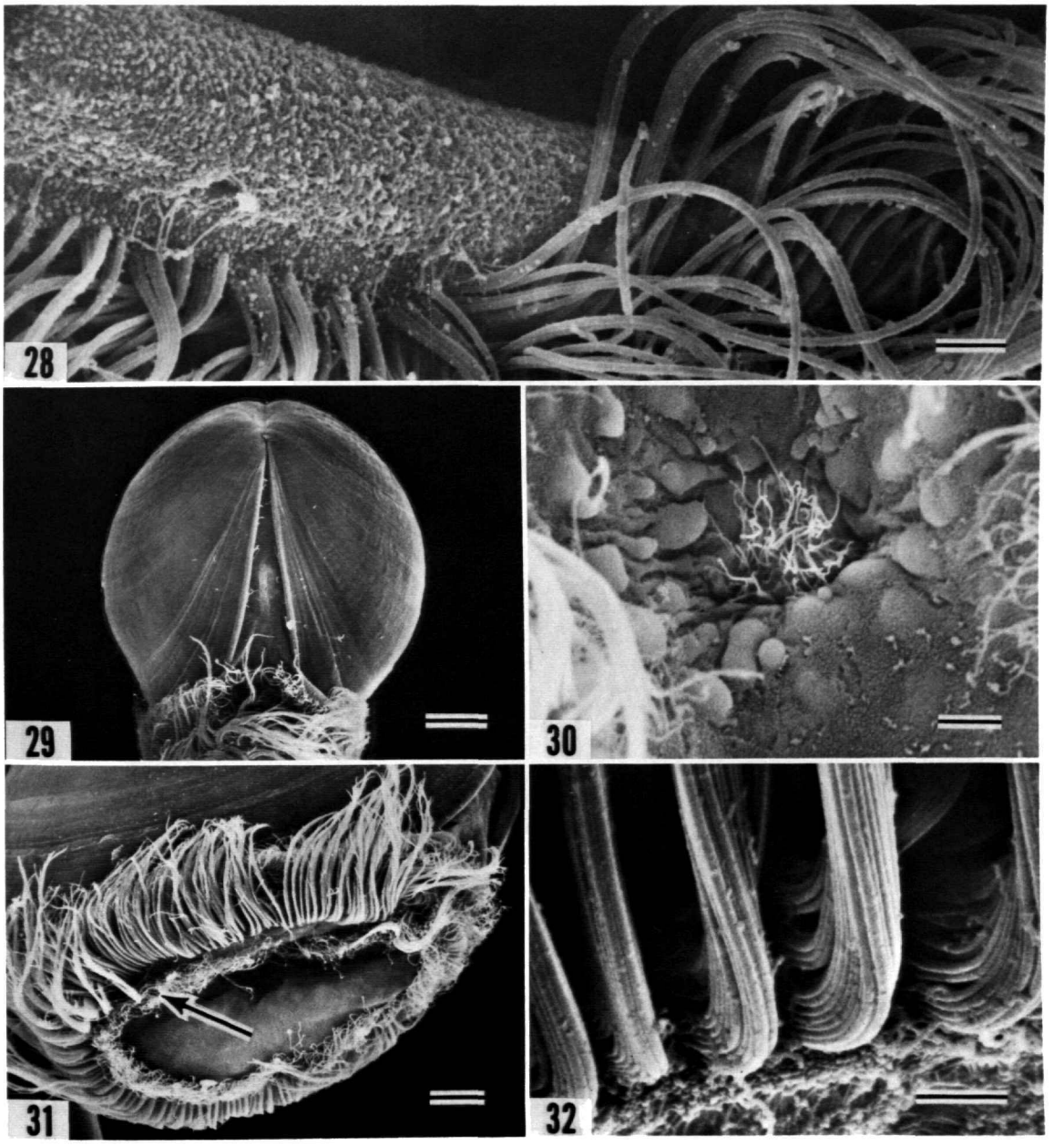

FIGURES 28–32.—*Ostrea edulis:* 28, specimen 373D, early prodissoconch II, between stages 1 and 2, detail of Figure 26, compound cilia of postoral band (× 5500, bar = 2 μm); 29 specimen 373D, anterior (× 470, bar = 20 μm); 30, specimen 373D, apical pit of velum (× 2000, bar = 5 μm); 31, specimen 372C, early prodissoconch II, between stages 2 and 3, slightly folded velum viewed obliquely from left side, inner preoral band (arrow) (× 410, bar = 20 μm); 32, detail of Figure 31, compound cilia of outer preoral band (× 7000, bar = 2 μm).

FIGURE 33.—*Ostrea edulis*, specimen 373B, mid-prodissoconch II, stage 3, posterior view (× 620, bar = 20 μm).

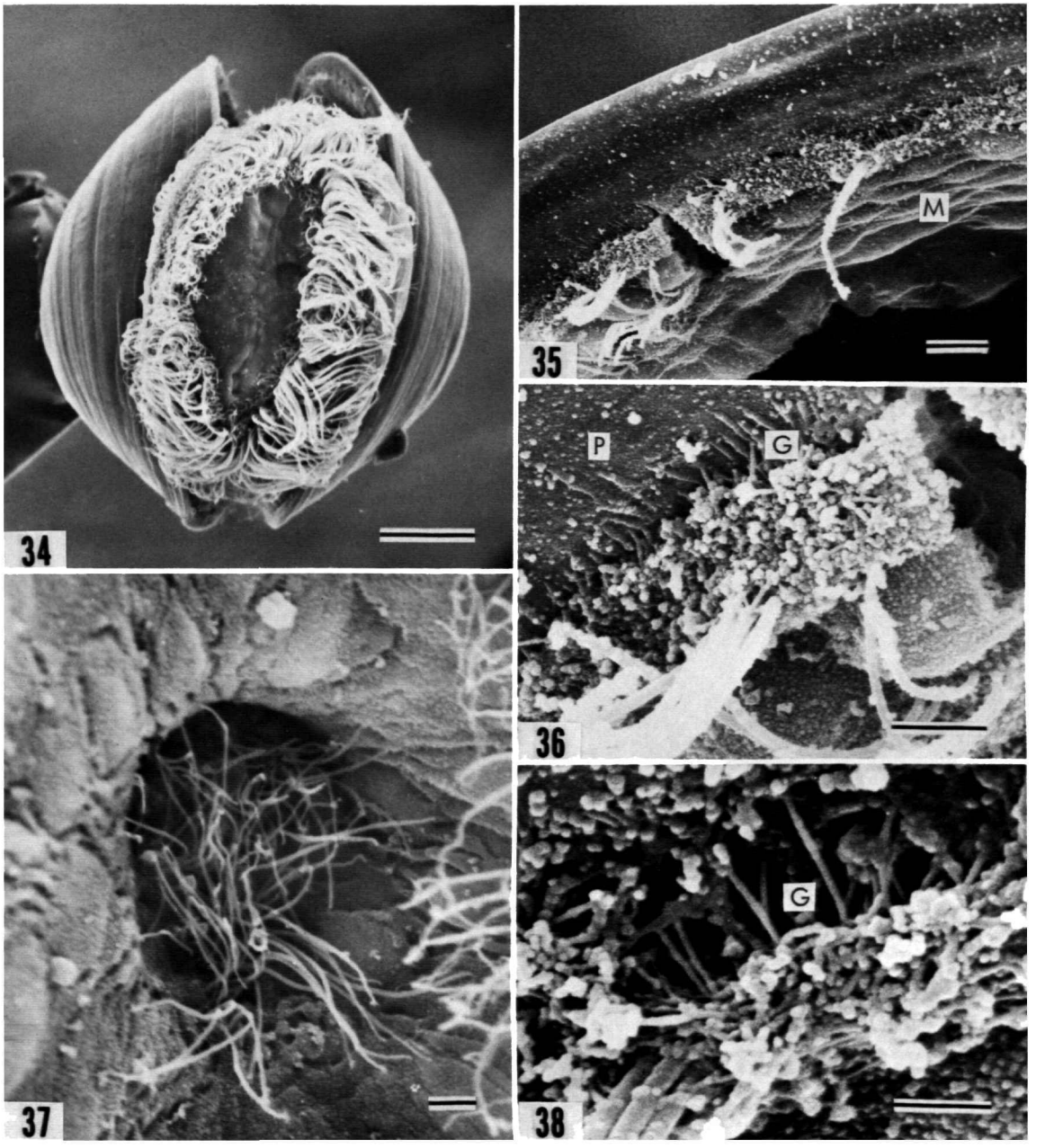

FIGURES 34–38.—*Ostrea edulis*, specimen 373B, mid-prodissoconch II, stage 3: 34, slightly folded velum (× 300, bar = 50 μm); 35, posterior edge of mantle (M) viewed obliquely from over edge of shell (× 2000, bar = 5 μm); 36, detail of Figure 35, periostracum (P) at contact with secretion-laden periostracal groove (G) (× 7500, bar = 2 μm); 37, detail of Figure 34, apical pit of velum (× 3500, bar = 2 μm); 38, detail of Figure 36, periostracal groove (G) (× 15000, bar = 1 μm).

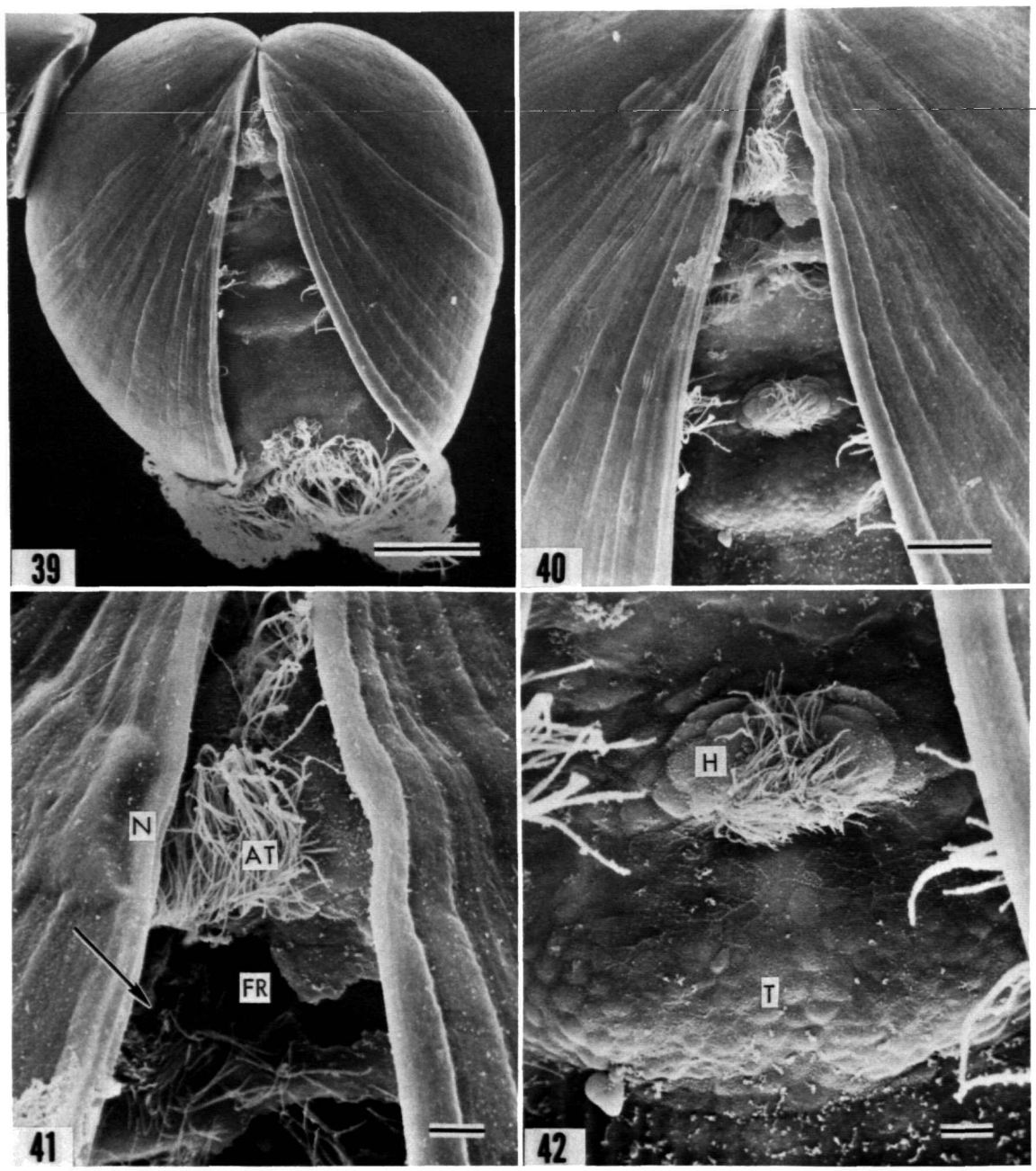

FIGURES 39–42.—*Ostrea edulis*, specimen 373B, mid-prodissoconch II, stage 3: 39, posterior view (× 330, bar = 50 μm); 40 detail of Figure 39 (× 650, bar = 20 μm); 41, detail of Figure 40, postanal ciliary tuft (AT) adjacent to posterodorsal notch (N), and anus (arrow) separated from tuft by fracture (FR) in body wall (× 1700, bar = 5 μm); 42, detail of Figure 40, foot primordium with well-developed heel (H) and incipient toe (T) (× 1700, bar = 5 μm).

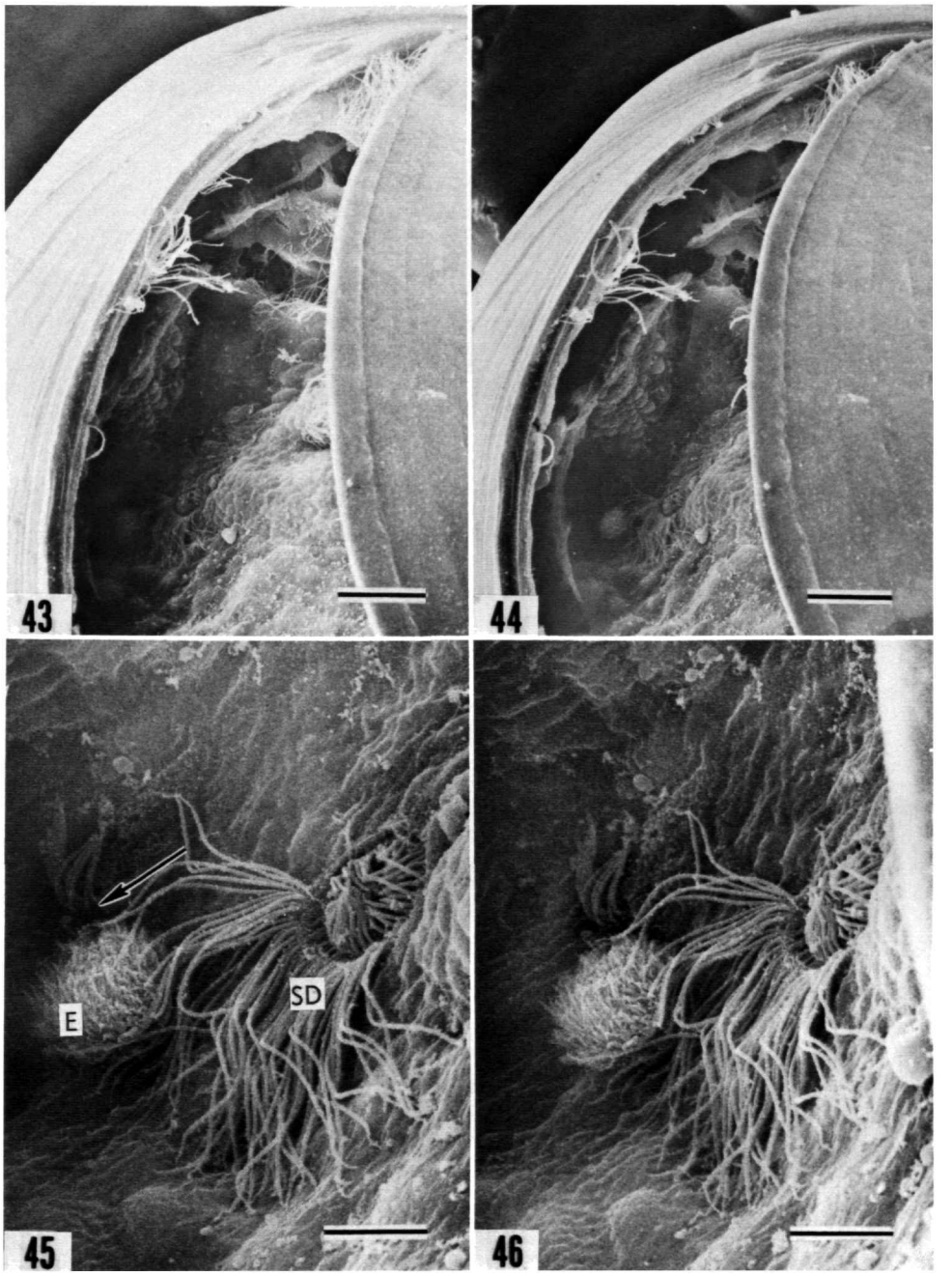

FIGURES 43–46.—*Ostrea edulis*, specimen 373B, mid-prodissoconch II, stage 3, stereomicrographs: 43 and 44, left gill cavity (× 650, bar = 20 μm); 45 and 46, detail of Figures 43 and 44, opening of static duct with long fringing cilia (SD), primordial microvillous eye (E), and possible protonephridial-duct opening (arrow) (× 3000, bar = 5 μm).

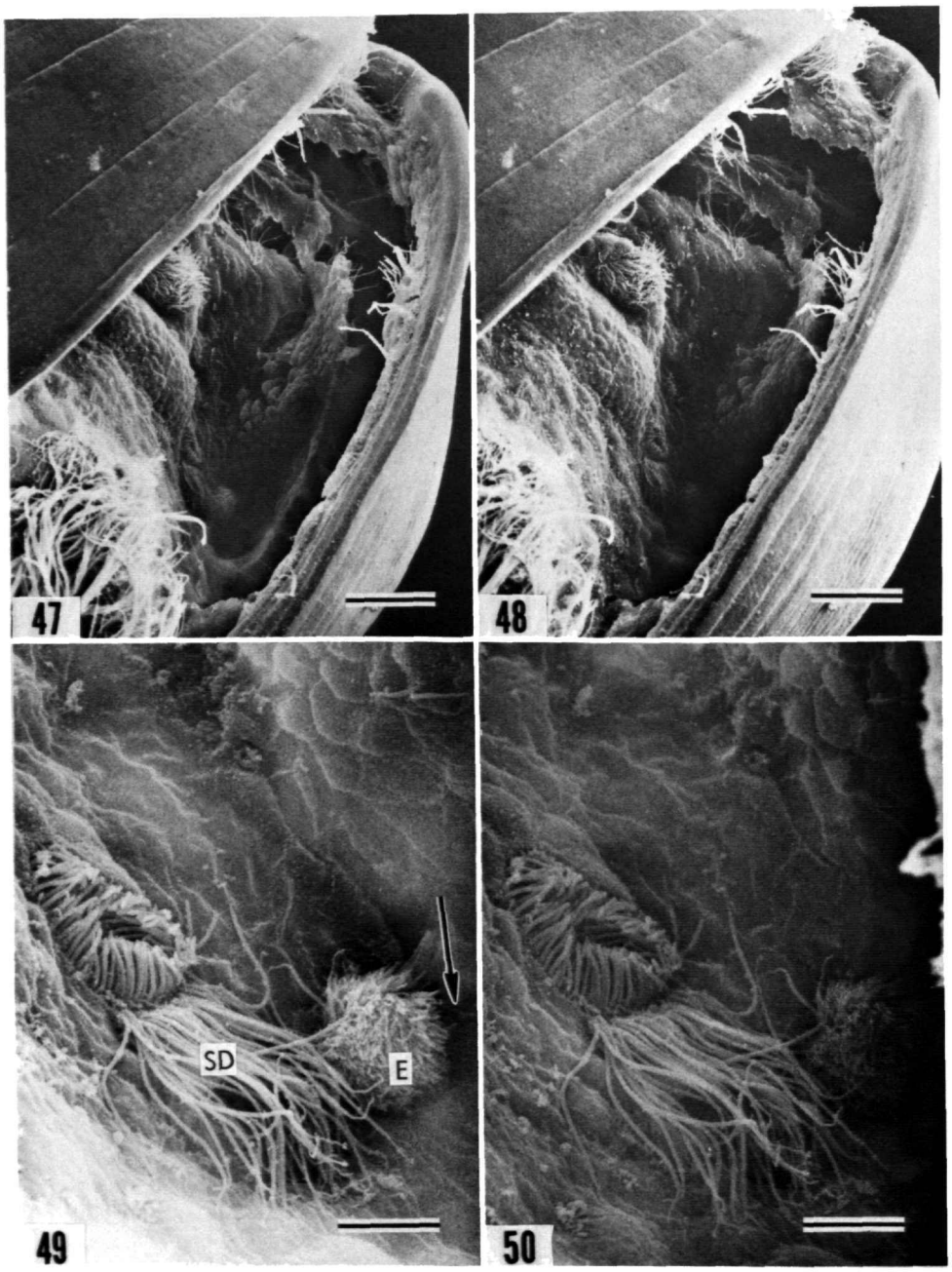

FIGURES 47–50.—*Ostrea edulis*, specimen 373B, mid-prodissoconch II, stage 3, stereomicrographs: 47 and 48, right gill cavity (× 650, bar = 20 μm); 49 and 50, detail of Figures 47 and 48, opening of static duct with long fringing cilia (SD), primordial microvillous eye (E), and possible protonephridial-duct opening (arrow) (× 3000, bar = 5μm).

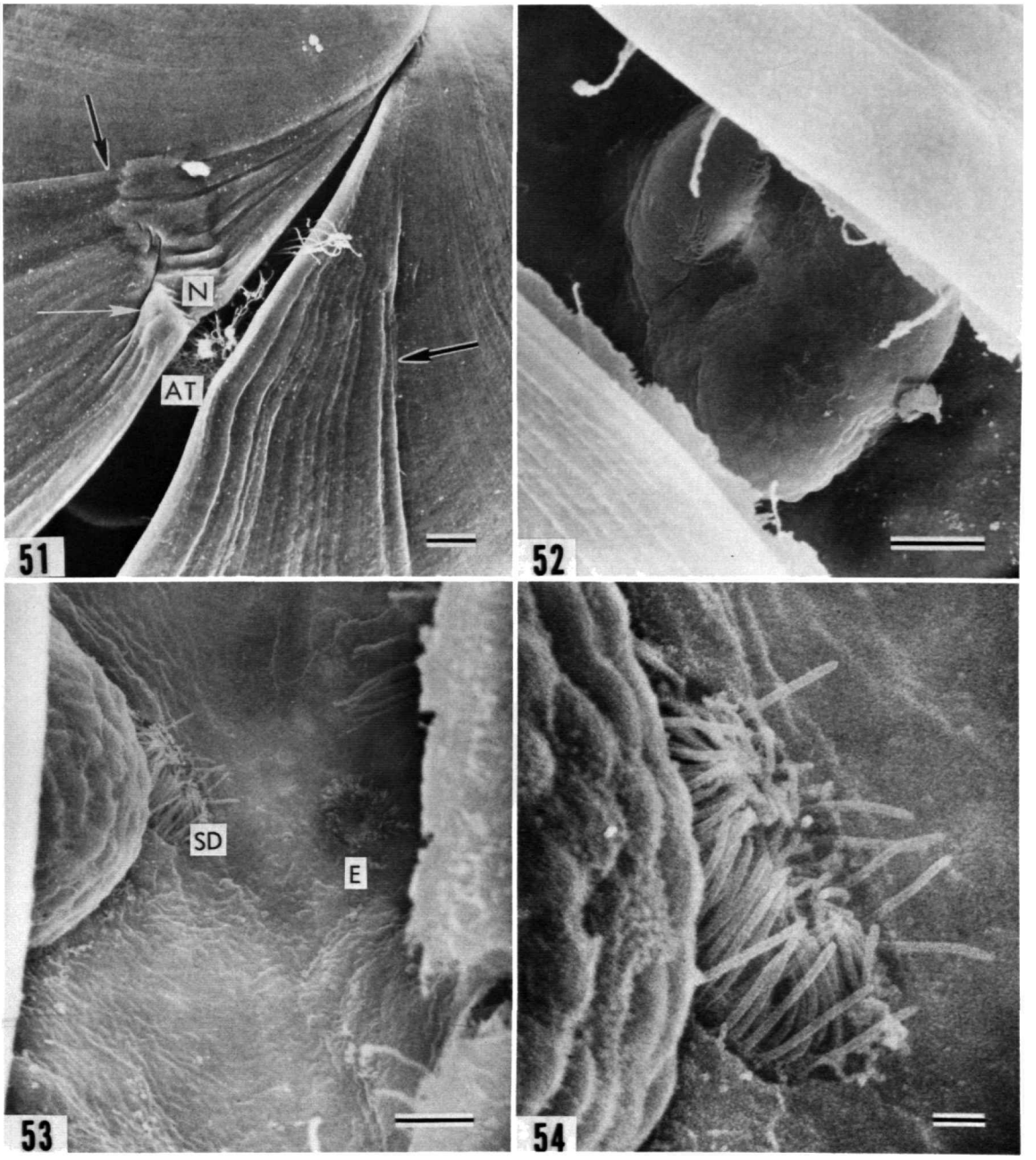

FIGURES 51–54.—*Ostrea edulis*, specimen 375C, mid-prodissoconch II, stage 5: 51, prodissoconch I-II boundary (black arrows), notch and growth track (N) with repaired injury (white arrow) in left valve, and postanal ciliary tuft (AT) (× 780, bar = 10 μm); 52, foot (× 1500, bar = 10 μm); 53, right gill cavity with opening of static duct (SD) and microvillous eye (E) (× 2470, bar = 5 μm); 54, detail of Figure 53, opening of static duct (× 8000, bar = 1 μm).

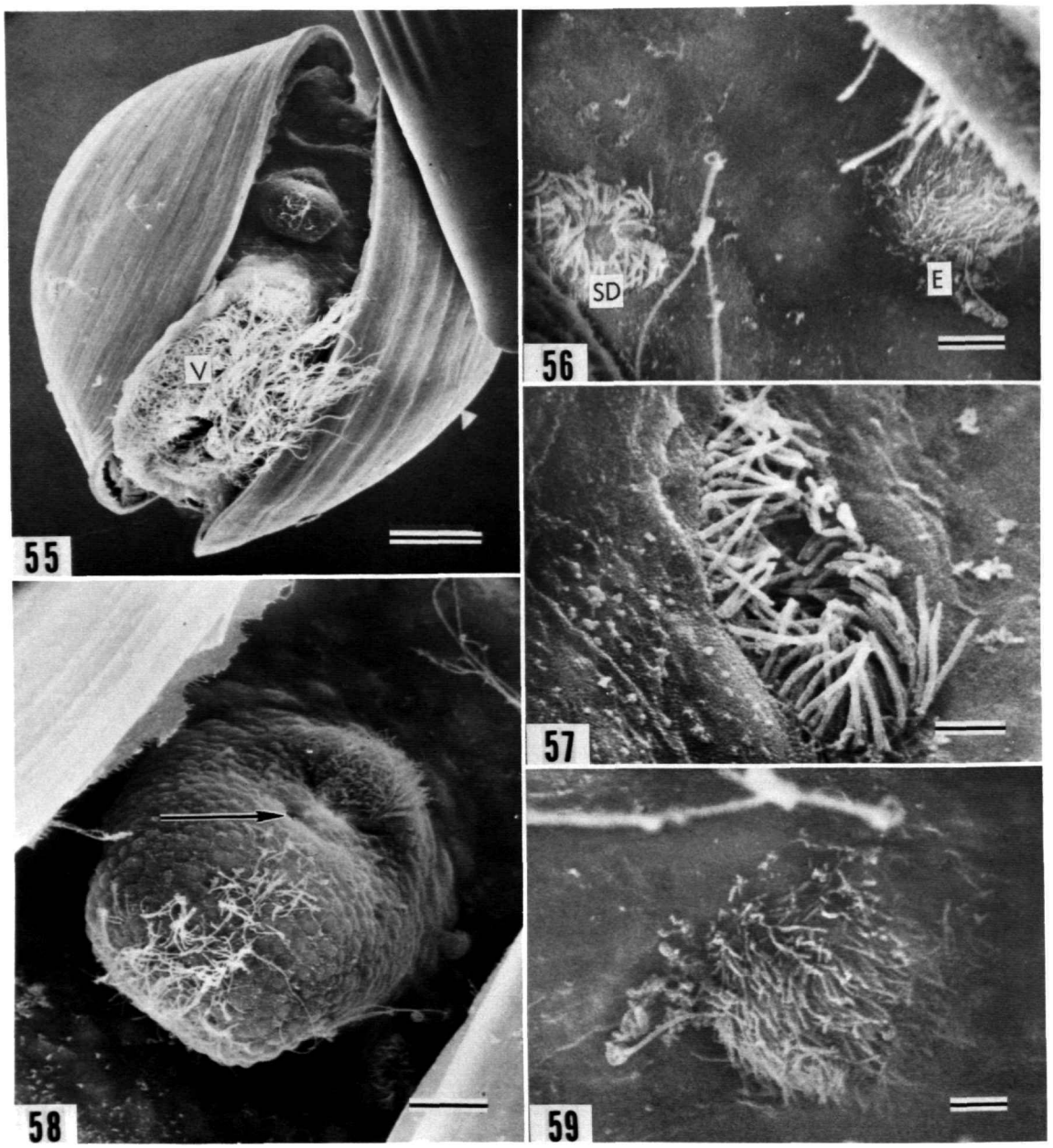

FIGURES 55–59.—*Ostrea edulis*, specimen 376B, late prodissoconch II, stage 7: 55, ventral view, velum (V) folded and partially retracted (× 280, bar = 50 μm); 56, right gill cavity, opening of static duct (SD) beside foot and microvillous eye (E) partially obscured by mantle edge (× 2100, bar = 5 μm); 57, detail of opening of right static duct, viewed obliquely from ventral side (× 5400, bar = 2 μm); 58, detail of foot viewed obliquely, opening of cement-gland duct (arrow) (× 1150, bar = 10 μm); 59, detail of Figure 56, microvillous eye (× 4500, bar = 2 μm).

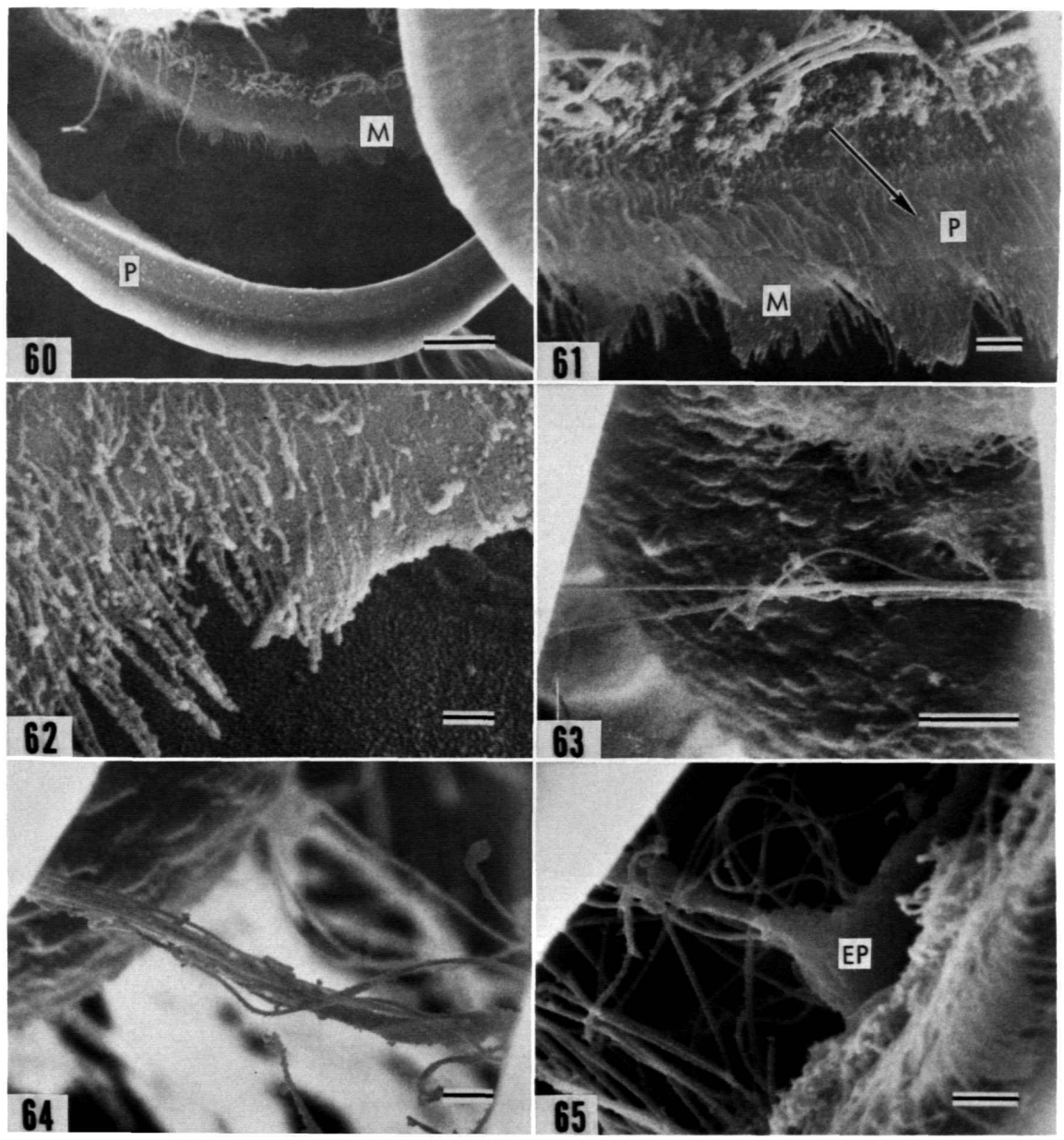

FIGURES 60–65.—*Ostrea edulis*, specimen 376B, late prodissoconch II, stage 7: 60, posteroventral mantle edge (M) contracted and pulled away from periostracum (P) (× 1050, bar = 10 μm); 61, detail of Figure 60, scalloped edge of outer fold of mantle (M) with periostracum (P) adhering to its inner surface (× 3600, bar = 2 μm); 62, outer surface of outer fold of mantle in anterodorsal region (× 7900, bar = 1 μm); 63, posterior view of cross-fused mantle cilia comprising primordial gill bridge (× 3100, bar = 2 μm); 64, detail of primordial gill bridge (× 3900, bar = 2 μm); 65, protrusion of epithelial cells (EP) at right end of primordial gill bridge (× 5000, bar = 2 μm).

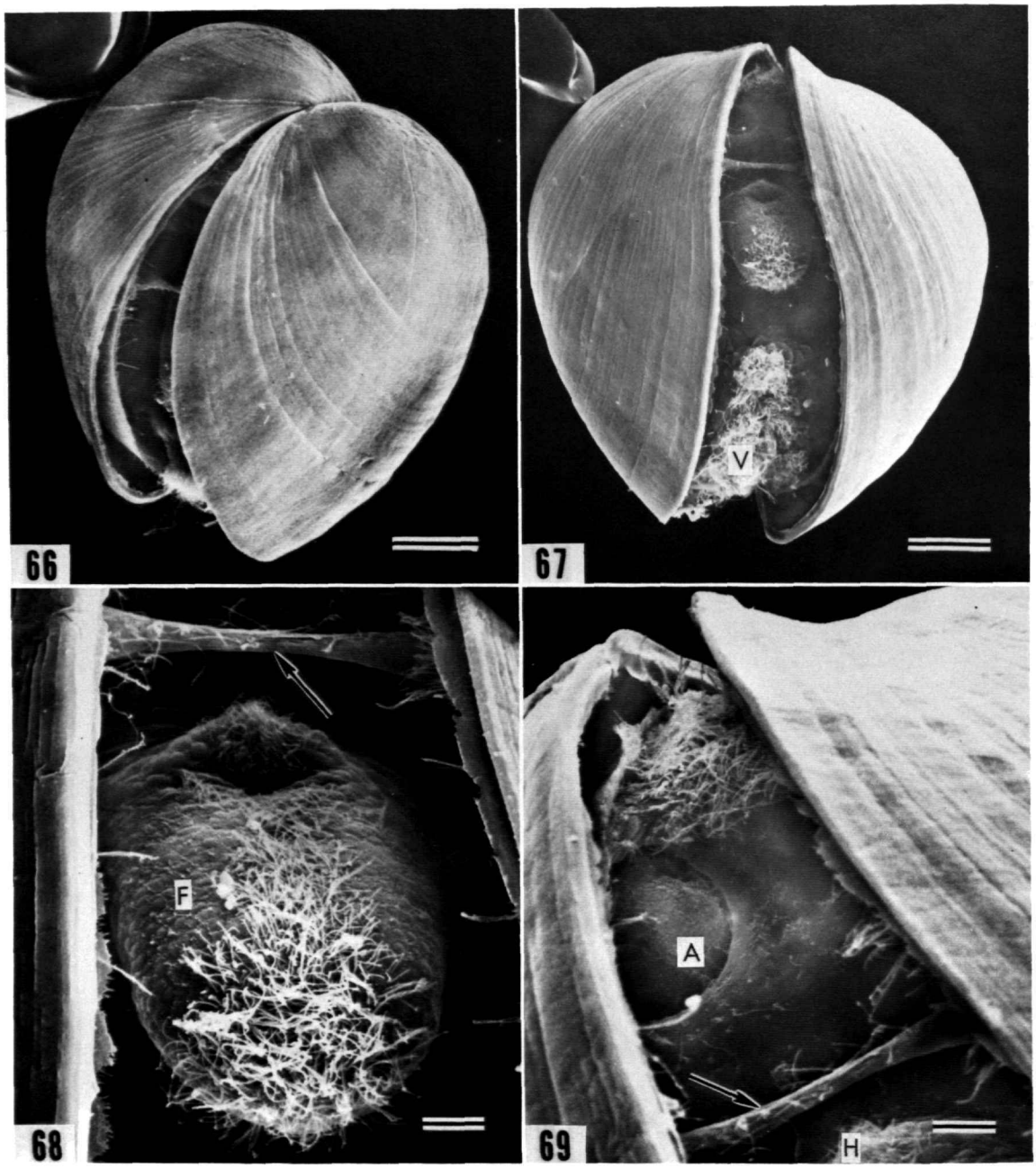

FIGURES 66–69.—*Ostrea edulis*, specimen 373A, late prodissoconch II, stage 8: 66, oblique posterior view (× 275, bar = 50 μm); 67, posteroventral view, velum (V) retracted (× 270, bar = 50 μm); 68, detail of Figure 67, foot (F) and gill bridge (arrow) (× 1000, bar = 10 μm); 69, posterodorsal region viewed from right ventral side, dilated anus (A) containing excrement, gill bridge (arrow), and heel of foot (H) (× 1000, bar = 10 μm).

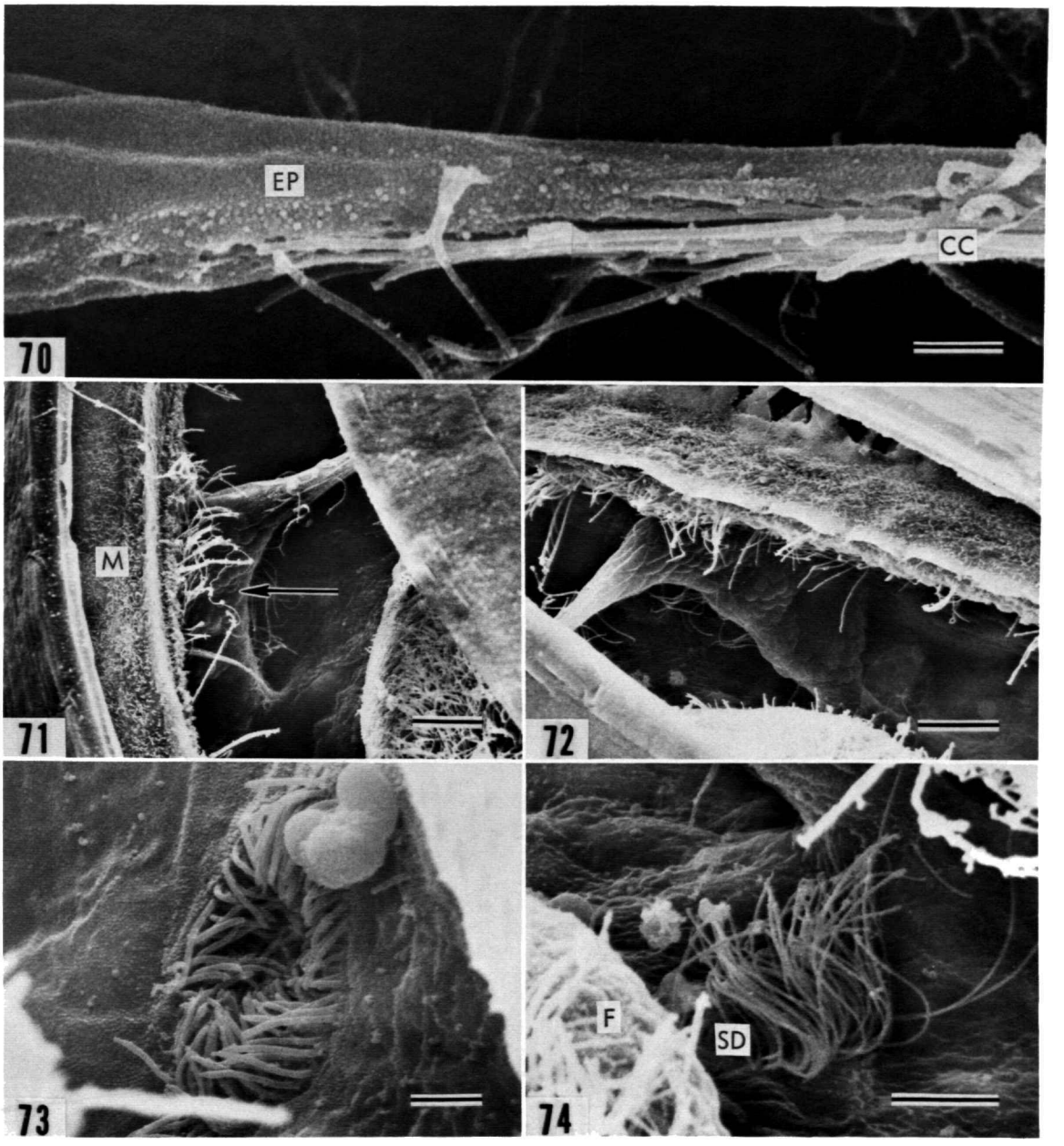

FIGURES 70–74.—*Ostrea edulis*, specimen 373A, late prodissoconch II, stage 8: 70, posterior view of gill bridge consisting of cross-fused cilia (CC) and epithelial cells (EP) (× 7000, bar = 2 μm); 71, left gill cavity viewed obliquely from posteroventral side, primordial gill (arrow) and gill bridge, mantle edge (M) with periostracal groove withdrawn from edge of shell (× 1100, bar = 10 μm); 72, right gill cavity (× 1270, bar = 10 μm); 73, oblique view of opening of static duct on left side of foot (× 5600, bar = 2 μm); 74, opening of static duct (SD) beneath long fringing cilia on right side of foot (F) (× 3400, bar = 5 μm).

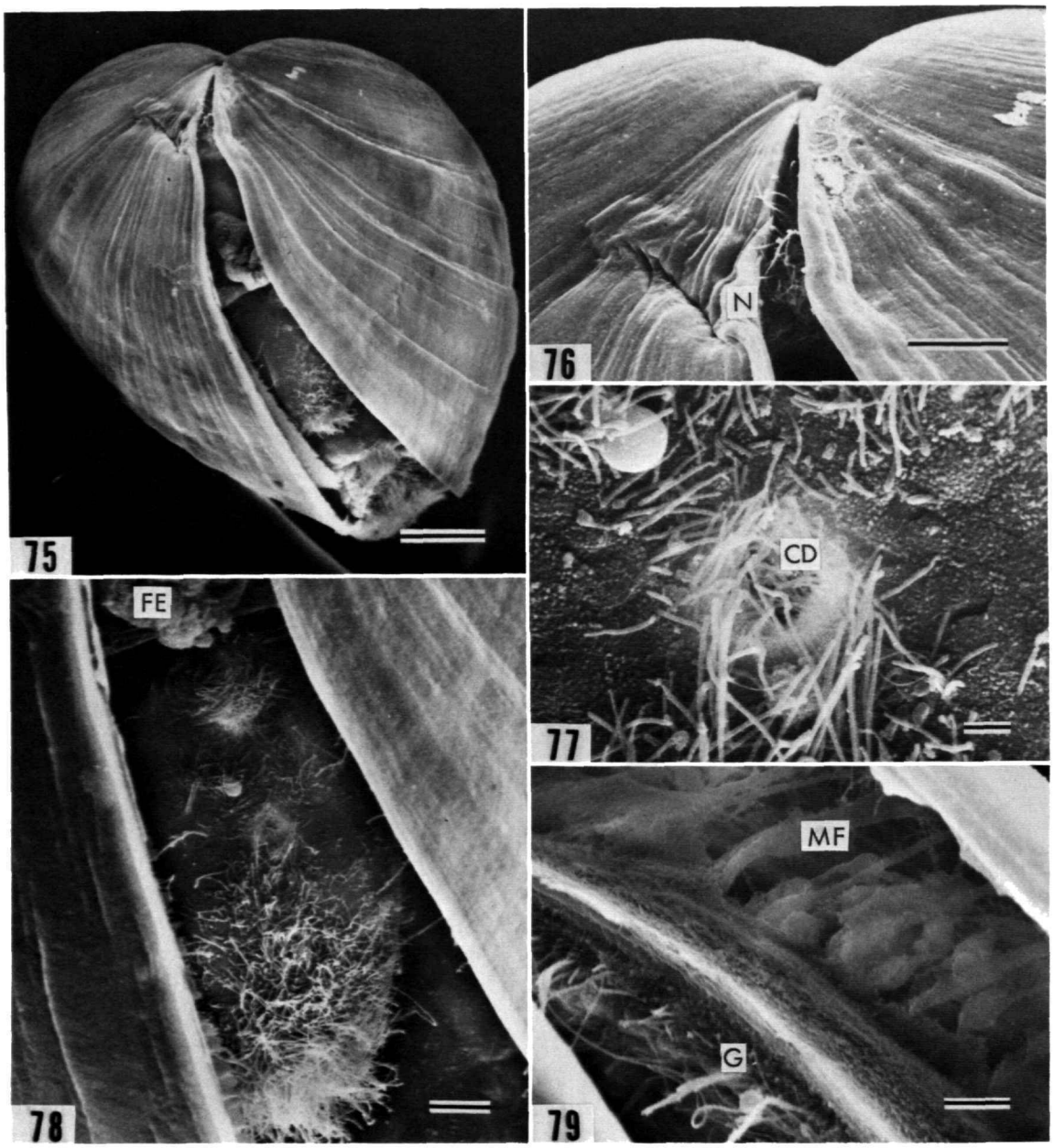

FIGURES 75–79.—*Ostrea edulis*, specimen 373C, late prodissoconch II, stage 9: 75, posterior view, velum retracted (× 270, bar = 50 μm); 76, detail of Figure 75, posterodorsal notch (N) and growth track with injury, postanal ciliary tuft (× 750, bar = 20 μm); 77, detail of Figure 78, opening of cement-gland duct (CD) (× 3600, bar = 2 μm); 78, foot, bordered on dorsal side by gill bridge partially obscured by feces (FE) (× 950, bar = 10 μm); 79, oblique view of outer surface of right mantle lobe withdrawn from shell, periostracal groove (G), and possible radial muscle fibers (MF) (× 2000, bar = 5 μm).

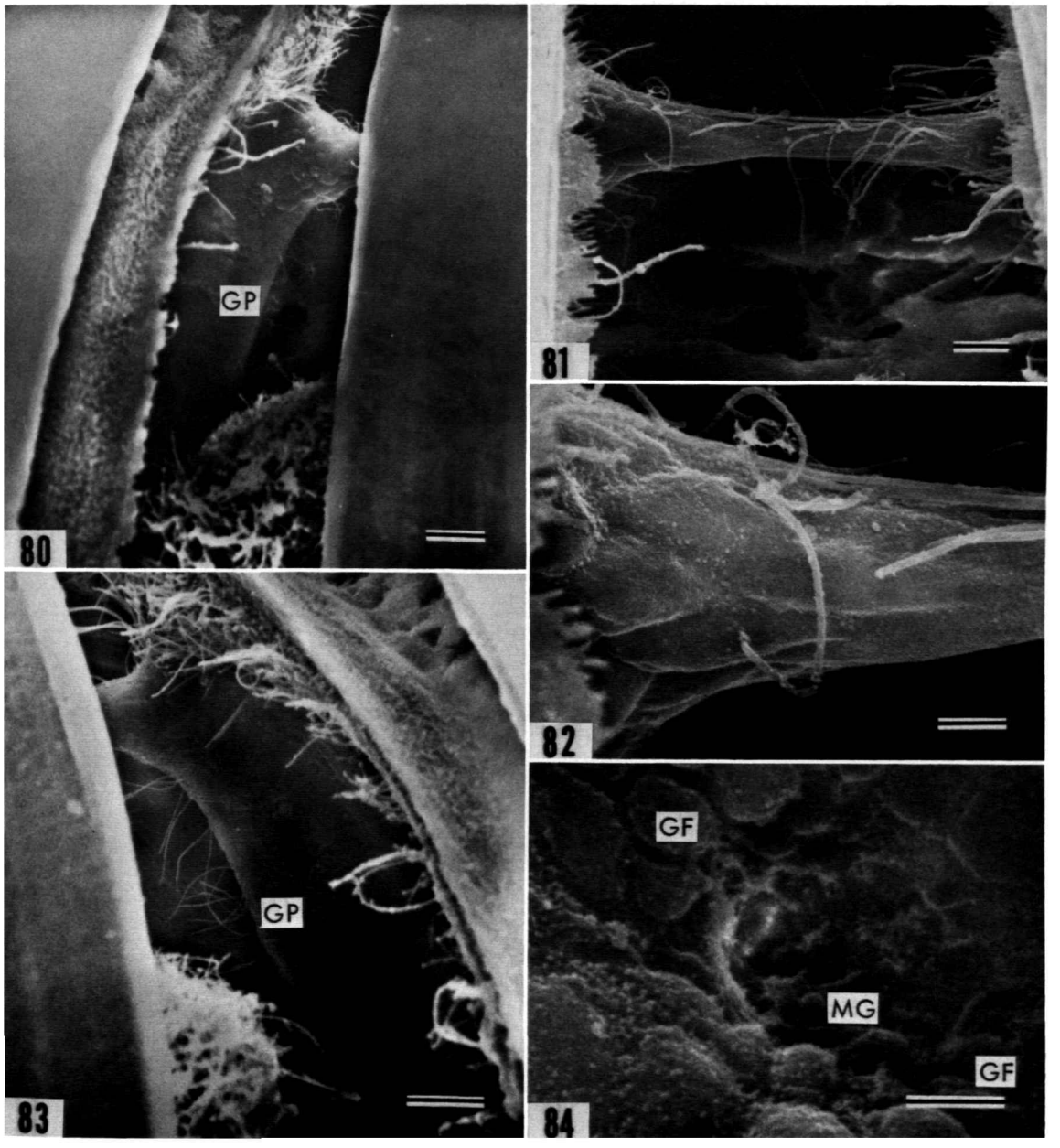

FIGURES 80–84.—*Ostrea edulis*, specimen 373C, late prodissoconch II, stage 9: 80, left gill primordium (GP) viewed from posteroventral side (× 900, bar = 10 μm); 81, gill bridge viewed from posterior, edge of outer fold of mantle and edge of shell on each side (× 1650, bar = 5 μm); 82, detail of Figure 81, left end of gll bridge with elongate epithelial cells and cilia (× 5340, bar = 2 μm); 83, right gill primordium (GP) viewed from posteroventral side (× 1200, bar = 10 μm); 84, detail of Figure 83, probable mucus-gland opening (MG) between primordia of gill filaments (GF) (× 7500, bar = 2 μm).

early stages of prodissoconch II. Prodissoconch-II growth along the margins of prodissoconch I gradually pushes the prodissoconch-I valves away from the plane of commissure and causes them to rotate on the hinge until they project dorsal to the hinge line, finally eliminating the D shape (compare Figure 11 to Figure 75).

The exterior surface of the earliest formed part of prodissoconch I has a sculptural pattern like that on the prodissoconch I of *Crassostrea virginica* described by Carriker and Palmer (1979a) and called by them the "punctate-stellate pattern" (Figures 85, 90, 92–94, 96, 97). In detail the pattern consists of two intergrading zones on each valve, a small, central "pitted zone" surrounded by a much larger "stellate-radial zone."

The pitted zone is oval in shape, roughly 50 by 30 μm, with its long diameter parallel to the dorsoventral axis of the shell and its dorsal edge separated from the hinge by a distance of about 15 to 20 μm. The pits are very shallow and range in diameter from less than 1 μm in the center of the zone to over 2 μm at the periphery of the zone. The entire pitted area tends to be somewhat depressed relative to the surrounding prodissoconch-I surface and generally tends to be planar or only very slightly convex. In some specimens, however, the surface of the pitted zone is thrown into relatively coarse folds which appear to involve both the periostracum and the outer surface of the outer calcified layer (Figure 98).

The stellate-radial zone begins at the periphery of the pitted zone with a series of 10 to 15 low, obscure, radially oriented ridges separated by V-shaped depressed areas which point into the pitted zone (Figures 85, 90, 96, 97). The ridges rapidly subside in elevation distally and disappear, the width of the ridged band being no more than about 25 μm and generally considerably less. The remaining surface of the stellate-radial zone is nearly smooth except for numerous exceedingly fine radial striae which diverge in V-shaped clusters. Fine commarginal growth lines (about two or three per micron) are also present (Figures 91, 94, 97), and which feature, radial or commarginal, shows in the micrograph depends on the angle of incidence of the electron beam. The earliest commarginal lines begin near the beginning of the stellate-radial zone, and the pattern that they trace on the shell surface suggests that the early calcified shell is dumbbell shaped and transversely elongate (Figure 85). Both the fine commarginal lines and the divaricate radial lines appear to persist through the prodissoconch-II stage but are obscured in the later stage by much coarser commarginal ridges and by the somewhat thicker periostracum (Figures 11, 23, 24, 39, 66, 92).

SHELL MICROSTRUCTURE.—The prodissoconch is covered by a periostracum so thin that it is difficult to examine and measure by scanning electron microscopy. Fracture sections and views of broken edges of periostracum suggest that its thickness is generally less than 0.1 μm in the early stages of prodissoconch I and that it may thicken slightly during the prodissoconch-II stage.

The outer surface of the calcified portion of the prodissoconch was examined after gentle removal of the periostracum by molecular bombardment (low-temperature plasma ashing) in oxygen (Figures 99–105). In the pitted zone of prodissoconch I, tiny grains or needles, which are assumed to be aragonite[2], are clustered in a polygonal pattern. In planar views of the surface, the grains or needles are on the order of 0.1 μm in diameter, and the polygons are from 1 to 3 μm in diameter. In the stellate-radial zone, the same type of granules or needles are present but are arranged in radially directed divergent rows that correspond to and probably produce the divergent radial pattern previously described on the periostracal surface. Approaching the prodissoconch-I/II boundary, the radial rows of granules become

[2] Stenzel (1964) determined by X-ray diffraction that the larval shell of *Crassostrea virginica* is aragonitic in composition; Carriker and Palmer (1979a) determined by the same methods that both the prodissoconch-I and prodissoconch-II stages of *C. virginica* are aragonite. There remains a possibility, however, that the earliest calcification adjacent to the periostracum in the pitted zone may be different. Watabe (1956) reported the presence of dahllite in the prodissoconch I of a pteriacean, *Pinctada martensii* (Dunker).

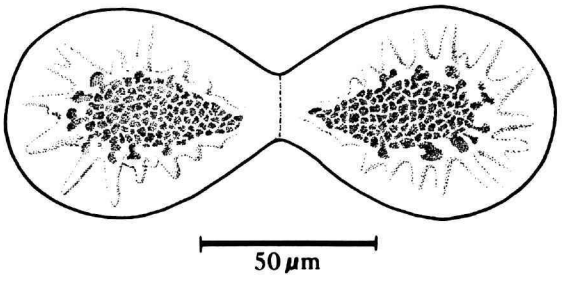

FIGURE 85.—Diagram of early prodissoconch I of *Ostrea edulis* shortly after evagination of the shell gland and before folding along the presumptive hinge. Pitted zones represent the two initial centers of calcification beneath a single, dumbbell-shaped periostracal sheet.

closer until on prodissoconch II the entire surface, including the growth track of the posterodorsal notch, consists of a thin, dense layer of closely packed granules (Figures 103, 143). Immediately beneath this granular surface are declined granular laths (Figures 106–108), described below.

Fractures through the prodissoconch of *Ostrea edulis* reveal a more complex structure than previously reported in bivalve larvae and demonstrate a gradual change in shell microstructure from the earliest portion of prodissoconch I to the end of prodissoconch II. As shown in Figures 109 through 116, three layers are present:

1. The outer layer, which underlies the periostracum, is generally about 0.7 μm in thickness in the early prodissoconch I but thins toward the prodissoconch-I margin and appears to be absent over the greater portion of prodissoconch II. The layer consists of exceedingly fine, irregular prisms that in the inner part of the layer vary from 0.05 to 0.1 μm in diameter. Next to the periostracum, the prisms attenuate into the fine needles described above. In scanning electron micrographs, the prisms comprising the outer layer appear to be columns of granules, as described by Carriker and Palmer (1979a) in the prodissoconch of *Crassostrea virginica.*

2. The inner layer, which forms the inner surface of the larval shell except at the free margins of the valves, is distinctly prismatic in structure. In scanning electron micrographs, the prisms appear to be uniform in texture rather than granular as in the outer layer. They are also coarser than the outer prisms, reaching diameters of about 0.3 μm. In fully developed prodissoconchs, the inner layer is thickest in the umbonal region, beneath the prodissoconch-I portion of the shell, where it may exceed 3 μm in thickness. The layer thins distally to less than 1 μm beneath the prodissoconch-II portion of the shell and finally to zero near the shell margin. The exact line of disappearance has not been determined, but it appears to be close to the line of attachment of mantle to shell, about 15 to 20 μm from the shell margin.

3. Beneath the pitted zone of prodissoconch I a third, middle layer is little more than a discontinuity between the inner and outer prismatic layers. This discontinuity thickens beneath the early portion of the stellate-radial zone and becomes a layer of randomly arrayed granules, a fabric that is generally referred to as "homogeneous." The increase in thickness is particularly noticeable in the dorsal region (Figure 111), where this layer comprises the hinge teeth and hinge plate. In the vicinity of the prodissoconch-I/II boundary, the middle layer increases greatly in thickness and, with the disappearance of the outer, prismatic layer, becomes the outer layer itself. At the shell margin, distal to the line of attenuation of the inner prismatic layer, the homogeneous layer is the only one present. In prodissoconch II the homogeneous layer also changes in character in that granules are no longer randomly arrayed but rather are clustered into laths that decline toward the shell margin from the outer surface to the inner surface (Figures 106–108, 115, 116). On the growth surface of this layer, which is the inner surface of the shell along the free margins, the granular laths are aligned in commarginal rows (Figure 117; see also Figure 148 of *Crassostrea gigas*).

These sculptural and textural changes during growth of the prodissoconch suggest a pattern of differentiation of epithelial cells during the transition from shell gland to mantle (Figure 86). As previously described, the first commarginal

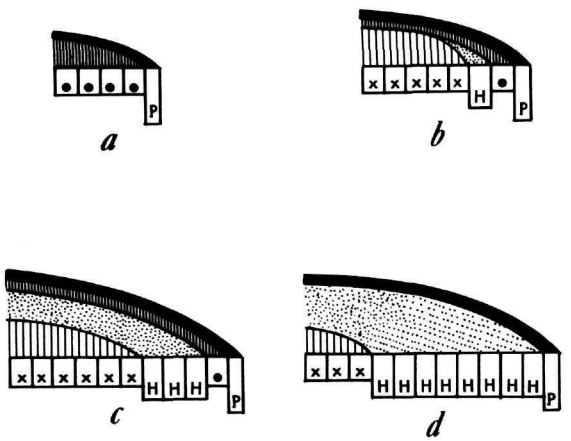

FIGURE 86.—Hypothetical relationship between layers of distinctive microstructure in the larval shell of *Ostrea edulis* and cellular differentiation during the transition from shell gland to mantle: *a*, shell-gland phase of calcification at the beginning of the prodissoconch-I stage; *b*, beginning of transition from shell gland to mantle, early to middle prodissoconch I; *c*, early phase of calcification by the mantle, middle to late prodissoconch I; and *d*, calcification by mantle, prodissoconch II. P and H represent cells secreting periostracum and homogeneous shell structure respectively. Cells bearing a dot (·) and an "x" represent successive secretory phases of cells originally present in the shell-gland phase.

growth line to form on prodissoconch I circumscribes a transversely elongate, somewhat dumbbell-shaped figure as shown in Figure 85. The pitted zones in the expanded lateral lobes of this initial shell probably represent two initial centers of calcification on the inner surface of a single, dumbbell-shaped periostracal sheet. Calcification probably begins simultaneously throughout the area of each pitted zone, as evidenced by the polygonal distribution pattern of crystals described above. It also seems likely that these centers of calcification as well as the periostracal sheet occupy a transverse depression with enlarged ends on the dorsal surface of the trochophore. The folded relief on some pitted zones suggests that distortion may occur during evagination of the shell gland, whereas the uniformly curved surface of the stellate-radial zone suggests that calcification in this region occurs after evagination.

Secretion of the stellate-radial zone of prodissoconch I is incremental, as evidenced by growth lines, and proceeds outward from the pitted zones in all directions including toward the hinge, as evidenced by the presence of radial elements between the pitted zones and the hinge (Figures 96, 137). Initial folding of the embryonic shell can occur only through the last remnant of uncalcified periostracum, which becomes the ligament at the site of the hinge (described below).

As previously described, the homogeneous shell ultrastructure that makes up nearly the entire thickness of prodissoconch II can be traced back to an origin in the discontinuity between the outer and inner prismatic layers present beneath the umbones. The beginning of the middle layer possibly indicates differentiation of a new commarginal band of cells near the periphery of the shell gland and a simultaneous change in secretory function of the older, more centrally located cells (Figure 86*b*). This is the kind of change that Cather (1967) used to mark the change from shell gland to mantle in a gastropod larva, and it seems desirable to use the same system in describing the ontogeny of bivalve larvae. Subsequent thickening of the middle shell layer thus may represent increase in size of a band of special secretory cells which persists until metamorphosis. Because this specialized band, and hence the mantle, begins well before the prodissoconch-I/II boundary, the boundary itself cannot be explained as a result of the change from shell gland to mantle.

At metamorphosis, the form, microstructure, and mineralogy of the shell suddenly change. The uniformly coiled, gibbous form of the prodissoconch is replaced by the irregular, flattened form of the dissoconch, which is now cemented to the substrate (Figures 118, 119). Both valves of the prodissoconch change abruptly from entirely aragonitic (Stenzel, 1964; Carriker and Palmer, 1979a) to nearly entirely calcitic (Taylor, Kennedy, and Hall, 1969), and the final, homogeneous shell microstructure of the prodissoconch changes to much coarser prisms and folia (Figures

121–131). The mature shell of *Ostrea edulis* is composed primarily of foliated calcite, with a thin outer layer of simple prismatic calcite on each valve. The only aragonite known to be present in the dissoconch is restricted to areas of muscle attachment (the myostraca) and to the ligament area (Carriker and Palmer, 1979b).

The prismatic calcitic outer layer of each valve of the dissoconch is initially no more than about 1 μm in thickness, consisting of tabular polygonal prisms bounded exteriorly by periostracum (Figures 121–129, 131). Scanning electron micrographs of the outer ends of prisms from which the periostracum has been removed show that initial growth of each prism is accretionary, beginning at a nucleation point that is offset from the center of the outer face of the prism toward the proximal side of the shell (Figure 123). As calcification proceeds concentrically around each nucleation point, the centers of calcification impinge upon one another and crowding produces the polygonal form. Once the close-packed polygonal condition has been reached, the prisms can only grow perpendicularly or at high angle to the periostracal surface. The diameters of prisms, measured at a distance of 1.5 μm from the edge of the prodissoconch, range from about 5 to 15 μm, with a somewhat larger size on the right valve than on the left.

Vertical growth of the calcitic prisms is terminated by the advancing front of an inner shell layer a short distance inside of the distal margin of the dissoconch (Figures 128, 129). This inner layer is foliated calcite (Taylor, Kennedy, and Hall, 1969), consisting of pointed laths inclined at a very low angle to the plane of the shell. Each lath has a thickness ranging from less than 1 μm to about 2 μm, a width from 0.5 to 3 μm, and an unknown length. Transition between prismatic and foliated microstructure is apparent both in fracture sections (Figures 127, 131) and on the growth surface of the shell (Figure 129).[3] Not only does foliated calcite cover the inner surface of the prismatic calcitic outer layer; it also extends inward over the inner surface of the prodissoconch and eventually completely fills the prodissoconch interior.

In addition to prismatic and foliated calcite, a third microstructure is also present in the earliest dissoconch. It is irregularly prismatic and apparently is associated with the attachment of the posterior adductor to the shell (Figures 126, 130). As would be expected by its limited area of secretion, the microstructure forms a thin, laterally restricted layer which forms on the inner surface of previously secreted foliated calcite and in turn is covered by later secreted foliated calcite. Such irregularly prismatic microstructures associated with muscle attachments were termed "myostraca" by Oberling (1964) and are known to be aragonitic in composition (Taylor, Kennedy, and Hall, 1969). What is of particular interest here is the very early appearance of the myostracum, actually beneath the rim of the prodissoconch but separated from this rim by a thin layer of foliated calcite (Figure 130).

The ultrastructure of this earliest myostracum is nearly identical to that of the inner shell layer of the prodissoconch (Figures 109–112, 114, 115). Although continuity between the two microstructures cannot be demonstrated in the scanning electron micrographs taken for this study, it is tempting to postulate that they are interconnected and that the mantle epithelium that gives rise to the inner layer of the prodissoconch may have features in common with the adhesive epithelium in areas of muscle attachment (Tompa and Watabe, 1976; Waller, 1980). If so, the combination of anatomical and biochemical features that produce the structure may be deeply rooted in the genetic program governing ontogeny of the shell.

HINGE AND MARGIN.—Ranson (1939) showed that the prodissoconch-I hinge of *Ostrea edulis* is linear and lacks teeth, and Werner (1939) demonstrated that this is also the case in other bivalves. In the present study, all of the specimens examined are beyond the prodissoconch-I stage,

[3] A similar transition has been reported in the Pectinacea and has contributed to a hypothesis that the prismatic microstructure is the evolutionary precursor of foliated microstructure (Waller, 1972).

but information on the early development of the hinge is provided by commarginal growth lines. The growth line that separates prodissoconch I from prodissoconch II can be traced to the hinge line and shows that there is little increase in length of hinge during the prodissoconch II stage. The prominent hinge teeth of prodissoconch II develop at the ends of the prodissoconch-I hinge (Figures 94, 96, 97).

The only ligament present in prodissoconch I is likely the same band of thickened periostracum that can be seen in early prodissoconch II (Figure 139). The valve margins of prodissoconch I are probably simple and not interlocking, as indicated by the presence of a largely prismatic microstructure during this stage. It is unlikely that the coarse, parallel prisms of this microstructure could be secreted on the interlocking shell margin.

Changes in number, spacing, shape, and size of hinge teeth during the development of prodissoconch II have been described by Pascual (1972) and will not be repeated here except to restate two points: (1) The posterior hinge teeth are larger than the anterior from the beginning of their development at the start of prodissoconch II. Early in prodissoconch-II development (at a shell length of about 230 μm in Pascual's samples), the anterior teeth begin to be filled in rapidly by new secretion of shell (Figure 138). Finally, at the end of the prodissoconch-II stage, only the posterior teeth remain in most specimens. (2) The central portion of the hinge between the hinge teeth is about equally developed in each valve throughout the prodissoconch-II stage. When the valves are closed, the central part of the hinge of one valve meets that of the other valve approximately along the plane of commissure (Figures 137, 138), although tiny denticulations or rugosities may be present (Figure 136).

The central region of the hinge is not the site of a resilium or tiny internal ligament, such as that illustrated by Stenzel (1971)[4], nor is there any indication of a fibrous inner layer, such as that indicated by Trueman (1951). The only ligament present during the prodissoconch-II stage is external, consisting of a band of thick periostracum (also noted by Calloway and Turner, 1979, and Lutz, 1979). Growth lines on the prodissoconch-II surface converge at the ends of this band and indicate that ligament length increases only slightly during the prodissoconch-II phase. Scanning electron microscopy of the hinge plates of young dissoconchs of *Ostrea edulis* show that the resilium first appears at or near metamorphosis at a point just anterior to the anterior hinge teeth (Figure 140). Pascual (1972) reached the same conclusion for *Ostrea stentina*, but Carriker and Palmer (1979a) found that in *Crassostrea virginica* the resilium appears earlier in the prodissoconch-II stage.

The anterior and posterior sides of the hinge teeth of prodissoconch II bear curved ridges (Figure 139) that fit into corresponding curved grooves on the sides of the corresponding sockets of the opposite valve. The curvature of these features is invariably concave toward the hinge line, and in fact the center of curvature lies approximately on the axis of rotation of the valves. Similar features are found on the larval hinge teeth of *Crassostrea virginica* (Carriker and Palmer, 1979a), *C. gigas* (herein, Figure 149), *Mytilus edulis* and *Modiolus modiolus* (Lutz and Hidu, 1979), and *Argopecten irradians* (Waller, unpublished data). As shown by Stanley (1978), such a ridge and groove system on the hinge teeth of mature bivalves serves to reduce shear between partially opened valves and produces a tighter interlocking system when the valves are in the process of opening and closing. The same function appears to be served in larval shells.

As described by Pascual (1972), the configuration of the hinge of species of *Ostrea* becomes much more variable in larval shells approaching metamorphosis than in younger shells. The anterior teeth may or may not disappear completely, and the rugosity produced by secondary denticulations on the primary teeth and across the central portion of the hinge may become extreme.

[4] Figure J37 in Stenzel (1971), showing a tiny central, internal ligament in the prodissoconch of *Ostrea edulis*, is said to be from Ranson (1939), but Ranson's original figure showed no such ligament.

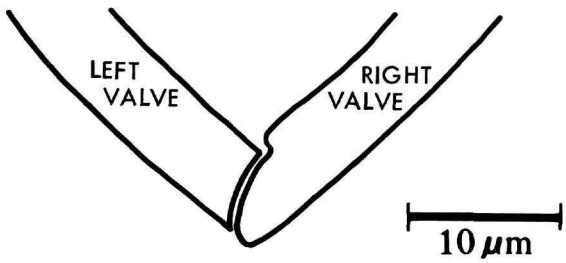

FIGURE 87.—Diagrammatic cross section of interlocking valve margins in *Ostrea edulis*.

In all of the prodissoconch-II stages of *Ostrea edulis* examined in the present study, the valves fit together in tongue-in-groove fashion by way of margins that differ between valves (Figures 87, 117, 132–135). Although these features are somewhat variable, they can be traced around the entire extent of the free margins of the shell except for the area of the posterodorsal notch of the left valve (described above). In the notch, the thin leading edge is either absent or folded back (Figures 22, 89). The tongue-in-groove arrangement provides a tight seal and prevents shear between closed valves.

Shell Morphology of Other Oyster Larvae

A number of features of the larval shell of *Ostrea edulis* are present in the shells of other oyster species of both the oviparous and larviparous types.

1. The punctate-stellate pattern present on the exterior surface of prodissoconch I of *Ostrea edulis* is also present in *Crassostrea virginica* (Carriker and Palmer, 1979a) and *Crassostrea gigas* (Waller, unpublished data).

2. The larval shell microstructure of *Crassostrea gigas* (Figures 145–147) is similar to that of *Ostrea edulis*. Although Carriker and Palmer (1979a) did not discuss microstructural change during growth of the prodissoconch, their figures indicate that shell microstructure in *Crassostrea virginica* is of the same type and undergoes the same kind of change during growth.

3. The prodissoconch-II shell margins of *Crassostrea gigas* (Figures 143, 144) are like those of *Ostrea edulis*. Scanning electron micrographs in Carriker and Palmer (1979a) indicate that the same interlocking arrangement also exists in *Crassostrea virginica*.

4. The posterodorsal notch and growth track in the prodissoconch II of *Ostrea edulis* are present in the left valves of many species of oyster larvae in this stage of development. In the Family Ostreidae, the presence of the notch has been documented in *Saccostrea echinata*, *Ostrea edulis*, *O. circumpicta*, *O. denselamellosa*, *O. futamiensis*, *Crassostrea virginica*, *C. ariakensis*, and *C. gigas* by Tanaka (1960), in *C. virginica* by Carriker and Palmer (1979a), in *Saccostrea glomerata* and *Ostrea corrugata* by P. Chanley (pers. comm., 1979), and in *C. gigas* by the present study (Figure 141–144). Furthermore, close inspection of light micrographs published by Ranson (1939) and Pascual (1971, 1972) reveals that a posterodorsal notch is probably present also in *Crassostrea angulata* and *Ostrea stentina*. In the Family Gryphaeidae, larval shells of *Neopycnodonte cochlear* shown herein (Figures 151, 152) also have a posterodorsal notch in prodissoconch II. According to P. Chanley (pers. comm., 1979), the notch is not present in *Ostrea lutaria* and *O. chilensis*.

5. Although patterns of hinge dentition differ in detail between species, the basic configuration of massive anterior and posterior teeth separated by a central space devoid of hinge teeth is similar in early stages of prodissoconch II in *Ostrea stentina* (Pascual, 1972), *Crassostrea angulata* (Pascual, 1972; Dinamani, 1976), *Saccostrea glomerata* (Dinamani, 1973, 1976), *C. gigas* (Dinamani, 1976; herein, Figure 150), and *C. virginica* (Dinamani, 1976; Carriker and Palmer, 1979a). In specimens examined with scanning electron microscope, curved ridges on the sides of teeth and sockets are present (Dinamani, 1976; Carriker and Palmer, 1979a; herein, Figure 149).

In contrast to these similarities between species,

important differences separate the larval shells of the oviparous and larviparous groups.

1. Although the sizes attained by the prodissoconch at metamorphosis may be similar between these two groups, there are great differences in the dimensions of the prodissoconch-I stage and hence in the ratio of size of prodissoconch I to size of prodissoconch II. Prodissoconch I is very small in the oviparous group, generally on the order of 70 μm in length, which ranges from 20% to 25% of the length of the fully formed prodissoconch II. In contrast, prodissoconch I lengths in larviparous species, including *Ostrea edulis* and *O. stentina* (herein and Pascual, 1972), range from 140 to 190 μm and therefore occupy a much greater proportion of the length of the total larval shell (50% to 60%).

2. Because the onset of asymmetry in the convexity of the two valves appears to begin at the prodissoconch-I/II boundary, the great differences in the proportions of these stages between oviparous and larviparous oysters lead to great differences in shape. In the fully developed prodissoconch II of species of *Crassostrea*, the left valve greatly exceeds the right valve in convexity, and therefore its umbo extends farther over the hinge than in species of *Ostrea* (Pascual, 1971, 1972; Carriker and Palmer, 1979a; herein, Figure 142). As a consequence of the relatively greater coiling of the left valve in species of *Crassostrea*, the track of its posterodorsal notch is longer and more obviously spiral than in species of *Ostrea* (Carriker and Palmer, 1979a; herein, Figure 142).

3. In both *Ostrea edulis* and *O. stentina*, the hinge teeth remain separated during prodissoconch-II development, while the anterior teeth gradually diminish in prominence. The central portion of the hinge between the teeth is equally developed in both valves. In contrast, in *Crassostrea angulata* (Pascual, 1971; Dinamani, 1976); *C. gigas* (Dinamani, 1976), and *C. virginica* (Dinamani, 1976; Carriker and Palmer, 1979a) the anterior and posterior teeth develop at the expense of the central portion of the hinge, and it is the posterior teeth that decrease in prominence. The central portion of the hinge is unequally developed between valves. The central area is a projection on the right valve and a depression on the left, so that the area itself serves as a sort of massive tooth and socket.

4. Although incremental growth is present in the prodissoconch-I phase because of the enlargement of the secretory epithelium of the shell-gland/mantle, there is a difference in the prominence of incremental lines between species. They are prominent on the prodissoconch-I surface of *Ostrea edulis* but nearly lacking in the same area of *Crassostrea gigas* (Figure 141) and *C. virginica* (Carriker and Palmer, 1979a).

Discussion

The prodissoconch-I/II boundary in larval shells of bivalves was shown by Ockelmann (1965) to be an important indicator of type of larval development and capability of dispersal. However, he offered no detailed explanation of how the boundary forms other than that it represents a change from calcification by the shell gland to that by the mantle edge, an explanation also put forth by many others.

Two lines of evidence suggest that a change in mode of calcification is not the cause of the prodissoconch-I/II boundary. First, if the shell gland is defined as the specialized glandular epithelium in the transverse dorsal invagination of the trochophore, then there is no correspondence in position between the boundary on the prodissoconch and this feature. As shown above, only the earliest stages of calcification of prodissoconch I, inside the first discernible growth line, are transversely elongate with respect to the larval body. The only feature that seems to suggest both evagination and a change in mode of calcification is the boundary between the central pitted zone on the umbo of prodissoconch I and the surrounding stellate-radial zone. Secondly, although the earliest phases of calcification in the oyster larva have never been described in detail, evidence from other groups of mollusks (see above review of early development) suggests that the change from shell gland to mantle is not accompanied by

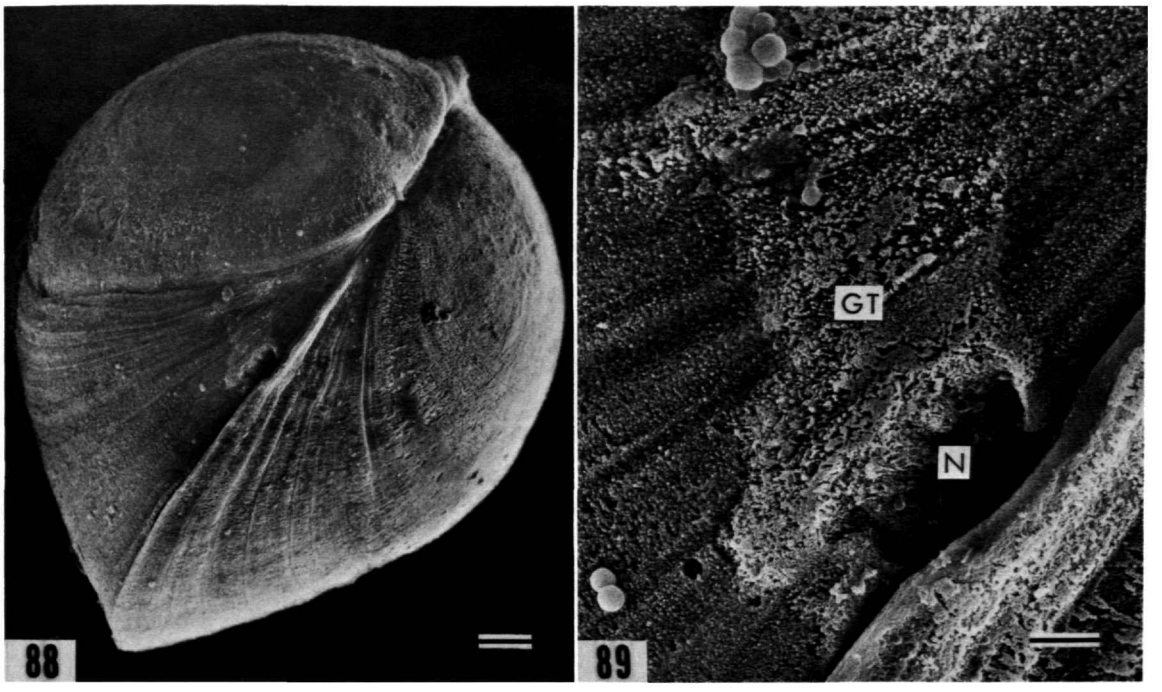

FIGURES 88 and 89.—*Ostrea edulis*, specimen 388C, late prodissoconch II, periostracum removed (5% NaOCl, 43 hours): 88, posterodorsal view (× 350, bar = 20 μm); 89, detail of Figure 88, posterodorsal notch (N) and growth track (GT) (× 2000, bar = 5 μm).

an abrupt change in mode of calcification. The prodissoconch-I/II boundary is therefore not only in the wrong place for this explanation to be valid, it is also the wrong type of boundary because it is sharp rather than gradational.

A number of observations described in the present study and previously reviewed in abstract (Waller, 1979) suggest a different cause of the prodissoconch-I/II boundary in oyster larvae and possibly in all planktotrophic larval bivalves: the boundary represents the time in the development of the shell at which the valves first completely enclose the body and close against one another along their free margins. The observations that support this interpretation are as follows:

1. The massive larval hinge teeth and tongue-in-groove valve edges, both of which serve to prevent shear between closed or nearly closed valves, develop primarily during the prodissoconch-II stage.

2. The sudden increase in the prominence of commarginal growth lines at the start of the prodissoconch-II stage is possibly due to the fact that these lines are produced by physiological changes dependent on valve closure as in mature bivalves (Lutz and Rhoads, 1977; Gordon and Carriker, 1978) as well as actual deflection of the mantle edge during closure, as suggested by the step-like configuration of these lines on the exterior surface. The much fainter growth lines present in the brooded prodissoconch-I stage possibly represent only physiological changes in the mantle cavity of the parent that affect the rate of calcification in the brooded larva, because there are no step-like deflections on the outer surface at this stage. Such prodissoconch-I growth lines are only very poorly developed in nonbrooded larvae, such as in specimens of *Crassostrea virginica* illustrated by Carriker and Palmer (1979a) and *C. gigas* illustrated herein (Figure 141).

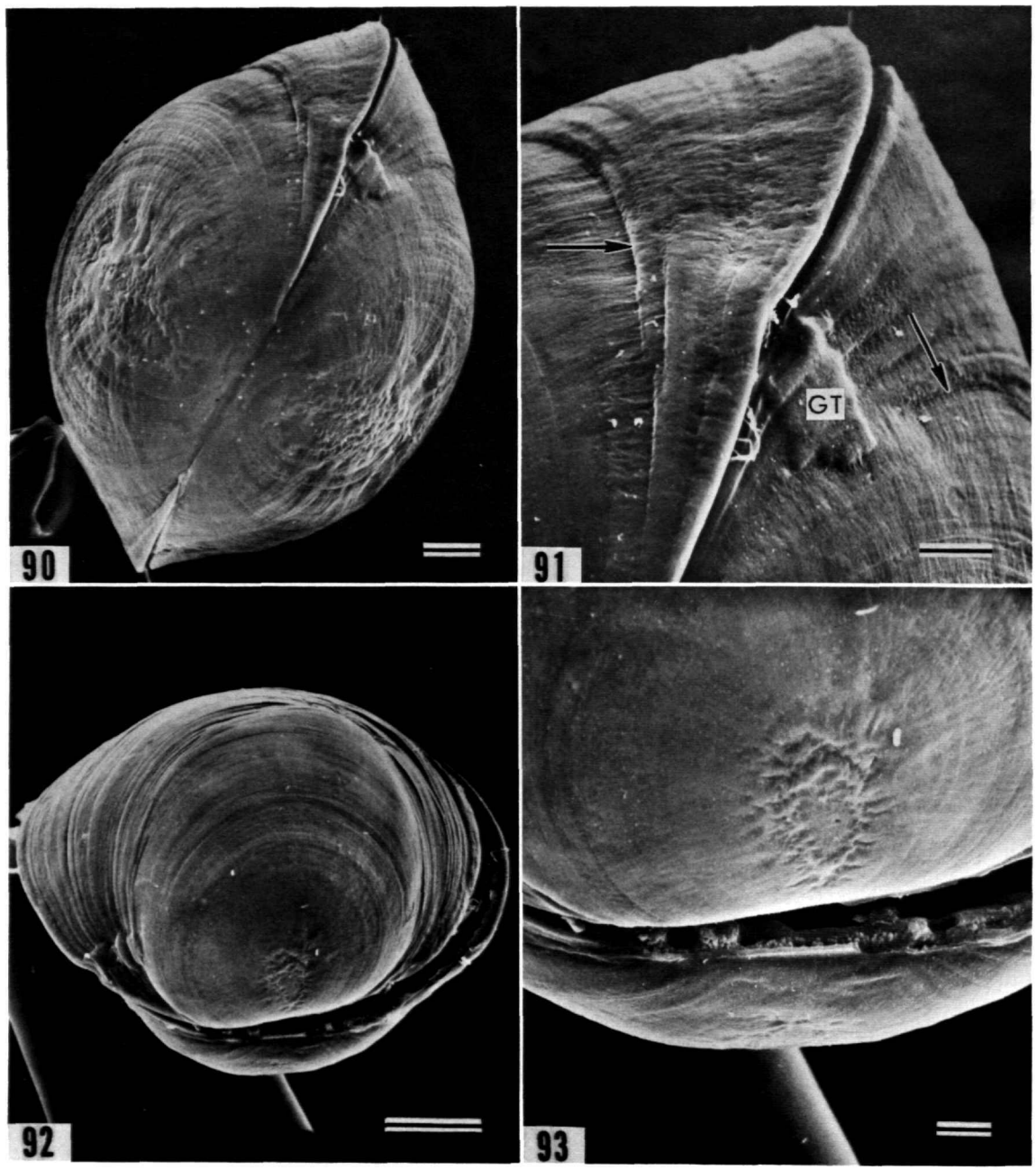

FIGURES 90–93.—*Ostrea edulis*, critical-point dried: 90, specimen 368B, early prodissoconch II, dorsal view (× 450, bar = 20 μm); 91, detail of Figure 90, posterodorsal notch and growth track (GT) and prodissoconch-I/II boundary (arrows) (× 1160, bar = 10 μm); 92, specimen 375B, middle prodissoconch II, left dorsal view (× 310, bar = 50 μm); 93, detail of Figure 92, prodissoconch-I region (× 820, bar = 10 μm).

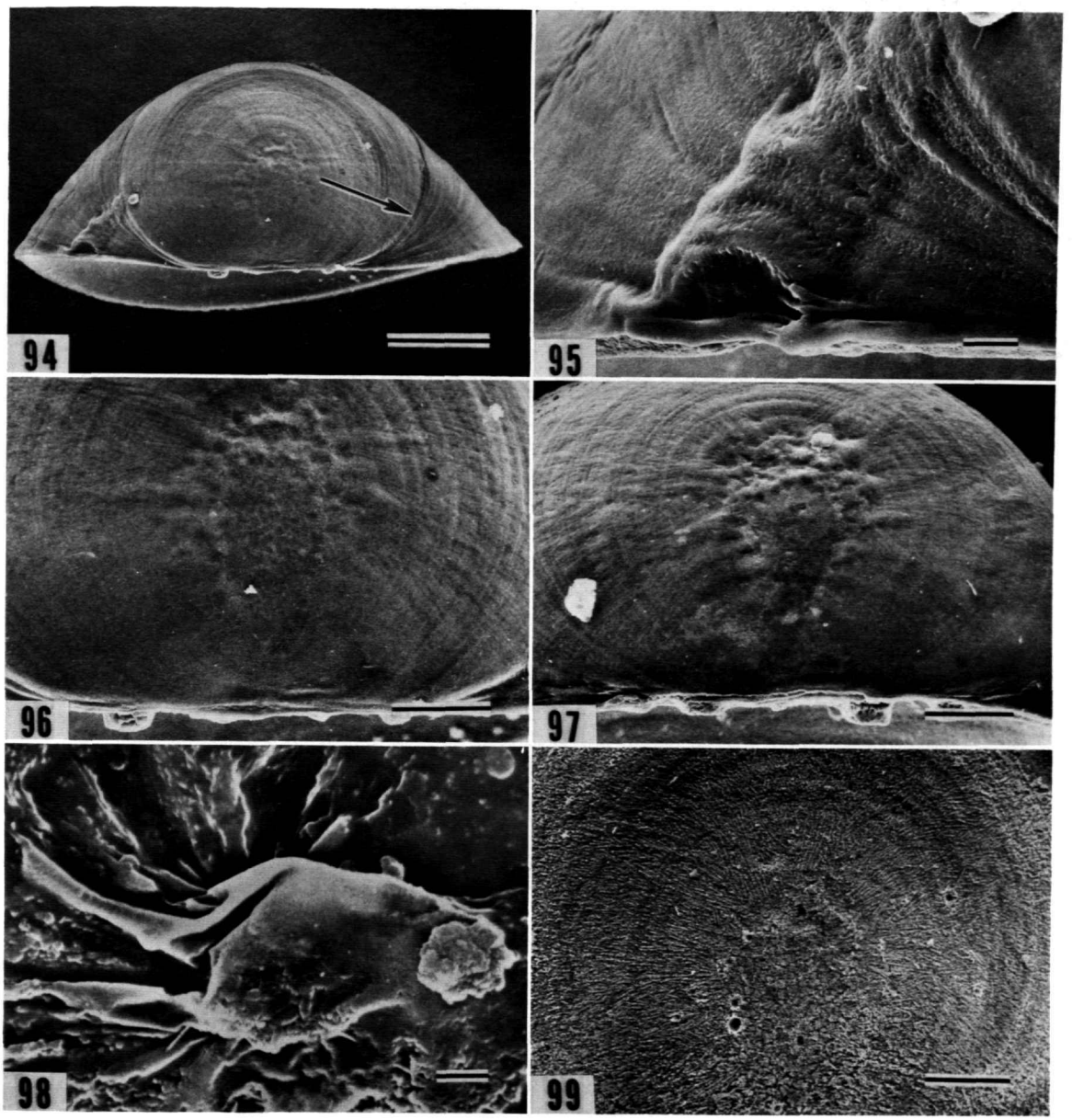

FIGURES 94–99.—*Ostrea edulis:* 94, specimen 387G, air dried, middle prodissoconch II, dorsal view of left valve, prodissoconch-I/II boundary (arrow) (× 310, bar = 50 μm); 95, detail of Figure 94, posterodorsal notch and growth track (× 1740, bar = 5 μm); 96, detail of Figure 94, pitted and stellate-radial zones (× 760, bar = 20 μm); 97, specimen 387E, early prodissoconch II, dorsal view of prodissoconch-I sculpture of right valve (× 740, bar = 20 μm); 98, specimen 385B, early dissoconch, right valve, folds in pitted zone of prodissoconch, hinge toward bottom (× 4000, bar = 2 μm); 99, specimen 388A, middle prodissoconch II, dorsal view of outer surface of prodissoconch-I region of left valve, periostracum removed (5% NaOCl, 43 hours) (× 680, bar = 20 μm).

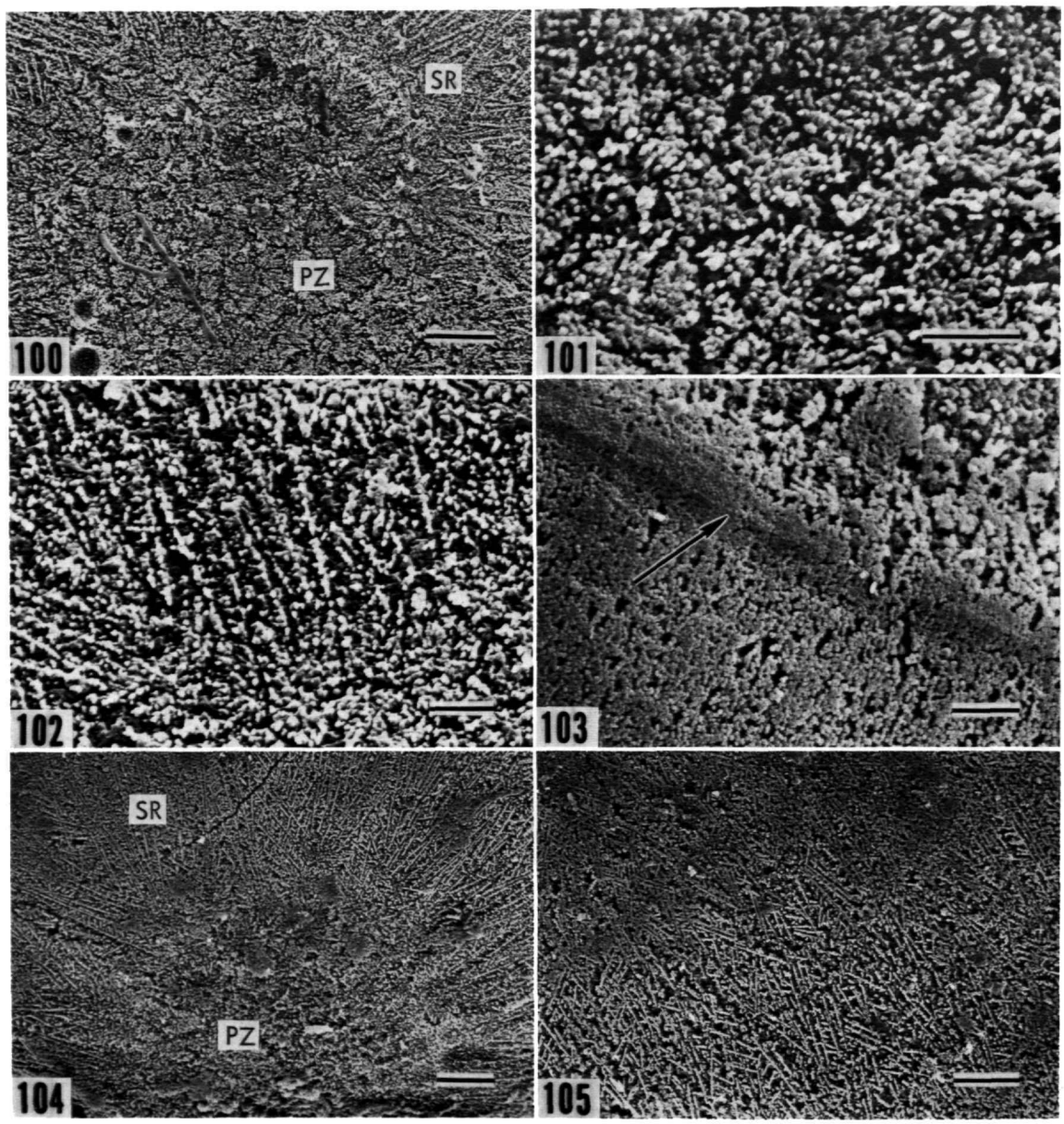

FIGURES 100–105.—*Ostrea edulis*, periostracum removed (5% NaOCl, 43 hrs.): 100, specimen 388A, mid-prodissoconch II, left valve, outer surface of pitted zone (PZ) and early stellate-radial zone (SR) (× 2060, bar = 5 μm); 101, detail of Figure 100, pitted zone (× 7500, bar = 2 μm); 102, detail of Figure 100, stellate radial zone, direction of growth toward upper left (× 5000, bar = 2 μm); 103, specimen 388A, outer surface of prodissoconch-II stage (lower left) adjacent to prodissoconch-I/II boundary (arrow) (× 5000, bar = 2 μm); 104, specimen 388B, early prodissoconch II, left valve, outer surface of pitted zone (PZ) and early stellate-radial zone (SR) (× 1700, bar = 5 μm); 105, specimen 388B, outer surface of middle stellate-radial zone, direction of growth toward lower right (× 2000, bar = 5 μm).

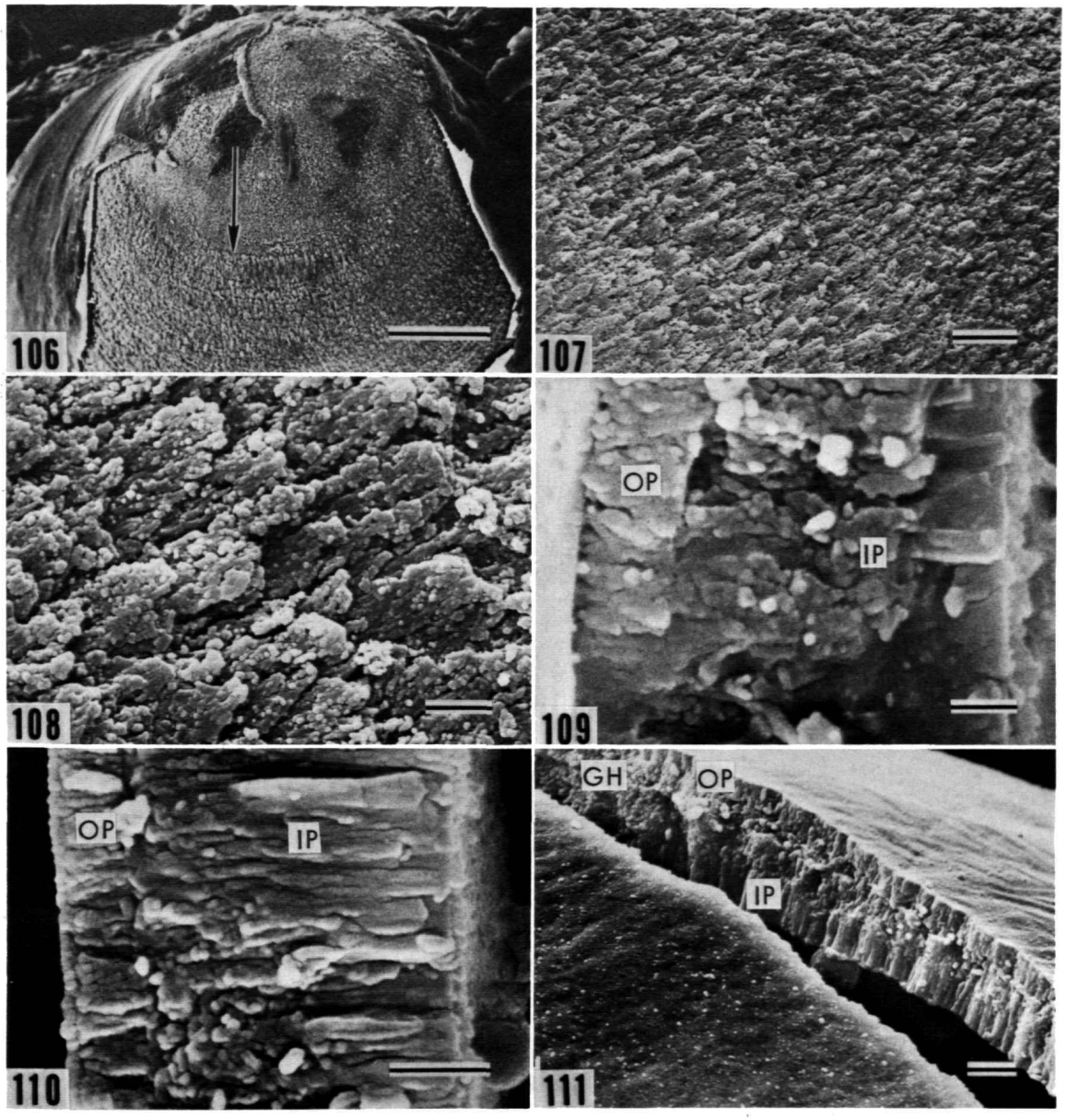

FIGURES 106–111.—*Ostrea edulis:* 106, specimen 384, left valve, periostracum and outermost shell layers partially removed by decay, prodissoconch-I/II boundary (arrow) (× 310, bar = 50 μm); 107, detail of Figure 106, granular laths of prodissoconch II, direction of growth to lower left (× 1000, bar = 10 μm); 108, detail of Figure 107 (× 5000, bar = 2 μm); 109, specimen 376C, mid-prodissoconch II, right valve, critical-point dried, radial fracture through pitted zone (× 20500, bar = 0.5 μm); 110, specimen 376C, radial fracture through early stellate-radial zone (× 15500, bar = 1 μm); 111, specimen 376C, fracture from early stellate-radial zone (lower right) to late stellate-radial zone (× 3800, bar = 2 μm) (OP = outer prismatic layer, GH = granular homogeneous layer, IP = inner prismatic layer).

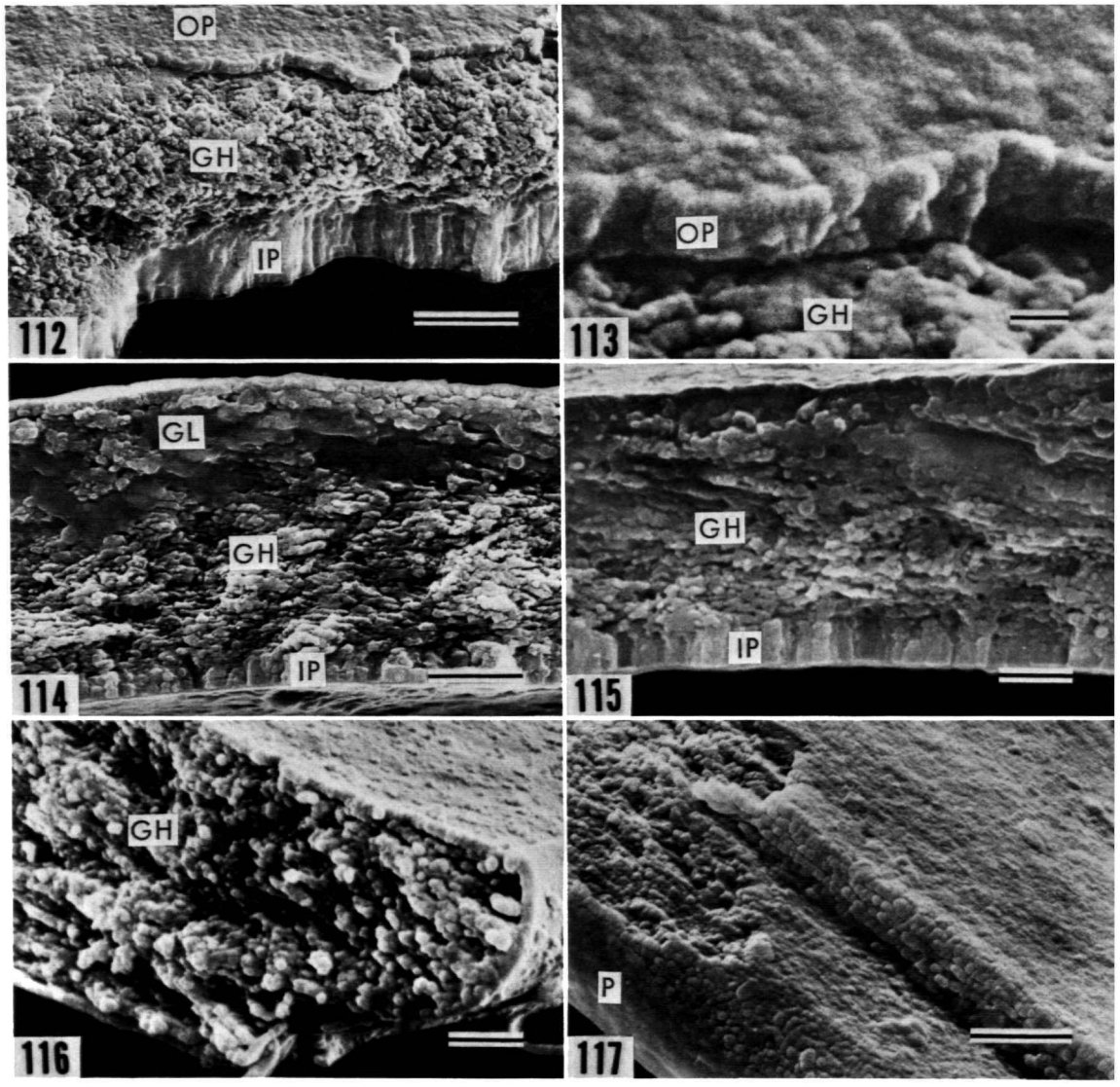

FIGURES 112–117.—*Ostrea edulis:* 112, specimen 387D, air dried, mid-prodissoconch II, right valve, commarginal fracture on distal side of prodissoconch-I/II boundary passing obliquely through vestige of outer prismatic layer (OP), granular homogeneous layer (GH), and inner prismatic layer (IP) (× 7600, bar = 2 μm); 113, detail of Figure 112 (× 41000, bar = 0.2 μm); 114, specimen 387D, fracture through prodissoconch-II stage perpendicular to shell surfaces but 45° to growth lines, outer granular homogeneous layer (GH), glue contamination (GL), inner prismatic layer (IP) (× 6800, bar = 2 μm); 115, specimen 387D, radial fracture through early prodissoconch-II stage, direction of growth to right (× 10500, bar = 1 μm); 116, specimen 377B, critical-point dried, late prodissoconch II, radial fracture through ventral margin of right valve, outer side toward upper right (× 10500, bar = 1 μm); 117, specimen 387E, air dried, mid-prodissoconch II, inner surface of anterior margin of right valve, periostracum (P) present near outer edge and removed elsewhere (× 7360, bar = 2 μm).

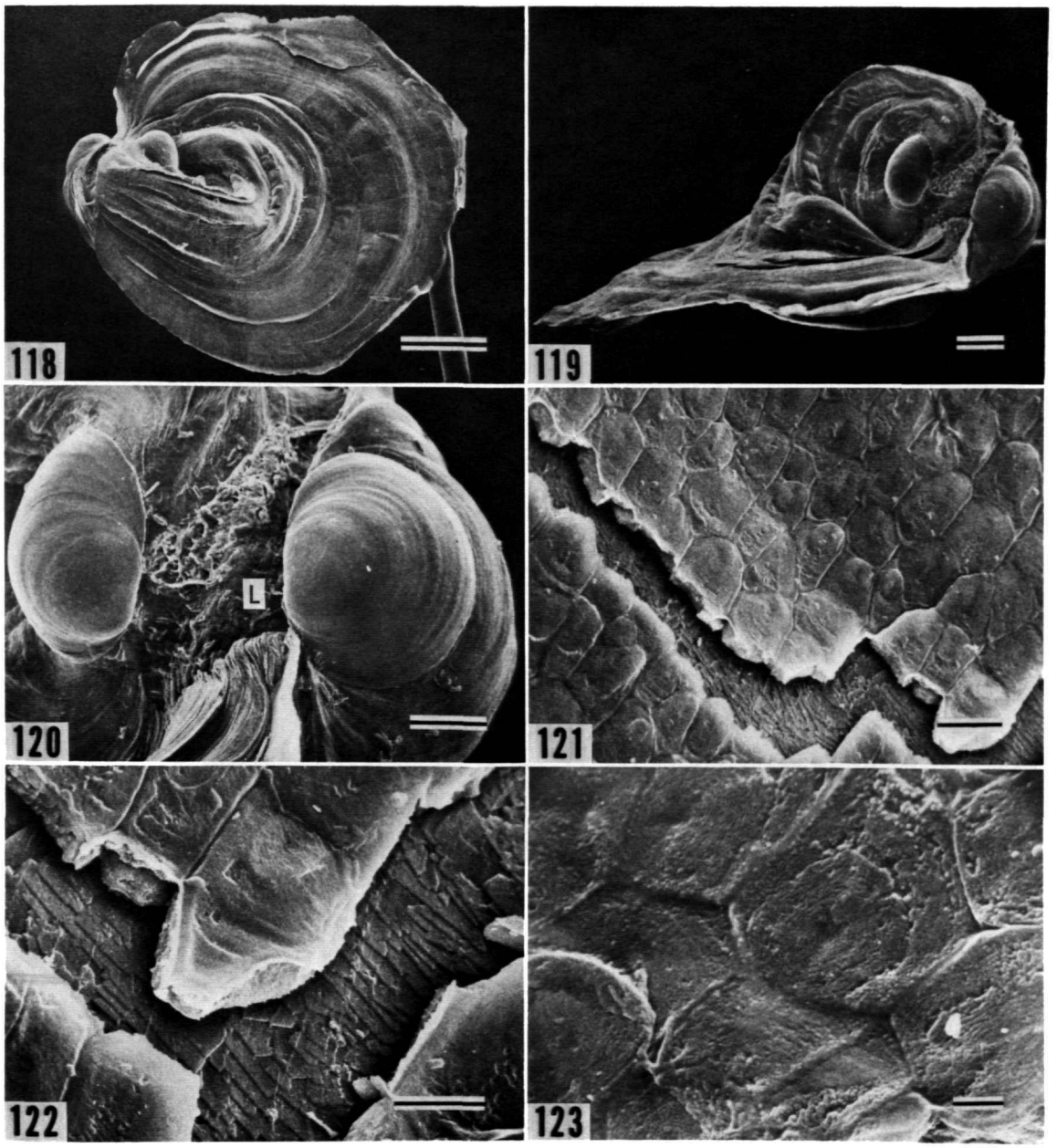

FIGURES 118–123.—*Ostrea edulis*, specimen 383, air dried, early dissoconch: 118, left side (× 27, bar = 500 μm); 119, dorsal view (× 38, bar = 200 μm); 120, detail of Figure 119, prodissoconch valves separated by dissoconch ligament area (L) (× 120, bar = 100 μm); 121, detail of Figure 118, near ventral edge, prismatic calcitic outer shell layer and underlying foliated calcite, direction of growth to lower left (× 1000, bar = 10 μm); 122, detail of Figure 121 (× 2760, bar = 5 μm); 123, outer surface of prismatic calcite of right valve showing accretionary lines on prism faces, direction of growth toward upper right (× 3900, bar = 2 μm).

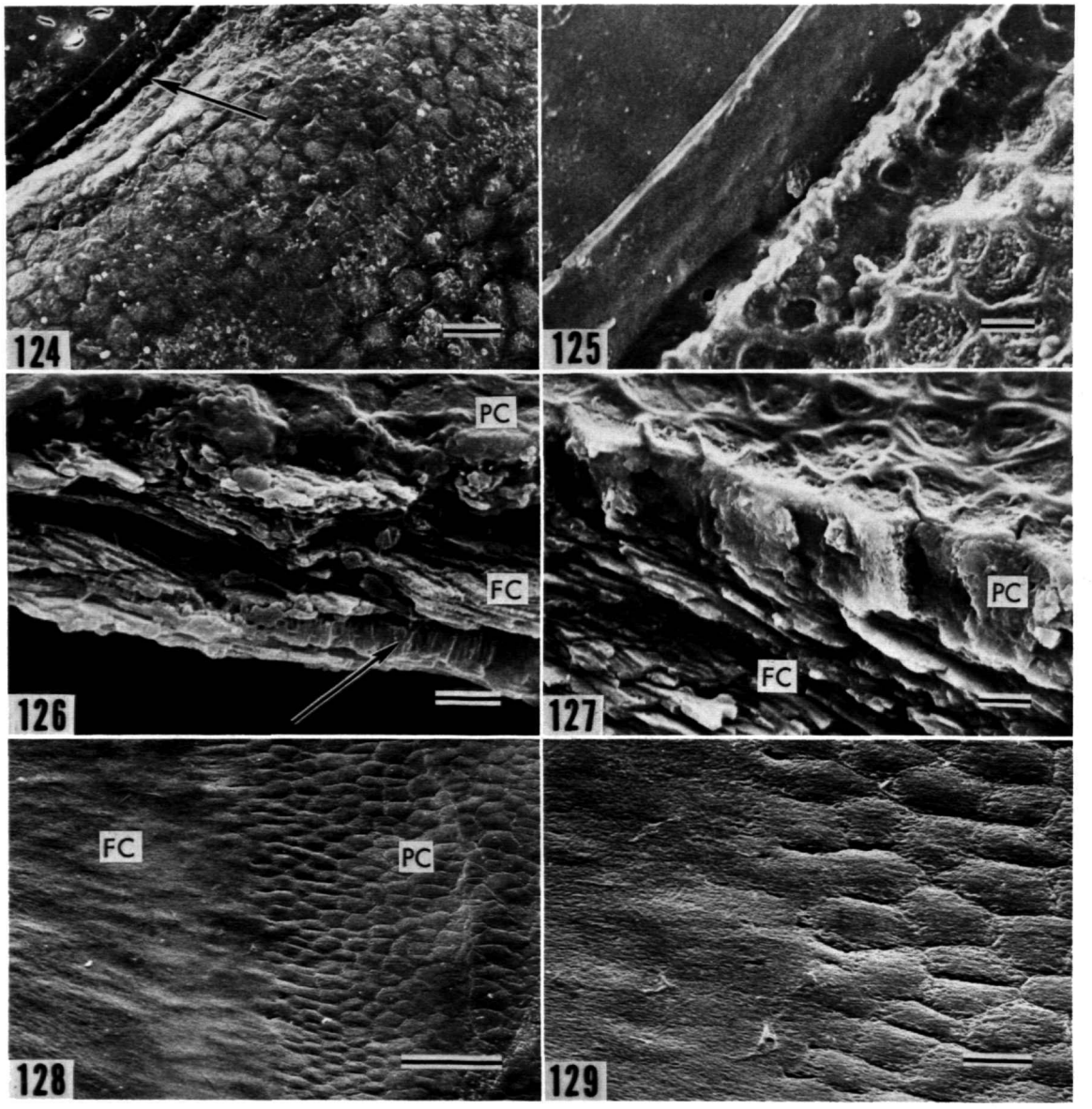

FIGURES 124–129.—*Ostrea edulis*, early dissoconchs, air dried: 124, specimen 384, outer surface of right valve at contact (arrow) between prodissoconch and dissoconch (× 840, bar = 10 μm); 125, detail of Figure 124 (× 4200, bar = 2 μm); 126, specimen 385B, radial fracture through early dissoconch of left valve, outer prismatic calcite (PC) underlain by foliated calcite (FC) and lens of adductor myostracum (arrow) (× 5500, bar = 2 μm); 127, specimen 385B, left valve, radial fracture, distal to lower right, outer prismatic calcite (PC) transitional to inner foliated calcite (FC) (× 4200, bar = 2 μm); 128, specimen 385B, oblique view of inner surface of right valve of dissoconch near ventral margin, prismatic calcitic outer layer (PC) and foliated inner layer (FC), direction of growth to right (× 300, bar = 50 μm); 129, detail of Figure 128 (× 1000, bar = 10 μm).

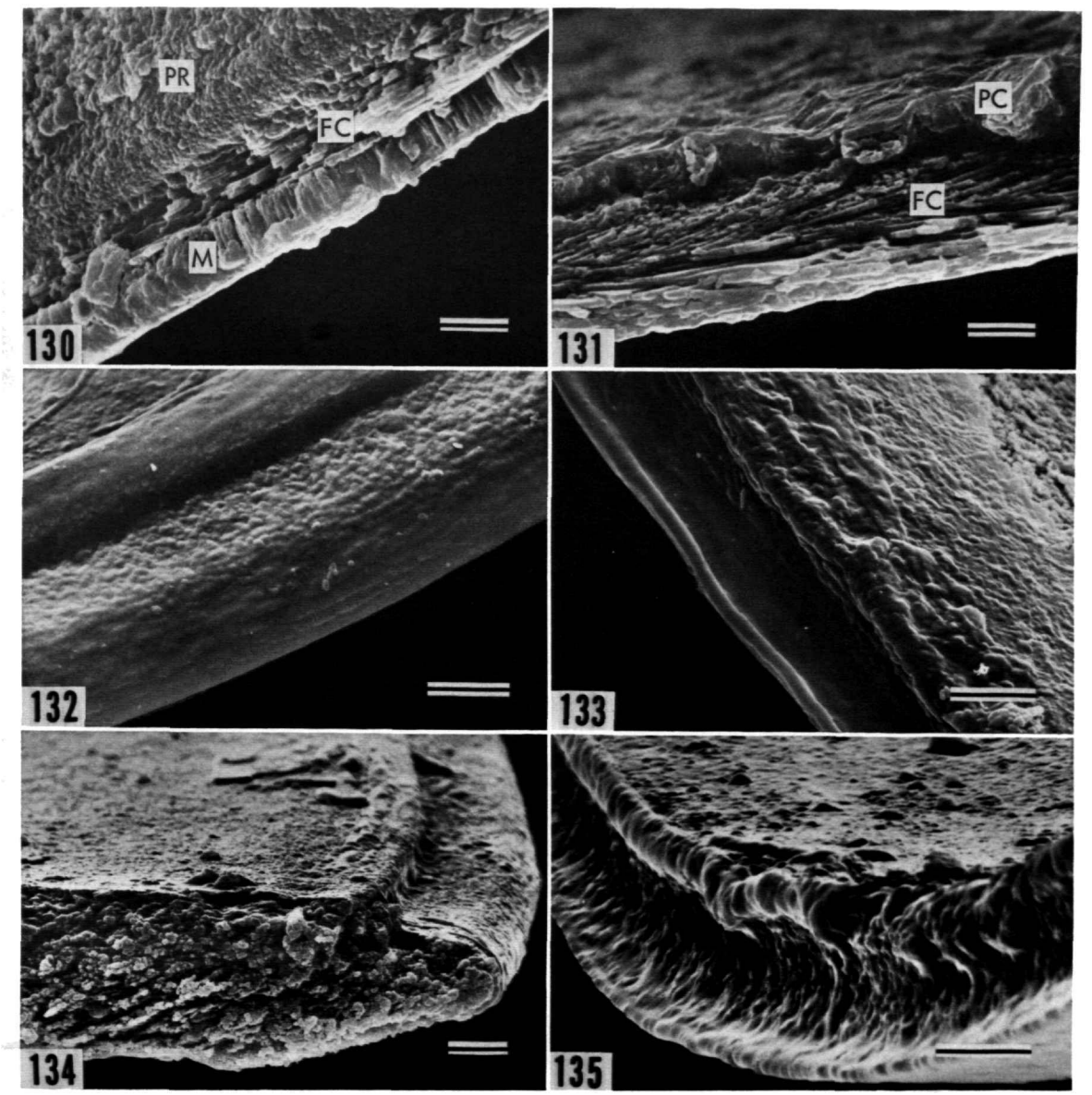

FIGURES 130–135.—*Ostrea edulis*, air dried: 130, specimen 385A, left valve of early dissoconch, commarginal fracture through dissoconch along margin of prodissoconch, myostracum (M) separated by foliated calcite (FC) from prodissoconch (PR) (× 5000, bar = 2 μm); 131, specimen 385A, radial fracture through early dissoconch, left valve, outer prismatic calcite (PC) underlain by foliated calcite (FC) (× 5000, bar = 2 μm); 132, specimen 387C, late prodissoconch II, inner side of right ventral margin, granular laths showing through thin periostracum (× 6200, bar = 2 μm); 133, specimen 387F, middle prodissoconch II, inner side of left ventral margin (× 6500, bar = 2 μm); 134, specimen 389L, middle prodissoconch II, radial fracture through right ventral margin, inner side at top (× 4450, bar = 2 μm); 135, specimen 387G, middle prodissoconch II, oblique view along ventral margin (× 7400, bar = 2 μm).

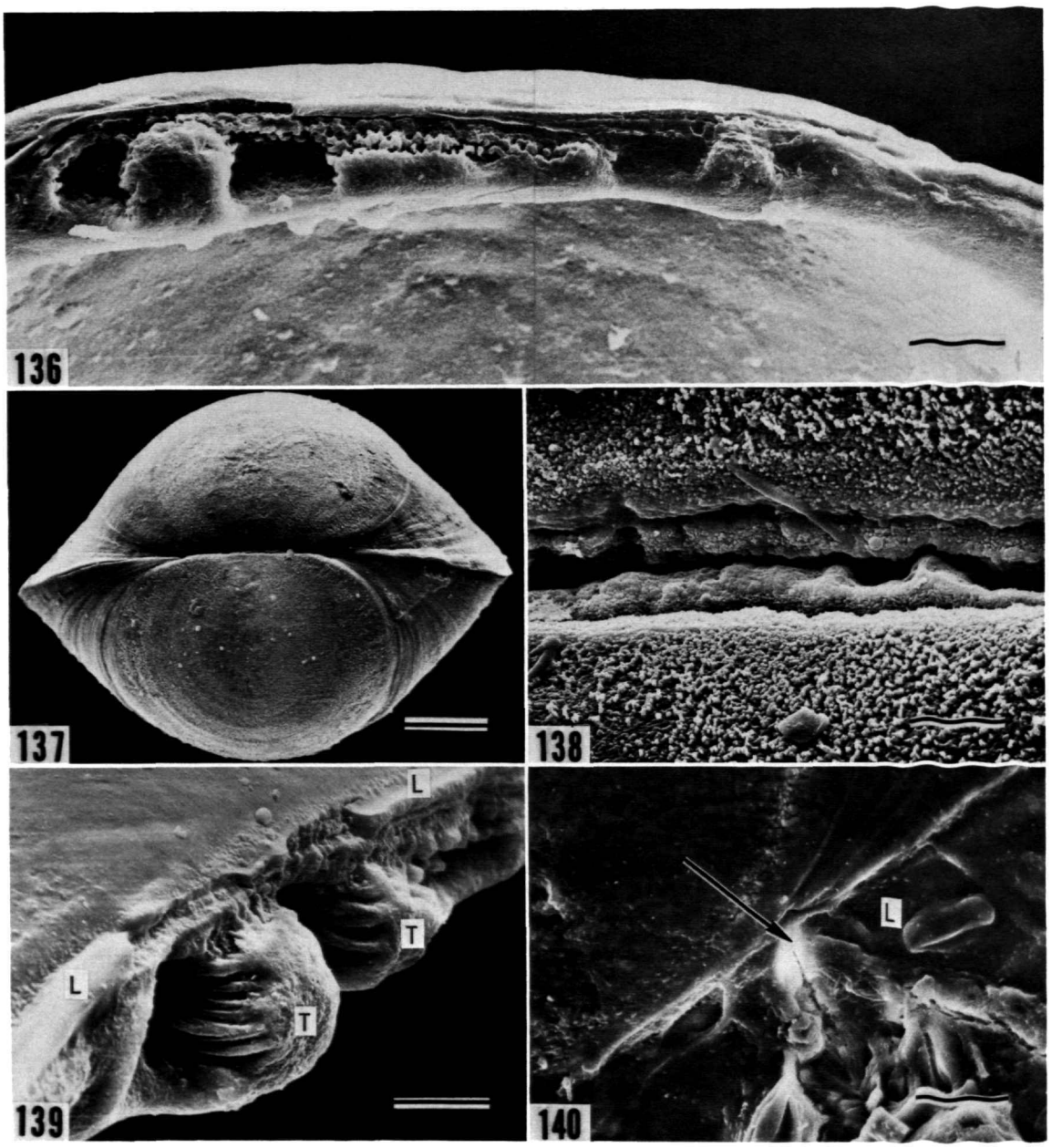

FIGURES 136–140.—*Ostrea edulis*, air dried: 136, specimen 387G, mid-prodissoconch II, left hinge (× 1450, bar = 10 μm); 137, specimen 388C, late prodissoconch II, periostracum removed (43 hrs. in 5% NaOCl), dorsal view of hinge, anterior to left (× 260, bar = 50 μm); 138, detail of Figure 137, central part of hinge between anterior and posterior teeth (× 3000, bar = 5 μm); 139, specimen 387F, mid-prodissoconch II, left valve, posterior hinge teeth (T) and periostracal ligament (L) (× 3000, bar = 5 μm); 140, specimen 385A, early dissoconch, ligament area (L) of left valve, origin of growth of resilium (arrow) (× 730, bar = 20 μm).

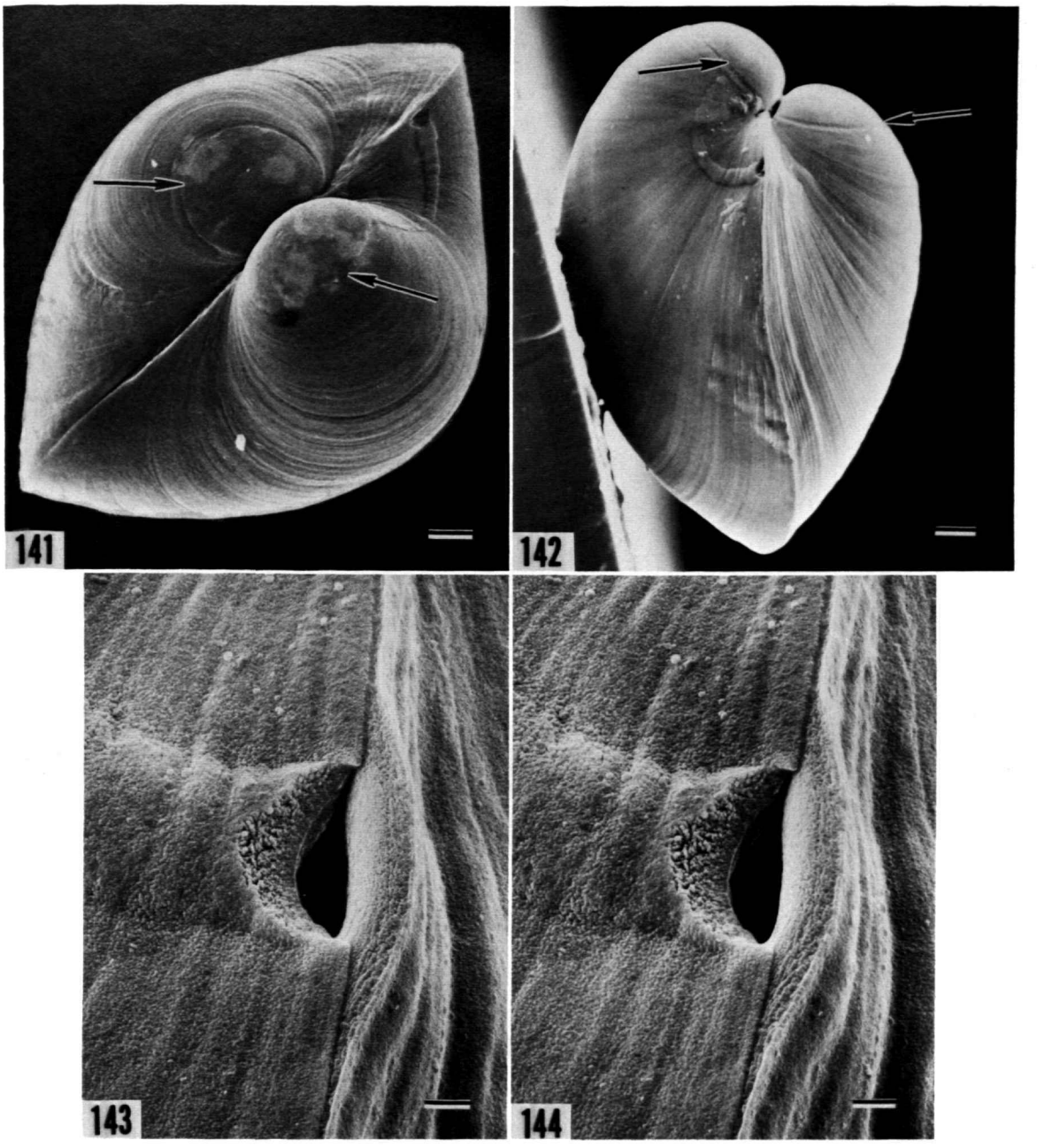

FIGURES 141–144.—*Crassostrea gigas*, late prodissoconch II: 141, specimen 362B, air dried, dorsal view, anterior toward lower left, prodissoconch-I/II boundary (arrows) (× 350, bar = 20 μm); 142, specimen 362A, air dried, posterior view, prodissoconch-I/II boundary (arrows) (× 325, bar = 20 μm); 143 and 144, specimen 367G, periostracum removed by plasma ashing, stereoscopic view of posterodorsal notch and interlocking valve margins (× 3400, bar = 2 μm).

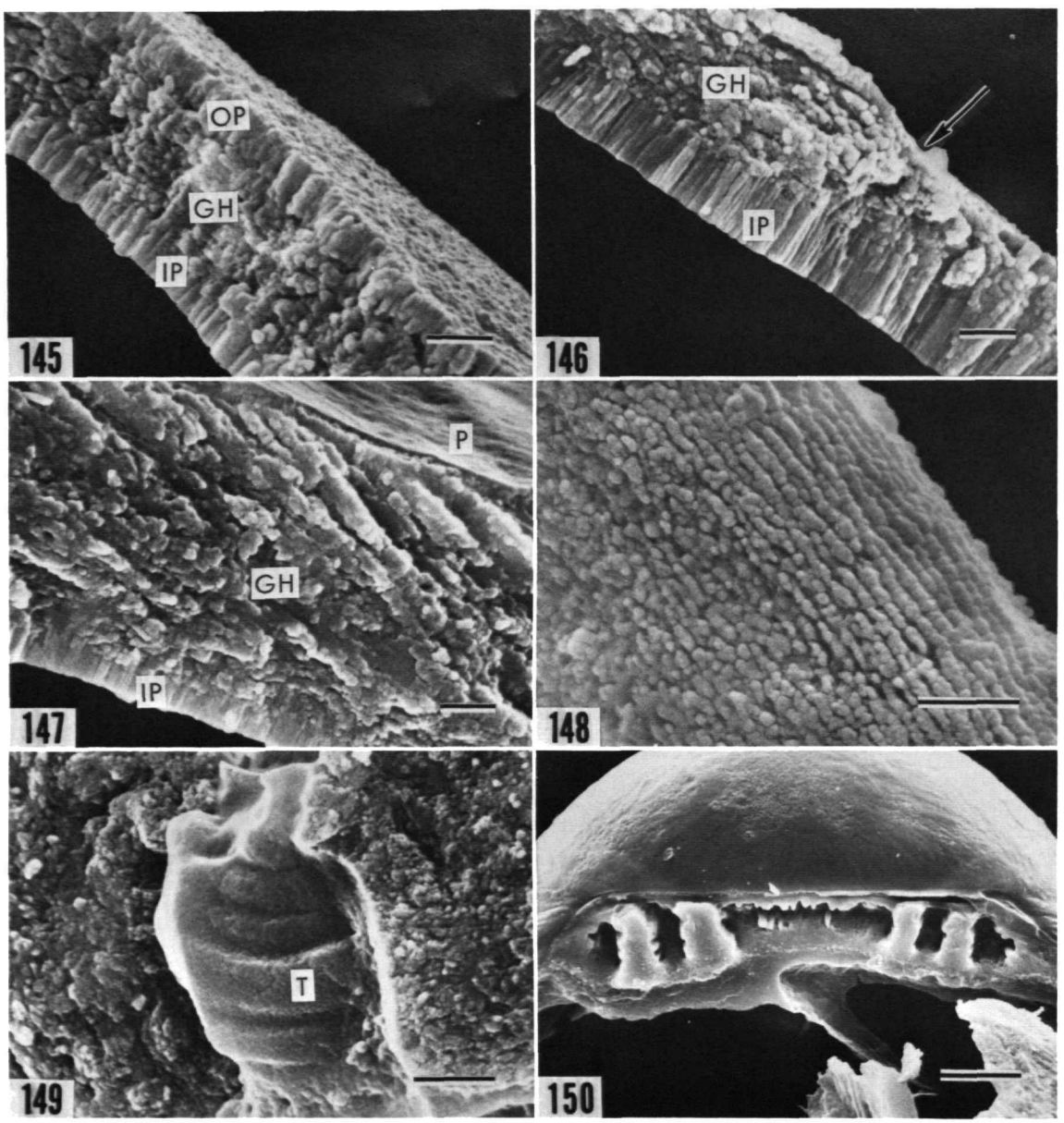

FIGURES 145–150.—*Crassostrea gigas*, middle and late prodissoconch II, air dried: 145, specimen 361G, radial fracture through prodissoconch-I stage, outer prismatic (OP), homogeneous (GH), and inner prismatic (IP) layers (× 10000, bar = 1 μm); 146, specimen 362D, radial fracture crossing prodissoconch-I/II boundary (arrow), homogeneous (GH) and inner prismatic (IP) layers, distal toward upper left (× 8700, bar = 1 μm); 147, specimen 361G, radial fracture through prodissoconch-II stage, periostracum (P), homogeneous layer (GH), and inner prismatic layer (IP), distal to right (× 8600, bar = 1 μm); 148, specimen 367A, inner surface of right posterodorsal edge, periostracum removed by plasma ashing (× 15400, bar = 1 μm); 149, specimen 362D, fracture perpendicular to hinge exposing posterior face of a hinge tooth (T) (× 6200, bar = 2 μm); 150, specimen 362K, hinge of left valve (× 1260, bar = 10 μm).

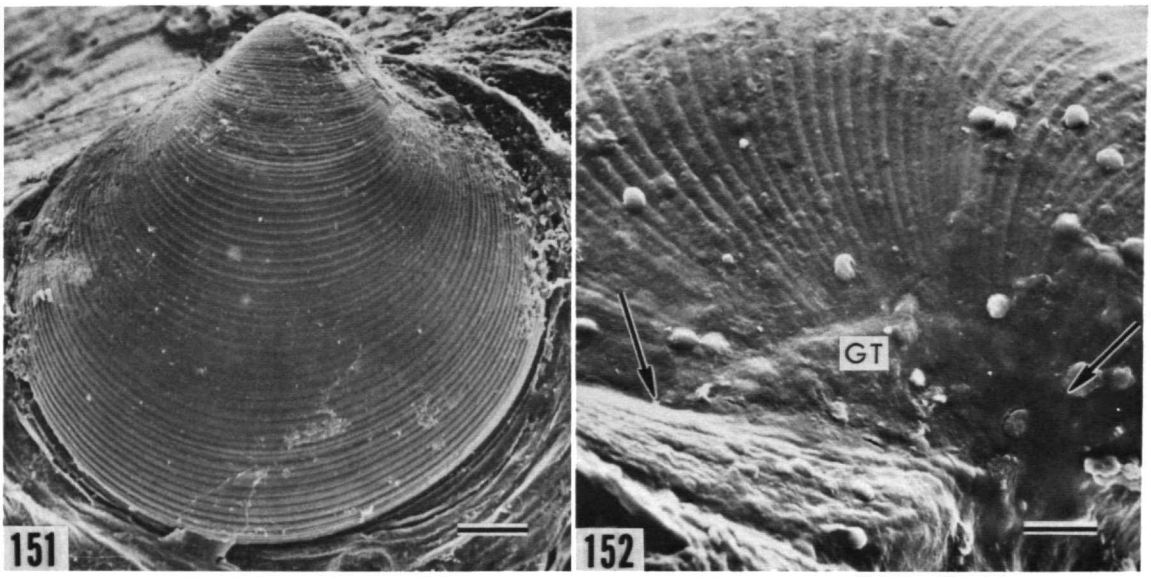

FIGURES 151–152.—*Neopycnodonte cochlear*, prodissoconchs preserved on beaks of mature shells: 151, USNM 196422, left valve (× 200, bar = 50 μm); 152, USNM 196422, left valve of another specimen, posterodorsal view of growth track (GT) of posterodorsal notch extending between prodissoconch-I/II boundary and prodissoconch-dissoconch boundary (arrows) (× 530, bar = 20 μm).

3. Injuries affecting both valve margins at the same point, which indicate that the valves closed on a foreign object or were injured simultaneously on both valve edges after being closed, are rare in the prodissoconch-I stage but common in the prodissoconch-II stage.

4. The prodissoconch-I/II boundary in *Ostrea edulis* appears to coincide approximately with time of release from parent, as indicated by specimens examined herein and by the material examined by Erdmann (1935). It is at this monent that complete valve closure would first be necessary for protection and survival.

The concept that the prodissoconch-I/II boundary represents the onset of valve closure facilitiates understanding the functional significance of some of the differences between oviparous and larviparous larvae. As pointed out by Ockelmann (1965), the size of prodissoconch I is correlated with size of egg. Oviparous species, which have a relatively small prodissoconch I, produce vast quantities of small eggs; larviparous species, with a relatively large prodissoconch I, produce relatively small quantities of much larger eggs. The prodissoconch I of larviparous bivalves is larger simply because an embryo of greater volume must be surrounded before valve closure is possible.

Although cell sizes may differ between the oviparous and larviparous groups and size itself is not an adequate indicator of rate of growth, evidence suggests that completion of the prodissoconch-I stage of larviparous individuals may take considerably longer than the corresponding stage of oviparous individuals [e.g., compare the seven-day brooding period of *Ostrea edulis* to the less-than-24-hour prodissoconch I of *Argopecten irradians*, an oviparous scallop (Waller, 1976; see also Amemiya, 1926)]. It is conceivable that in oviparous species small egg size evolved not only to balance high mortality with high numbers of potential progeny, but also to reduce the time

needed to achieve protection from a closed shell to a minimum by reducing the volume to be covered by the initial closure.

A striking feature of the larval oyster shell is the posterodorsal notch in the left-valve margin and the spiral track that this notch leaves on the exterior surface of the shell during its migration with shell growth. Observations reported above demonstrate that the notch forms exactly adjacent to the postanal ciliary tuft and also that the mantle edge and shell microstructure in the area of the notch are no different from those on either side of it. It thus appears that the beating of the postanal cilia actually deflects the thin periostracal envelope of the margin at this point, and that the deflection is made permanent by subsequent calcification.

Although the postanal tuft is medial in position, it is not likely that the cilia beat more strongly against one valve than the other. Why, then, is the notch much more prominent on the left valve than on the right? The answer seems to lie in the fact that the cross-sectional configurations of the valve margins differ, a thin sharp edge being present on the left side, a thick rounded edge on the right. Deflection of the left-valve margin probably requires less mechanical force than does deflection of the right.

As stated in the review of early development, the postanal tuft is a continuation of the telotroch present during the trochophore stage and thus is present throughout the prodissoconch-I phase of larval shell development. The sudden appearance of the notch at or near the prodissoconch-I/II boundary can readily be explained if the above cause of this boundary—that it represents the onset of valve closure—is valid. It is at this time that the valve margins would first be within reach of the beating postanal cilia. The notch disappears at the prodissoconch/dissoconch boundary, because the postanal tuft disappears at metamorphosis and the newly formed rectum extends the anus ventrally, away from the inner, dorsal wall of the mantle cavity as in mature oysters.

It appears that the posterodorsal notch is a prominent feature throughout the Ostreidae. It is unclear, however, why this feature is so strongly developed in oysters but absent or only very poorly developed in the plankototrophic larval shells of other bivalve groups. Thus far, a comparable but less well-developed feature has been observed only on a member of the Pholadacea (observable in Figure 2 of Calloway and Turner, 1979). It is not known whether absence of a posterodorsal notch results from differences in the position of the postanal tuft, in its degree of ciliation, or in the configurations of the shell margins.

Another striking feature of oyster larvae is the appearance of the bridge between the posterior extremities of the left and right gills well before metamorphosis and before the development of the gills themselves. As demonstrated above, this bridge may arise by fusion of cilia present on opposite mantle lobes of the veliger. Cells then grow medially from the mantle edge along the ciliary bridge, and a bridge of tissue is completed at a time when the gill primordia are first becoming differentiated from the mantle epithelium. Superficially, this gill bridge has the appearance of an adductor muscle and arises by the very process by which adductor muscles are thought to have originated during the course of molluscan evolution (Yonge, 1957). Here, however, it is unlikely that any muscle fibers are present in the bridge, and the actual adductors arise during the course of larval development in the mesoderm by the aggregation of free mesenchymal cells (Erdmann, 1935).

Summary and Conclusions

Scanning electron microscopy of anesthetized, critical-point dried veliger larvae of *Ostrea edulis* L. revealed many anatomical features of body and shell not previously observed by other techniques. In summary, these features are as follows.

Velum

1. The apical pit contains a tuft of fine, short cilia that barely project above the sides of the pit and are possibly sensory.

2. The apical pit is separated from the periphery of the velar crown by an expanse of nonciliated, microvillous epithelium. The periphery of the velum is girdled by four ciliary bands: an inner preoral band of fine cilia of unknown function, an outer preoral band of long compound cilia that function in locomotion and food gathering, an adoral band of fine cilia concerned with movement of food particles to the mouth, and a postoral band of compound cilia that appear to assist the cilia of the outer preoral band in trapping food and to adjust locomotory forces.

3. The locomotory cilia of the outer preoral band beat in a plane that is oblique to the velar margin. The obliquity and intensity of this beat more than counter the opposing rotational force imparted by laeoplectic metachronal waves, and the larva thus rotates in a clockwise direction.

4. The postoral tuft is a distinct structure of relatively rigid cilia and is not merely the posterior edge of the postoral ciliary band. The tuft is possibly sensory and may facilitate streaming of excess mucus and food posteriorly.

Foot

The heel and opening of the byssal-gland complex develop before the toe. The toe gradually bulges from the body wall and gradually becomes ciliated along its midline and finally over its entire surface. The opening of the cement-gland duct appears before the foot is fully formed.

Structures in Gill Cavities

1. Static-duct openings are continuously present throughout all stages studied and probably remain open until metamorphosis. Analysis of curvature of fixed cilia suggest that cilia in the lumen of a static duct beat inward toward the statocyst; long cilia fringing the ventral side of each duct opening beat dorsally, over the opening. These patterns support the idea that early statoliths and statoconia may originate externally.

2. Cerebral eyes, which in *Ostrea edulis* become pigmented late in the veliger stage, originate very early, probably before release from parent. In early veligers they are hemispherical tufts of microvilli. Later, these tufts submerge in the epithelium, eventually becoming cup-shaped eyes.

3. A pitlike ciliated structure near each eye is possibly an opening of a protonephridial duct.

Gill Primordia

The gill bridge, which in mature *Ostrea edulis* connects the posterior ends of left and right gills to one another, appears early in veliger development. It originates by cross-fusion of tufts of cilia formed at the edge of opposite mantle lobes. Epithelial cells gradually migrate along the bridge and fuse at the midline, producing a bridge that is at first both ciliary and epithelial and later completely epithelial. The mode of formation is precisely like that hypothesized for bivalve adductors, but here there are no muscle cells involved, and the larval adductors originate during development by an altogether different process.

The gill primordia begin as anterior-posterior ridges of epithelium; filament primordia in the form of transverse ridges on the initial ridge develop later. Asymmetry begins in the mid-veliger stage, with the right gill primordium having fewer primordial filaments than the left. Structures interpreted as mucus glands are already present between the filament primordia. Although it is doubtful that the gills are functional at this early stage, the basic incurrent-excurrent pattern through the mantle cavity seems to be established.

Anal Region and Posterodorsal Shell Notch

Feces are formed by compaction of waste in the lumen of the gut and rectum and are moved by ciliary action through the anus, which is offset to the left of the midline. Fecal material is forcefully ejected to the exterior in a trajectory that crosses the plane of commissure toward the right side of the shell. At least part of the expulsive

force is generated by the postanal ciliary tuft, which lies dorsal to the anus along the posterodorsal margin of the shell. The action of cilia of this tuft also deforms the shell margin, particularly the margin of the left valve, which is more deformable than the margin of the right valve. The result is a distinct posterodorsal notch and growth track on the left valve. The notch originates at the prodissoconch-I/II boundary, because this boundary marks the onset of valve closure and contact between valve margins and the postanal ciliary tuft. The notch disappears at the prodissoconch-dissoconch boundary, because the postanal ciliary tuft disappears at metamorphosis.

Mantle Edge

The mantle edge is two-fold through all veliger stages. The leading edge of the inner fold has long microvilli, some of which appear to be embedded in the periostracum. This fold also has scattered cilia. The outer fold, which lies beneath the newly generated periostracum, attenuates to a sharp edge consisting of long, densely matted microvilli or cell processes. The outer surface of the outer fold is covered with long microvilli, many of which remain embedded in the shell after the mantle is removed. Mantle contraction in dried specimens suggests that radial muscles in the mantle are not present until the mid-veliger stage. These muscles appear to insert into the shell along a commarginal pallial line, as in mature bivalves.

Shell

Exterior microsculptural patterns and microstructure of the shell both reveal a progression of changes during the ontogeny of the prodissoconch that can be explained in terms of a gradually enlarging and differentiating shell gland and mantle. The prodissoconch begins at two centers of calcification on a single periostracal sheet after the invaginated stage of the shell gland. These centers have a pitted appearance on the exterior; gentle removal of the periostracum by plasma ashing reveals a polygonal pattern of tiny crystals beneath the periostracum. Thereafter, beneath a stellate-radial external sculpture, calcification is marginal and incremental, the increments possibly reflecting physiological irregularities in the mantle cavity of the parent in which the larva develops.

Fracture sections show that the shell becomes three-layered during the prodissoconch-I stage, with the middle layer beginning as little more than a discontinuity between outer and inner prismatic layers. This middle layer increases in prominence in prodissoconch I and finally dominates the structure of the shell in prodissoconch II.

An hypothesis of cellular differentiation of the mantle edge, advanced to explain the changing shell microstructures, leads to the conclusion that the change from shell gland to mantle is gradual and that it occurs well before the prodissoconch-I/II boundary.

The fine aragonitic microstructures of the prodissoconch change abruptly to relatively coarse prismatic and foliated calcitic microstructures in the dissoconch. The foliated structure extends inward and covers the inner surface of the prodissoconch. Myostracal layers appear in the earliest dissoconch and may be continuous with the inner prismatic layer of the larval shell. This suggests that attachment of mantle to larval shell may have features in common with postlarval adhesive mantle.

Hinge teeth develop primarily during the prodissoconch-II stage and have curved ridges on their sides that offset shear between partially closed valves as in mature bivalves. The early ligament is formed by the periostracum; the resilium does not appear until near or possibly after metamorphosis. When the resilium appears, it is anterior to the anterior larval hinge teeth, not in the center of the larval hinge as shown in some previous studies. The margins of prodissoconch II fit together in tongue-in-groove fashion to provide a tight seal and to prevent shear between closed valves.

On the basis of a limited comparison, many of the features of the larval shell of *Ostrea edluis* are also present in the larval shells of other oyster species: pitted and stellate-radial sculptural patterns of prodissoconch I, configuration and ontogeny of shell microstructures, interlocking valve margins, posterodorsal notch and growth track and its ontogeny, and basic pattern of hinge teeth and ligament. Important differences, however, separate species in oviparous and larviparous groups. Compared to the larval shells of larviparous species, those of oviparous species have a much smaller prodissoconch I compared to prodissoconch II. As a result of greater coiling during the prodissoconch-II stage, oviparous larval shells also have a more convex shape, with umbones overhanging the hinge line further. Fine incremental growth lines, present on prodissoconch I of *O. edulis*, appear to be absent from prodissoconch I of oviparous species. Important differences between species also occur in the ontogeny of hinge teeth.

The prodissoconch-I/II boundary has been explained in the past as the result of a change in mode of calcification from that by shell gland to that by the mantle. However, the actual differentiation of the mantle edge appears to precede the boundary, and the sharpness of the boundary is not at all reflected in the transitional change from shell gland to mantle. Instead, evidence detailed here for the first time suggests that the boundary marks the onset of valve closure.

Precisely how these observations should enter into an interpretation of the evolution of oysters is unclear at present, because as yet there are no comparable details on larvae of other bivalves. It is likely, however, that as study of other groups both by scanning and transmission electron microscopy progresses, a comparative anatomy will eventually develop that will allow, for the first time, assessment of the role of larvae in the evolutionary diversification of the Bivalvia.

Literature Cited

Allen, J. A.

1961. The Development of *Pandora inaequivalvis* (Linné). *Journal of Embryology and Experimental Morphology*, 9(2):252–268, 5 figures, 2 tables.

Amemiya, I.

1926. Notes on Experiments on the Early Developmental Stages of the Portuguese, American and English Native Oysters, with Special Reference to the Effect of Varying Salinity. *Journal of the Marine Biological Association of the United Kingdom*, 14(1): 161–175, 1 figure, 6 tables.

Anderson, T. F.

1951. Techniques for the Preservation of Three-dimensional Structures in Preparing Specimens for the Electron Microscope. *Transactions of the New York Academy of Science*, series 2, 13(3):130–133.

1956. Electron Microscopy of Micro-organisms. *In* G. Oster and A. Pollistor, editors, *Physical Techniques in Biological Research*, volume 3 (*Cells and Tissues*), chapter 5, pages 177–240, 22 figures, 1 table. New York: Academic Press.

Ansell, A. D.

1962. The Functional Morphology of the Larva, and the Post-larval Development of *Venus striatula* (Da Costa). *Journal of the Marine Biological Association of the United Kingdom*, 42(2):419–443, 13 figures.

Barber, V. C.

1968. The Structure of Mollusc Statocysts, with Particular Reference to Cephalopods. *Symposia of the Zoological Society of London*, number 23:37–62, 15 figures.

Becker, R. P., and O. Johari

1978. *Scanning Electron Microscopy—1978*. Volume 2, 1134 pages. AMF O'Hare, Illinois: Scanning Electron Microscopy, Inc. [Post Office Box 66507].

Bernard, F.

1896. Deuxième Note sur le developpement et la morphologie de la coquille chez les Lamellibranches (Taxodontes). *Bulletin de la Societe Geologique de France*, series 3, 24:54–82, 15 figures.

Boyde, A.

1978. Pros and Cons of Critical Point Drying and Freeze Drying for SEM. *In* R. P. Becker and O. Johari, editors, *Scanning Electron Microscopy—1978*, 2:303–314. AMF O'Hare, Illinois: Scanning Electron Microscopy, Inc. [Post Office Box 66507].

Boyle, P. J., and R. D. Turner

1976. The Larval Development of the Wood Boring Piddock *Martesia striata* (L.) (Mollusca: Bivalvia: Pholadidae). *Journal of Experimental Marine Biology and Ecology*, 22:55–68, 4 figures, 2 tables.

Brach, J.

1690. Observ. CCIII, De ovis Ostreorum. *Ephemeridum Academia Leopoldina Naturae Curiosorum*, VIII:506–508.

Brooks, W. K.

1880. The Development of the Oyster (*Ostrea virginiana* [sic] List). *Johns Hopkins University, Studies from the Biological Laboratory*, 4:1–83, 10 plates.

Buddenbrock, W. von

1915. Die Statocyste von *Pecten*, ihre Histologie und Physiologie. *Zoologisches Jahrbuch Abteilung für allgemeine Zoologie und Physiologie*, 35:301–356, 15 figures, plates 7–8.

Calloway, C. B., and R. D. Turner

1979. New Techniques for Preparing Shells of Bivalve Larvae for Examination with the Scanning Electron Microscope. *Bulletin of the American Malacological Union for 1978*, pages 17–24, 3 plates.

Carazzi, D.

1902. Contributo all'istologia e alla fisiologia dei Lamellibranchi. *Internationale Monatsschrift für Anatomie und Physiologie*, 20:57–87, 5 figures, plates 3 and 4.

Carriker, M. R.

1961. Interrelation of Functional Morphology, Behavior, and Autecology in Early Stages of the Bivalve *Mercenaria mercenaria*. *Journal of the Elisha Mitchell Scientific Society*, 77(2):168–241, 39 figures, 13 tables.

Carriker, M. R., and R. E. Palmer

1979a. Ultrastructural Morphogenesis of Prodissoconch and Early Dissoconch Valves of the Oyster *Crassostrea virginica*. *Proceedings of the National Shellfisheries Association*, 69:103–128, 63 figures.

1979b. A New Mineralized Layer in the Hinge of the Oyster. *Science*, 206:691–693, 2 figures, 1 table.

Cather, J. N.

1967. Cellular Interactions in the Development of the Shell Gland of the Gastropod, *Ilyanassa*. *The Journal of Experimental Zoology*, 166(2):205–223, 24 figures.

Cole, H. A.

1938. The Fate of the Larval Organs in the Metamorphosis of *Ostrea edulis*. *Journal of the Marine Biological*

Association of the United Kingdom, 22:469–484, 8 figures.

Cragg, S. M., and J. A. Nott
1977. The Ultrastructure of the Statocysts in the Pediveliger Larvae of *Pecten maximus* (L.) (Bivalvia). *Journal of Experimental Marine Biology and Ecology*, 27(1):23–36, 14 figures, 1 table.

Cranfield, H. J.
1973a. A Study of the Morphology, Ultrastructure, and Histochemistry of the Foot of the Pediveliger of *Ostrea edulis*. *Marine Biology*, 22(3):187–202, 16 figures, 3 tables.
1973b. Observations on the Behaviour of the Pediveliger of *Ostrea edulis* during Attachment and Cementing. *Marine Biology*, 22(3):203–209, 2 figures, 2 tables.
1973c. Observations on the Function of the Glands of the Foot of the Pediveliger of *Ostrea edulis* during Settlement. *Marine Biology*, 22(3):211–223, 13 figures, 4 tables.
1974. Observations on the Morphology of the Mantle Folds of the Pediveliger of *Ostrea edulis* L. and Their Function during Settlement. *Journal of the Marine Biological Association of the United Kingdom*, 54:1–12, 4 figures, 2 plates, 1 table.
1975. The Ultrastructure and Histochemistry of the Larval Cement of *Ostrea edulis* L. *Journal of the Marine Biological Association of the United Kingdom*, 55:497–503, 1 figure, 3 plates, 1 table.

Culliney, J. L., P. J. Boyle, and R. D. Turner
1972. New Approaches and Techniques for Studying Bivalve Larvae. *In* W. L. Smith and M. H. Chanley, editors, *Culture of Marine Invertebrate Animals*, pages 257–271, 2 figures. New York: Plenum Publishing Corp.

Dantan, J.-L.
1916. La Larve de *l'Ostrea edulis* (L.). *Annales de L'Institut Oceanographique (Foundation Albert I^er^, Prince de Monaco)*. 7(6): 20 pages, 3 figures, 2 plates.

Davaine, C.
1853. Recherches sur la génération des huitres. *Comptes Rendus des Séances et Mémoires de la Société de Biologie, Paris*, series 1, 4(1852):297–339, 2 plates.

Demian, E. S., and F. Yousif
1973a. Embryonic Development and Organogenesis in the Snail *Marisa cornuarietis* (Mesogastropoda: Ampullariidae), I: General Outlines of Development. *Malacologia*, 12(1):123–150, 24 figures, 1 table.
1973b. Embryonic Development and Organogenesis in the Snail *Marisa cornuarietis* (Mesogastropoda: Ampullariidae), IV: Development of the Shell Gland, Mantle and Respiratory Organs. *Malacologia*, 12(2):195–211, 13 figures.

Dinamani, P.
1973. Embryonic and Larval Development in the New Zealand Rock Oyster, *Crassostrea glomerata* (Gould). *The Veliger*, 15(4):295–299, 19 figures, 1 table.
1976. The Morphology of the Larval Shell of *Saccostrea glomerata* (Gould, 1850) and a Comparative Study of the Larval Shell in the Genus *Crassostrea* Sacco, 1897 (Ostreidae). *Journal of Molluscan Studies*, 42: 95–107, 7 figures.

Eakin, R. M.
1965. Evolution of Photoreceptors. In *Cold Spring Harbor Symposia on Quantitative Biology*, 30:363–370, 2 figures. Cold Spring Harbor, Long Island, N. Y.: Cold Spring Harbor Laboratory of Quantitative Biology.

Erdmann, W.
1935. Untersuchungen über die Lebensgeschichte der Auster, 5: Über die Entwicklung und die Anatomie der "Ansatzreifen" Larve von *Ostrea edulis* mit Bemerkungen über die Lebensgeschichte der Auster. *Wissenschaftliche Meeresuntersuchungen Kommission zur Wissenschaftlichen Untersuchung der Deutschen Meere in Kiel und der Biologischen Anstalt auf Helgoland*, new series, 19(6): 25 pages, 5 figures, 8 plates.

Fernando, W.
1931. The Origin and Development of the Pericardium and Kidneys in *Ostrea*. *Proceedings of the Royal Society of London*, series B, 107(752):391–397, plates 29–32.

Fujita, T.
1929. On the Early Development of the Common Japanese Oyster. *Japanese Journal of Zoology*, 2(3):353–358, plate 7.
1934. Note on the Japanese Oyster Larva. In *Proceedings of the Fifth Pacific Sciences Congress, Canada 1933*, 5: 4111–4117, 5 figures, 1 table. Toronto: University of Toronto Press.

Galtsoff, P. S.
1964. The American Oyster. *United States Department of the Interior, Fish and Wildlife Service, Bureau of Commercial Fisheries, Fishery Bulletin*, 164: iii + 480 pages, 400 figures, 46 tables.

Gordon, J., and M. R. Carriker
1978. Growth Lines in a Bivalve Mollusk: Subdaily Patterns and Dissolution of the Shell. *Science*, 202: 519–521, 4 figures.

Gray, J.
1928. *Ciliary Movement*. viii + 162 pages, 105 figures, 16 tables. Cambridge: Cambridge University Press.
1930. The Mechanism of Ciliary Movement, VI: Photographic and Stroboscopic Analysis of Ciliary Movement. *Proceedings of the Royal Society of London*, series B, 107(751):313–332, 10 figures, plates 20–22.

Hatschek, B.
1880. Ueber Entwicklungsgeschichte von *Teredo*. *Arbeiten aus dem Zoologischen Institute der Universität Wien und der Zoologischen Station in Triest*, 3(1):1–44, 3 plates.

Hickman, R. W., and Ll. D. Gruffydd
1971. The Histology of the Larva of *Ostrea edulis* during Metamorphosis. In *Fourth European Marine Biology Symposium, Bangor, Wales, 1969*, pages 281–294, 4 figures. Cambridge: Cambridge University Press.

Hori, J.
1933. On the Development of the Olympia Oyster, *Ostrea lurida* Carpenter, Transplanted from United States to Japan. *Bulletin of the Japanese Society of Scientific Fisheries*, 1(6):269–276, 17 figures.

Horst, R.
1883–1884. The Development of the Oyster (*Ostrea edulis* L). [Translation from Dutch by Herman Jacobson.] *United States Commission of Fish and Fisheries, Report of the Commissioner for 1884*, part 12 [1886]: 891–910, 2 plates.

Knight-Jones, E. W.
1954a. Notes on Invertebrate Larvae Observed at Naples during May and June. *Pubblicazioni della Stazione Zoologica di Napoli*, 25(1):135–144, 2 figures, 1 table.
1954b. Relations between Metachronism and the Direction of Ciliary Beat in Metazoa. *Quarterly Journal of Microscopical Science*, 95:503–521.

Kniprath, E.
1977. Zur Ontogenese des Schalenfeldes von *Lymnaea stagnalis*. *Wilhelm Roux's Archives of Developmental Biology*, 181:11–30, 7 figures.
1979. The Functional Morphology of the Embryonic Shell-Gland in the Conchiferous Molluscs. *Malacologia*, 18:549–552, 2 figures.

Korringa, P.
1941. Experiments and Observations on Swarming, Pelagic Life and Setting in the European Flat Oyster, *Ostrea edulis* L. [Thesis, University of Amsterdam, 1940.] *Archives Néerlandaises de Zoologier*, 5: 249 pages, 24 figures.

Kumé, M., and K. Dan
1968. *Invertebrate Embryology*. [Translation from Japanese by J. C. Dan.] xvi + 605 pages, illustrated. Belgrade: NOLIT Publishing House. [Published for the National Library of Medicine, Public Health Service, United States Department of Health, Education, and Welfare, and the National Science Foundation, Washington, D. C. Originally published by Bai Fu Kan Press, Tokyo, 1957.]

Lacaze-Duthiers, M. H.
1854. Nouvelles Observations sur le développment des huîtres. *Comptes Rendus Hebdomadaires des Seances de l'Academie des Sciences*, 39:1197–1200.

Leeuwenhoek, A. van
1695. *Arcana Naturae detecta*. Volume II, letters 92 and 94.

Lutz, R. A.
1979. The Bivalve "Larval Ligament Pit" as an Exclusively Post-larval Feature (Abstract). *Proceedings of the National Shellfisheries Association*, 69:197.

Lutz, R. A., and H. Hidu
1979. Hinge Morphogenesis in the Shells of Larval and Early Post-Larval Mussels (*Mytilus edulis* L. and *Modiolus modiolus* (L.). *Journal of the Marine Biological Association of the United Kingdom*, 59:111–121, 1 figure, 1 plate, 1 table.

Lutz, R. A., and D. C. Rhoads
1977. Anaerobiosis and a Theory of Growth Line Formation. *Science*, 198:1222–1227, 2 figures.

Meisenheimer, J.
1900. Entwicklungsgeschichte von *Dreissensia polymorpha* Pall. *Zeitschrift für wissenschaftliche Zoologie*, 69:1–137, 18 figures, 13 plates.

Millar, R. H.
1955. Notes on the Mechanism of Food Movement in the Gut of the Larval Oyster, *Ostrea edulis*. *Quarterly Journal of Microscopical Science*, 96(4):539–544, 3 figures.

Morton, J. E.
1958. *Mollusca*. First edition, 232 pages, 23 figures. London: Hutchinson and Company.

Oberling, J. J.
1964. Observations on Some Structural Features of the Pelecypod Shell. *Mitteilungen der Naturforschenden Gesellschaft in Bern*, new series, 20: 60 pages, 3 figures, 6 plates.

Ockelmann, K. W.
1965. Developmental Types in Marine Bivalves and Their Distribution along the Atlantic Coast of Europe. *In* L. R. Cox and J. F. Peake, editors, *Proceedings of the First European Malacological Congress (London, September 17–21, 1962)*, pages 25–35, 5 figures. London: Conchological Society of Great Britain and Ireland and the Malacological Society of London.

Orton, J. H.
1937. *Oyster Biology and Oyster-Culture, Being the Buckland Lectures for 1935*. 211 pages. London: Edward Arnold and Co.

Owen, G., and J. M. McCrae
1976. Further Studies on the Latero-frontal Tracts of Bivalves. *Proceedings of the Royal Society of London*, series B, 194:527–544, 28 figures, plates 1–7.

Pascual, E.
1971. Morfología de la charnela larvaria de *Crassostrea angulata* (Lmk.) en diferentes fases de su desarrollo.

Investigacion Pesquera, 35(2):549–563, 10 figures.

1972. Estudio de la conchas larvarias de *Ostrea stentina*, Payr. y *Ostrea edulis* L. *Investigacion Pesquera*, 36(2): 297–310, 8 figures.

Plate, L.

1924. Gleichgewichtserhaltung und Schwerkraftorgane. *In* L. Plate, editor, *Allgemeine Zoologie und Abstammungslehre*, part 2, pages 92–131, figures 88–130. Jena: Gustav Fischer.

Ranson, G.

1939. Le Provinculum de la prodissoconque de quelques Ostréides. *Bulletin du Muséum d'Histoire Naturelle* (Paris), series 2, 11:318–332, 4 figures, 1 plate.

1960. Les prodissoconques (coquilles larvaires) des Ostréides vivants. *Bulletin de l'Institut Oceanographique* (Foundation Albert I^{er}, Prince de Monaco), 1183: 41 pages, 136 figures.

Raven, C. P.

1958. *Morphogenesis: The Analysis of Molluscan Development*. 311 pages, 66 figures. New York: Pergamon Press.

Rees, C. B.

1950. The Identification and Classification of Lamellibranch Larvae. *Hull Bulletins of Marine Ecology*, 3(19):73–104, 4 figures, 5 plates.

Rice, E. L.

1908. Gill Development in Mytilus. *Biological Bulletin*, 14(2):61–77, 9 figures.

Senô, H.

1929. A Contribution to the Knowledge of the Development of *Ostrea denselamellosa* Lischke. *Journal of the Imperial Fisheries Institute*, 24(5):129–135, 3 plates.

Sleigh, M. A.

1962. *The Biology of Cilia and Flagella*. xiii + 223 pages, 53 figures, 18 plates, 14 tables. Oxford: Pergamon Press.

1974. *Cilia and Flagella*. xi + 500 pages, illustrated. London and New York: Academic Press.

Stanley, S. M.

1978. Aspects of the Adaptive Morphology and Evolution of the Trigoniidae. *Philosophical Transactions of the Royal Society of London*, series B, 284(1001):247–258, figures 29–32, 2 plates.

Stenzel, H. B.

1964. Oyster: Composition of the Larval Shell. *Science*, 145(3628):155–156, 2 figures.

1971. Oysters. *In* R. C. Moore, editor, *Treatise on Invertebrate Paleontology*, part N, volume 3, Mollusca 6, Bivalvia, pages 953–1224. Lawrence, Kansas: Geological Society of America and University of Kansas Press.

Strathmann, R. R., T. L. John, and J. R. C. Fonseca

1972. Suspension Feeding by Marine Invertebrate Larvae: Clearance of Particles by Ciliated Bands of a Rotifer, Pluteus, and Trochophore. *Biological Bulletin*, 142:505–519, 5 figures.

Tanaka, Y.

1960. Identification of Larva of *Saxostrea echinata* (Quoy et Gaimard). *Venus (Japanese Journal of Malacology)*, 21(1):32–38, 7 figures, 2 plates.

Taylor, J. D., W. J. Kennedy, and A. Hall

1969. The Shell Structure and Mineralogy of the Bivalvia, Introduction: Nuculacea-Trigonacea. *Bulletin of the British Museum (Natural History), Zoology*, supplement 3: 125 pages, 77 figures, 29 plates.

Tompa, A. S., and N. Watabe

1976. Ultrastructural Investigation of the Mechanisms of Muscle Attachment to the Gastropod Shell. *Journal of Morphology*, 149(3):339–351, 1 figure, 3 plates.

Trueman, E. R.

1951. The Structure, Development, and Operation of the Hinge Ligament of *Ostrea edulis*. *Quarterly Journal of Microscopical Science*, 92(2):129–140, 8 figures.

Turner, R. D., and P. J. Boyle

1975. Studies of Bivalve Larvae Using the Scanning Electron Microscope and Critical Point Drying. *Bulletin of the American Malacological Union, Inc.*, 1974:59–65, 4 plates, 2 tables.

Waller, T. R.

1972. The Functional Significance of Some Shell Microstructures in the Pectinacea (Mollusca: Bivalvia). In *International Geological Congress, 24th Session, Montreal Canada*, 7(Paleontology):48–56, 3 figures, 1 table.

1976. The Development of the Larval and Early Postlarval Shell of the Bay Scallop, *Argopecten irradians* (Abstract). *Bulletin of the American Malacological Union, Inc.*, 1976:46.

1979. Formation of a Posterodorsal Notch in Larval Oyster Shells and the Prodissoconch-I/II Boundary in the Bivalvia (Abstract). *Bulletin of the American Malacological Union, Inc.*, 1978:55–56.

1980. Scanning Electron Microscopy of Shell and Mantle in the Order Arcoida (Mollusca: Bivalvia). *Smithsonian Contributions to Zoology*, 313: 58 pages, 46 figures, 1 table.

Watabe, N.

1956. Dahllite Identified as a Constituent of Prodissoconch I of *Pinctada martensii* (Dunker). *Science*, 124(3223):630, 1 table.

Werner, B.
1939. Über die Entwicklung und Artunterscheidung von Muschellarven des Nordseeplanktons, unter besuderer Berucksichtigung der Schalen-entwicklung. *Zoologische Jahrbucher*, 66(1):1–54, 22 figures, 3 tables.

Yonge, C. M.
1926. Structure and Physiology of the Organs of Feeding and Digestion in *Ostrea edulis*. *Journal of the Marine Biological Association, United Kingdom*, 14(2):295–386, 42 figures, 20 tables.
1957. Mantle Fusion in the Lamellibranchia. *Pubblicazioni della Stazione Zoologica di Napoli*, 29:151–171, 11 figures.
1960. *Oysters*. 207 pages, 72 figures, 17 plates. London: Collins.

REQUIREMENTS FOR SMITHSONIAN SERIES PUBLICATION

Manuscripts intended for series publication receive substantive review within their originating Smithsonian museums or offices and are submitted to the Smithsonian Institution Press with approval of the appropriate museum authority on Form SI–36. Requests for special treatment—use of color, foldouts, casebound covers, etc.—require, on the same form, the added approval of designated committees or museum directors.

Review of manuscripts and art by the Press for requirements of series format and style, completeness and clarity of copy, and arrangement of all material, as outlined below, will govern, within the judgment of the Press, acceptance or rejection of the manuscripts and art.

Copy must be typewritten, double-spaced, on one side of standard white bond paper, with 1¼" margins, submitted as ribbon copy (not carbon or xerox), in loose sheets (not stapled or bound), and accompanied by original art. Minimum acceptable length is 30 pages.

Front matter (preceding the text) should include: **title page** with only title and author and no other information, **abstract page** with author/title/series/etc., following the established format, **table of contents** with indents reflecting the heads and structure of the paper.

First page of text should carry the title and author at the top of the page and an unnumbered footnote at the bottom consisting of author's name and professional mailing address.

Center heads of whatever level should be typed with initial caps of major words, with extra space above and below the head, but with no other preparation (such as all caps or underline). Run-in paragraph heads should use period/dashes or colons as necessary.

Tabulations within text (lists of data, often in parallel columns) can be typed on the text page where they occur, but they should not contain rules or formal, numbered table heads.

Formal tables (numbered, with table heads, boxheads, stubs, rules) should be submitted as camera copy, but the author must contact the series section of the Press for editorial attention and preparation assistance before final typing of this matter.

Taxonomic keys in natural history papers should use the alined-couplet form in the zoology and paleobiology series and the multi-level indent form in the botany series. If cross-referencing is required between key and text, do not include page references within the key, but number the keyed-out taxa with their corresponding heads in the text.

Synonymy in the zoology and paleobiology series must use the short form (taxon, author, year:page), with a full reference at the end of the paper under "Literature Cited." For the botany series, the long form (taxon, author, abbreviated journal or book title, volume, page, year, with no reference in the "Literature Cited") is optional.

Footnotes, when few in number, whether annotative or bibliographic, should be typed at the bottom of the text page on which the reference occurs. Extensive notes must appear at the end of the text in a notes section. If bibliographic footnotes are required, use the short form (author/brief title/page) with the full reference in the bibliography.

Text-reference system (author/year/page within the text, with the full reference in a "Literature Cited" at the end of the text) must be used in place of bibliographic footnotes in all scientific series and is strongly recommended in the history and technology series: "(Jones, 1910:122)" or ". . . Jones (1910:122)."

Bibliography, depending upon use, is termed "References," "Selected References," or "Literature Cited." Spell out book, journal, and article titles, using initial caps in all major words. For capitalization of titles in foreign languages, follow the national practice of each language. Underline (for italics) book and journal titles. Use the colon-parentheses system for volume/number/page citations: "10(2):5–9." For alinement and arrangement of elements, follow the format of the series for which the manuscript is intended.

Legends for illustrations must not be attached to the art nor included within the text but must be submitted at the end of the manuscript—with as many legends typed, double-spaced, to a page as convenient.

Illustrations must not be included within the manuscript but must be submitted separately as original art (not copies). All illustrations (photographs, line drawings, maps, etc.) can be intermixed throughout the printed text. They should be termed **Figures** and should be numbered consecutively. If several "figures" are treated as components of a single larger figure, they should be designated by lowercase italic letters (underlined in copy) on the illustration, in the legend, and in text references: "Figure 9b." If illustrations are intended to be printed separately on coated stock following the text, they should be termed **Plates** and any components should be lettered as in figures: "Plate 9b." Keys to any symbols within an illustration should appear on the art and not in the legend.

A few points of style: (1) Do not use periods after such abbreviations as "mm, ft, yds, USNM, NNE, AM, BC." (2) Use hyphens in spelled-out fractions: "two-thirds." (3) Spell out numbers "one" through "nine" in expository text, but use numerals in all other cases if possible. (4) Use the metric system of measurement, where possible, instead of the English system. (5) Use the decimal system, where possible, in place of fractions. (6) Use day/month/year sequence for dates: "9 April 1976." (7) For months in tabular listings or data sections, use three-letter abbreviations with no periods: "Jan, Mar, Jun," etc.

Arrange and paginate sequentially EVERY sheet of manuscript—including ALL front matter and ALL legends, etc., at the back of the text—in the following order: (1) title page, (2) abstract, (3) table of contents, (4) foreword and/or preface, (5) text, (6) appendixes, (7) notes, (8) glossary, (9) bibliography, (10) index, (11) legends.